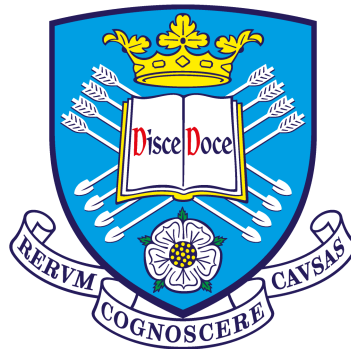


Stability Analysis for the Implementation of Game Theory-based On-Line Pricing Schemes in Micro-Grids

Fernando Genis Mendoza

A thesis submitted in partial fulfillment of the requirements for the
degree of
Doctor of Philosophy



Automatic Control and Systems Engineering

The University of Sheffield

United Kingdom

July 2021

To the loving memory of my father, and to my family back home.

“...“Playing” is not simply a pastime,
it is the primordial basis of
imagination and creation.

Truth be told, *Homo Ludens* (Those
who Play) are simultaneously
Homo Faber (Those who Create).”

Hideo Kojima

Acknowledgements

First and foremost, I would like to express my deepest gratitude to my supervisor Dr George Konstantopoulos. His rescue, his advice and his encouragement helped me focus when I struggled and enabled me to surpass challenges that I did not think I was capable of. After working with me, his patience has reached new bounds and I cannot thank him enough. Speaking of patience, I also would like to give special thanks to my mentor and friend Prof Dario Bauso, his talks were always an inspiration and without his aid and exceptional lessons, this work would not have been fruitful. A big thank you also goes to Prof Toru Namerikawa for his support, it has been an honour collaborating with someone of such academic excellence. I am also grateful to Pablo Baldivieso for believing and making sense of my work when others would not, especially during the last straw of this whole journey.

All of this has been possible because of the endless love, care, and support from my dear wife Lalis. She is my strength, driving force and muse at the same time. I owe to my parents Fernando and Rosa their unconditional support, discipline and teachings that have ultimately led me to this point. And to my sister Alma for taking care of everything else and pushing me to pursue this endeavour.

I want to thank my PhD colleagues, I appreciate your friendship and sharing your experiences (good and bad) in this path we decided to take. I would also like to thank all the ACSE staff that allowed me to work as a GTA, more specifically Tara Baldacchino and Roderich Gross.

Lastly, I thank the Mexican National Council of Science and Technology for the financial support that made my postgraduate studies possible (CONACyT Scholarship No. 440742).

Declaration

I hereby declare that the present thesis was composed by myself in its entirety and the work contained herein is my own except when stated otherwise. The work included in Chapter 3 was done in collaboration with Prof Dario Bauso and Prof Toru Namerikawa. Chapter 4 was done in collaboration with Prof Dario Bauso with some input from my supervisor Dr George Konstantopoulos. Chapter 5 was carried out in collaboration with Dr George Konstantopoulos with advice from Prof Dario Bauso. Chapter 6 is a collaborative work with Dr Pablo R. Baldivieso-Monasterios, Dr George Konstantopoulos and Prof Dario Bauso. Chapter 3 has been published in the peer-reviewed journal *IET Smart Grid* and part of it was first presented at the *2017 International Conference on Wireless Networks and Mobile Communications (WINCOM)*. Chapter 4 was presented at the *2019 European Control Conference (ECC)* and part of Chapter 6 has been presented at the *2021 European Control Conference*. Chapter 5 has been published in *IET Smart Grid* as well. A manuscript corresponding to Chapter 6 has been submitted to a peer-reviewed journal and is still under review at the time of submission of this thesis. A list with all the mentioned publications can be found on the next pages.

Abstract

An existing challenge in power systems is the implementation of optimal demand management through dynamic pricing. This research project deals with on-line pricing schemes for electricity in micro-grid network systems and the ways in which their implementation affects the physical system's response. Two approaches were devised in this study: First, the ways in which micro-grid networks can be modelled as less prescriptive multi-agent consensus systems; examining their response under uncertainties and gaining insights on the relation between the network topology, the heterogeneous parameters of its components, and the system's response. Secondly, deriving game-theoretic novel pricing schemes and integrating them with the physical system model to perform a stability analysis. The proposed schemes consider the rational behaviour of the end-users and the entailing tension with the energy supplier(s); demonstrating the ways in which the decisions of the players involved influence the physical system. The study aims to clarify the interconnection between the market and physical layers of the problem, leading to a better future implementation of such schemes. The first part of this thesis studies networks of heterogeneous micro-grids, treating them as agents and modelling their dynamics as an averaging process that is subject to uncertain non-linear parameters. The second part introduces a pricing scheme based on the Stackelberg game with incentive strategies in a micro-grid, where the leader is the energy supplier, and the follower the consumer. The scheme is then improved and carried out in a droop-controlled low-voltage resistive AC micro-grid. The final part of this research is about the design of a scheme based on coalitional game theory, where there are multiple competing energy retailers attracting consumers. For all the propositions above, analysis and simulations that illustrate system stability, agent rationality, profit improvement, and the convergence to different equilibria in the physical and market responses are implemented.

List of Publications

Journal Publications

1. F. Genis Mendoza, D. Bauso and T. Namerikawa, “**Transient and stability analysis of heterogeneous micro-grid networks subject to uncertainties**”, *IET Smart Grid*, Volume 3, Issue 6, December 2020, p. 851 – 859. Available: 10.1049/ietstg.2020.0049
2. F. Genis Mendoza, D. Bauso and G. Konstantopoulos, “**On-Line Pricing for Demand-Side Management in a Low-Voltage Resistive Micro-Grid via a Stackelberg Game with Incentive Strategies**”, *IET Smart Grid*, September 2021, p. 1 – 14. Available: 10.1049/stg2.12053

Conference Proceedings

1. F. Genis Mendoza, D. Bauso and T. Namerikawa, “**Transient dynamics of heterogeneous micro grids using second order consensus**”, *2017 International Conference on Wireless Networks and Mobile Communications (WINCOM)*, Rabat, Morocco, 2017, pp. 1-6. Available: 10.1109/WINCOM.2017.8238210
2. F. Genis Mendoza, D. Bauso and G. Konstantopoulos, “**Online Pricing via Stackelberg and Incentive Games in a Micro-Grid**”, *2019 18th European Control Conference (ECC)*, Naples, Italy, 2019, pp. 3520-3525, Available: 10.23919/ECC.2019.8795772
3. F. Genis Mendoza, P. R. Baldivieso-Monasterios, D. Bauso and G. Konstantopoulos, “**Demand-Side Management in a Micro-Grid with Multiple Retailers: A Coalitional Game Approach**”, *2021 20th European Control Conference (ECC)*, 2021.

Poster Presentation

1. F. Genis Mendoza, and G. Konstantopoulos, “**An Application of the Stackelberg Game in On-Line Pricing for Resistive Micro-Grids (Preliminary Results)**”, *2019 Engineering Researcher Symposium (ERS)*, The University of Sheffield, Poster Winner - Automatic Control and Systems Engineering

Contents

1	Introduction	1
1.1	Background and Motivation	1
1.1.1	Multi-Agent Systems	3
1.1.2	On-Line Pricing	4
1.1.3	Game Theory	5
1.2	Research Questions	5
1.3	Overview and Main Contributions	6
2	Literature Review	9
2.1	Network Models	9
2.2	Modelling for Networks of AC Micro-Grids	10
2.3	Line Diagrams and Parameter Approximation	12
2.4	Analysis of Linear and Non-Linear Systems	13
2.5	Consumer-Supplier Models and Ex-Ante Price	13
2.6	Stackelberg Game and Incentive Strategies	14
2.7	Demand Response and Load Modelling	16
2.8	Stackelberg Game and Micro-Grids	16
2.9	Resistive Network Model	17
2.10	Droop Controller	19
2.11	Coalitional Games in Micro-Grids	20
2.12	Conclusion	21
3	Stability of a Network of Micro-Grids under Uncertainties	23
3.1	Introduction	23
3.1.1	Summary and Contributions	24

3.2	Problem Statement and Model	24
3.3	Preliminary Derivations	28
3.3.1	Transient Dynamics of the Micro-Grid Network System	28
3.3.2	Gershgorin Disc Theorem	29
3.4	Stability and Response Analysis	29
3.4.1	Eigenvalue Location and Response Bounding	29
3.4.2	Effect of Inertia on Eigenvalues	32
3.4.3	Clusterization	35
3.5	Stability Under Uncertainties	36
3.5.1	Amplitude of Uncertainty	37
3.5.2	Lyapunov Approach	39
3.6	Numerical Examples	40
3.6.1	Graph Modeling from Existing Network	41
3.6.2	Change of Topology	42
3.6.3	Parameter Varying and Heterogeneity	44
3.7	Conclusion	46
4	On-line Pricing in a Micro-Grid via a Stackelberg Game with Incentive Strategies	49
4.1	Introduction	49
4.1.1	Main Contributions	50
4.1.2	Problem Statement	50
4.2	Micro-Grid and On-Line Pricing Models	50
4.2.1	Micro-Grid Model	51
4.2.2	Demand Response	51
4.2.3	Consumer and Supplier Functions	52
4.3	System Integration and Analysis	54
4.3.1	Normalized Stackelberg Game Formulation	55
4.3.2	Stability of Open-Loop Configuration	57
4.3.3	Price as a Function of Power and Demand	60
4.4	Numerical Examples	65
4.4.1	Micro-Grid with Exogenous Price Input	65
4.4.2	Micro-Grid with Closed-Loop Market Dynamics	68

4.5	Conclusion	68
5	Personalised Pricing in a Resistive Micro-Grid via a Stackelberg Game with Incentive Strategies	71
5.1	Introduction	71
5.1.1	Summary and Contributions	71
5.1.2	Problem Statement	72
5.1.3	Notation Preliminaries	72
5.2	Micro-Grid Model	72
5.2.1	Network Model Considerations	73
5.2.2	Resistive Micro-Grid Model	73
5.2.3	Definition and Properties of the Conductance Matrix	74
5.2.4	Additional Model Conventions	75
5.2.5	P-V Droop Controller	75
5.3	Problem Formulation	76
5.4	System Integration and Stability Analysis	77
5.4.1	Consumer and Supplier Functions	77
5.4.2	Stackelberg Game Formulation	78
5.4.3	Closed Loop Configuration	81
5.4.4	Closed-Loop Stability	82
5.4.5	Implementing a Bounded Droop Control Architecture	85
5.5	Numerical Examples	89
5.6	Conclusion	91
6	Pricing and Stability via Coalitional Games in a Resistive Micro-Grid	95
6.1	Introduction	95
6.1.1	Problem Statement and Contributions	96
6.2	System Model, Definition and Preliminaries	97
6.2.1	Sets and Coalitions Definition	97
6.2.2	Consumer and Retailer Profit Functions	98
6.2.3	Stackelberg Game Review	100
6.2.4	Network Systems Review	100
6.2.5	Definition and Properties of the Conductance Matrix	101

6.3	Coalitional Game with Multiple Retailers	102
6.3.1	Cost Definition and Minimum Spanning Tree Problem	102
6.3.2	Savings Imputation via Shapley Value	104
6.3.3	Retailer's Cost Network Derivation	105
6.3.4	Price, Consumption and Coalition Forming	107
6.3.5	Properties and Stability of the Coalitional Game	110
6.3.6	Stackelberg Equilibrium	114
6.4	Risk Sharing and Reduction of Statistical Dispersion	115
6.5	Implementation with Physical Dynamics	117
6.5.1	Micro-Grid and Demand Dynamics	118
6.5.2	Physical Stability Analysis	120
6.6	Numerical Examples	122
6.6.1	Coalition Formation and Profit Calculation	122
6.6.2	Game and Physical Dynamics Integration	127
6.7	Conclusion	128
7	Conclusions	133
7.1	Discussion and Conclusions	133
7.2	Impact on the Community	134
7.3	Future Directions	134

List of Figures

1.1	Micro-grid elements and representation example.	2
1.2	On-line pricing and rational end-user behavior example.	4
1.3	Payoff matrix of Rock-Paper-Scissors game, where the payoff for a player is equal to 1 when winning, 0 when there is a tie and -1 when losing.	5
2.1	One-line diagram derived from part of the London City Road Network as in [1]	12
2.2	Following game where a seller announces an item of price p , value K to the buyer and no value to the seller. The buyer can decide to buy or not to buy, choosing the latter yields a payoff of 0 to both players. The seller has to consider the buyer's responses while formulating p	14
2.3	Equivalent model of a transmission line between nodes i and j in a micro-grid network.	18
2.4	P-V droop control slope example.	20
3.1	Equivalent circuit representing the connection between micro-grids i and j , with shunt conductances $Y_i = 1/Z_i$	26
3.2	System block representation of micro-grid i	26
3.3	Graph topology analogous to the micro-grid network in [1].	27
3.4	Gershgorin disc configuration example.	31
3.5	Micro-grid i subject to disturbances.	36
3.6	Sector definition example (dashed) for non-linearity ψ_i	37
3.7	Reduced network model based on the one-line diagram of the London City Road Network from [1].	41
3.8	State of the micro-grid frequency over time.	42

3.9	State of the power flow in each micro-grid over time.	43
3.10	Derived graph for a different section of the network in [1].	43
3.11	Frequency response in a different topology.	44
3.12	Weighted directed graph of the London City Road network [1].	45
3.13	Frequency and power flow responses for the directed, weighted and approximated configuration while subject to uncertainties.	46
4.1	Block system of a micro-grid with demand response ΔP_L , power P_{flow} and frequency f subject to exogenous price input Λ	52
4.2	Supplier and consumer functions and quantities.	54
4.3	Stackelberg equilibrium points as a function of γ	57
4.4	Block system of the micro-grid with closed-loop on-line pricing.	61
4.5	Open-loop response of (top) price, (middle) power flow, and (bottom) frequency.	66
4.6	Open-loop response of (top) price, (middle) power flow, and (bottom) frequency; by increasing the damping coefficient oscillations are reduced.	67
4.7	Open-loop response of (top) price, (middle) power flow, and (bottom) frequency; by selecting large gain values, the demand exceeds the power available in the grid.	67
4.8	Closed-loop response of (top) power flow, and (bottom) frequency.	68
4.9	Closed-loop response of (top) power flow, and (bottom) frequency; by increasing the damping coefficient oscillations are reduced.	69
4.10	Closed-loop response of (top) power flow, and (bottom) frequency; by selecting large gain values, the demand exceeds the power available in the grid.	69
5.1	Resistive micro-grid in a network representation, comprised by loads \bullet and generators \blacksquare , resistive distribution lines, and shunt conductances.	74
5.2	Gershgorin disc configuration example, center and radius for the i th disc of J	84
5.3	Bounded droop controller phase portrait example.	85
5.4	Simulation of a network connected to the main grid with one load and two varying generators.	90

5.5	Voltage plots for the one load configuration.	91
5.6	Simulation of a network connected to the main grid with two loads and two varying generators.	92
5.7	Voltage plots for the two load configuration.	92
6.1	Example cost network from retailer r_1 , and its minimum spanning tree (dashed). Other retailers r_j also assign similar costs (gray).	103
6.2	Resistive micro-grid in a network representation, comprised by loads/consumers \bullet and generators/retailers \blacksquare , resistive distribution lines, and shunt conductances.	118
6.3	Cost networks defined by each retailer for the same set of consumers.	123
6.4	Price and coalition consumption responses over time.	124
6.5	Consumers' individual power demand over time.	124
6.6	Consumers' immediate profits for every time period.	125
6.7	Retailers' immediate profits for every time period.	125
6.8	Total consumption and profits from all consumers in the problem.	126
6.9	Consumers' coalition selection over time.	126
6.10	Resistive network configuration for the physical dynamics integration example.	127
6.11	Resistive network node powers when subject to the proposed coalitional game.	129
6.12	Resistive network node voltages when subject to the proposed coalitional game.	129
6.13	Desired cumulative consumptions for each retailer coalition given a respective price.	130
6.14	Consumers coalition selection when subject to physical dynamics.	130

List of Tables

2.1	Most important literature by topic.	22
3.1	London City Road Grid Power Capabilities	45
6.1	Parameters for Retailers and Consumers.	123

Chapter 1

Introduction

The present thesis deals with the dynamic modeling of power systems and electricity pricing mechanisms via elements of control theory and game theory respectively. From the dynamic and market setups here derived, an analysis on stability is performed when integrating both kinds of systems.

In this chapter, a background of the topics related to this research project is provided along with the motivations that led to its formulation.

This dissertation contains seven chapters. Chapter 3, Chapter 4, Chapter 5 and Chapter 6 comprise the main body of this thesis.

1.1 Background and Motivation

The study of network systems (or system of systems) has numerous applications, one of rising interest is the smart-grid paradigm, sometimes referred to as micro-grid, which is characterised by the management of energy resources such as power and frequency in a large group of electricity users with a local supply and consumers that act as loads [2]. A micro-grid can either operate in conjunction with the main electricity grid or independently (islanded mode). The balance of power between the elements and their management is achieved by a local controller. An example of a micro-grid and its elements is illustrated in Fig. 1.1.

The AC micro-grid is the dominant type of micro-grid and is the main focus of the present work. However, two configurations are presented in this study. The first one is based on the swing equation [3, 4] which deals with the frequency f_i and power P_i

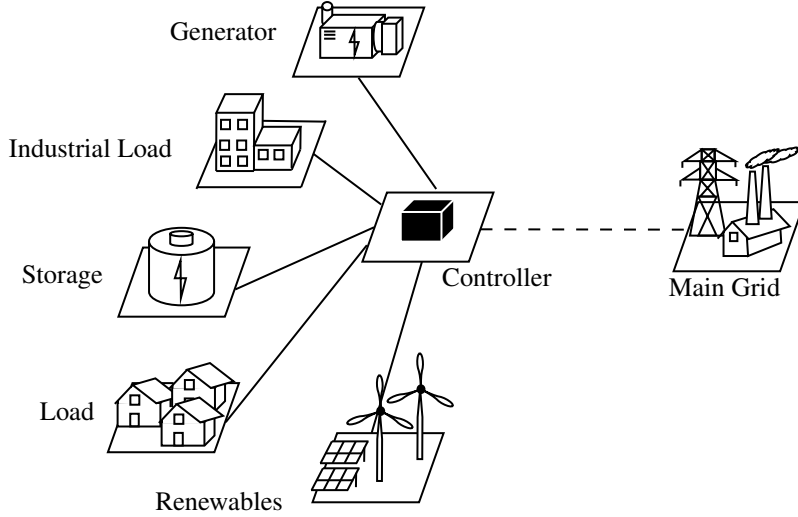


Figure 1.1: Micro-grid elements and representation example.

dynamics of a micro-grid i in a network:

$$\begin{aligned} \dot{P}_i &= \sum_{j \in \mathcal{N}_i} T_{ij}(f_j - f_i), \\ \dot{f}_i &= \frac{1}{M_i} P_i - \frac{D_i}{M_i} f_i, \end{aligned} \quad (1.1)$$

where D_i and M_i are damping and inertia coefficients, and T_{ij} is a synchronizing coefficient between the connected micro-grids i and j in a neighborhood of nodes \mathcal{N}_i . The second is the resistive micro-grid, which as we will explain later, can be considered similar to a DC micro-grid, where the power expression for a power unit (or node) i in a network can be expressed as

$$P_i = V_i^2 \left(\frac{1}{R_{ii}} + \sum_{j \in \mathcal{N}_i} \frac{1}{R_{ij}} \right) - \sum_{j \in \mathcal{N}_i} \frac{V_i V_j}{R_{ij}}, \quad (1.2)$$

where V_i is the node voltage, R_{ii} its shunt resistance and R_{ij} the equivalent resistance of the transmission line that connects nodes i and j in \mathcal{N}_i .

On the other hand, one of the most relevant problems at present in the research field of demand-side management is the search for a real-time pricing scheme that successfully improves the profits of both energy consumers and suppliers while also improving the efficiency of the power grid. This study focuses on bringing together the market and physical dynamics that are involved, determining the functioning of a micro-grid network as a whole.

As commonly employed in the field of economics, game theory concepts allow modelling the dynamics of a market and the rationale of consumers and suppliers. The implementation of pricing mechanisms based on game theory for electrical networks is not novel *per se*. In contrast, as we will show later in the literature review, there are still open challenges that need to be explored when these kinds of pricing mechanisms are put in conjunction with the physical system. For instance, given a pricing scheme, a detailed stability analysis should be conducted to ensure the correct operation of the micro-grid. These open research areas are expected to some degree since the analysis of just one system is complex, let alone for a group of interconnected ones. This further motivates the search for a simpler representation of the network system that can help us predict its behaviour and the agents interacting in it in a reliable manner.

The main chapters of this thesis contain problems related to power systems modelling, network theory, real-time electricity pricing and game theory. Despite the fact that the setup of each chapter is independent of each other, they constitute a whole evolving work; where each contributes to the refinement of this research and its application. To set the stage about the setup and concepts involved, let us provide a brief background.

1.1.1 Multi-Agent Systems

Recently there has been increased interest in large scale interconnected multi-agent systems due to their potential to be implemented in numerous areas such as energy, transportation, social networks, cloud computing and others [5]. Multi-agent systems are powerful mathematical constructs that describe the interaction between a number of entities, sometimes also referred to as players or agents, such entities can possess decision-making capabilities as well as means of sensing and communication between them. Generally, said capabilities are achieved by the use of information technologies, hence their present-day relevance. The models for these kinds of systems can accommodate the information, the influence of it to the agents' behaviour, as well as the response of the system itself and the impact of the agents to it. Previous work about the modelling of such systems provides numerous results about their mathematical foundations and equilibrium concepts. However, there are limited writings about the stability analysis, equilibrium selection and robustness under uncertainty; additionally, the inclusion

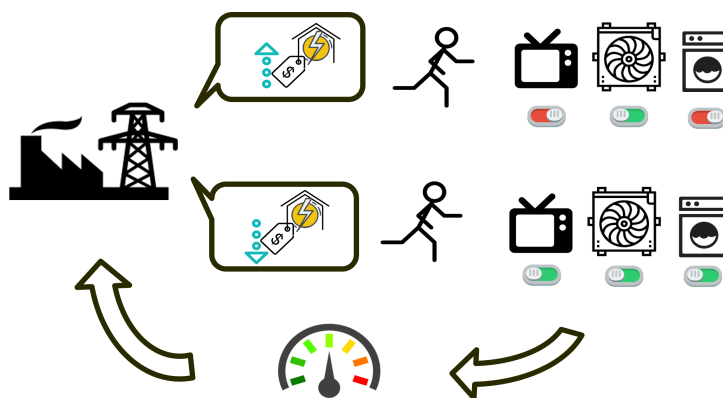


Figure 1.2: On-line pricing and rational end-user behavior example.

of schemes to shift the agents' response is an interesting approach to the study of the mentioned literature challenges. As we will mention later, micro-grid networks can also be represented as systems that need to reach a consensus (i.e. a certain frequency value for all micro-grids) [4].

1.1.2 On-Line Pricing

One of the aims of this research is to subject micro-grid systems to on-line electricity pricing mechanisms and the ways in which these can be designed. Pricing mechanisms on electrical power systems constitute a viable way to shift the demand peaks and thus to improve efficiency [3]. The underlying assumption is that the consumer and the supplier are rational and try to maximise their profits. Under such an assumption, a change of the price by the independent system operator modifies the consumer's behaviour [6]. An example of such seller-buyer dynamics is exemplified in Fig. 1.2 where the demand of the users is shifted as a reaction to the announced price. The analysis of the resulting dynamics is a core element in the literature on on-line pricing. On-line pricing requires the implementation of incentive mechanisms in real-time to increase the profits of the supplier by charging more when the production costs are higher instead of applying a flat rate. Similarly, incentives can be used to let the consumer know when is more convenient to carry out the more power-consuming tasks [7]. Effective methods to determine the electricity price dynamically present several challenging open problems including: Global optimality for both consumers and suppliers, the uncertainties in the consumers' behaviours and preferences, and more importantly, the safe operation of the electrical systems when subjected to such mechanisms.

		Player 2		
		rock	paper	scissors
Player 1	rock	(0,0)	(-1,1)	(1,-1)
	paper	(1,-1)	(0,0)	(-1,-1)
	scissors	(-1,1)	(1,-1)	(0,0)

Figure 1.3: Payoff matrix of Rock-Paper-Scissors game, where the payoff for a player is equal to 1 when winning, 0 when there is a tie and -1 when losing.

1.1.3 Game Theory

The pricing schemes presented in this study are modelled using concepts from game theory. Game theory studies the interaction between rational individuals and their strategies in a cooperative or competitive environment [8]. It is applied to a plethora of domains, from finance to social sciences. A very basic example of strategy and payoff modeling is found in Fig. 1.3. This feature of capturing rationality is useful in the modeling of suppliers and consumers. We employ concepts of game theory such as the Stackelberg equilibrium [8] and coalitional games [9] to describe the ways in which a price is derived in the pricing schemes we have designed, and in consequence, the choices from the consumers that result in power demand.

1.2 Research Questions

This research project addresses the aforementioned responses and behaviours in two ways: firstly the analysis and explanation of observed phenomena. Secondly, the prediction and design of the network system response. Part of this project focuses on the strategic interaction between the players and their influences, specifically the effect that individual actions have on the system and vice versa. More concretely, this research is about studying pricing schemes based on game theory and the ways in which these can be implemented in the physical power network. We intend to answer the following research questions: How can we model these complex networks of systems in a less rigid, less complicated way? What is the role of the network topology and its parameters? How do the strategies of the agents affect such systems responses? And more importantly: How can we induce such strategies and implement them in a stabilizing manner?

1.3 Overview and Main Contributions

To accentuate the importance of the present work, an abridgement of the main contributions is given in the sequel. The interrelation between the different contributions is also explained with the intention of allowing the reader to follow the work progress in the chapters that follow.

Chapter 2 presents the state of the art and the reviewed literature that inspired and motivated the present research. A brief comparison of the previous works with the current investigation is enclosed.

Chapter 3 presents an analysis of the transient dynamics of a network of micro-grids, mainly the influence of oscillations during the system response, where every single micro-grid is modelled incorporating heterogeneous parameters for damping and inertia. *This study sheds light on the ways in which different damping coefficients influence the frequency and power flow responses as well as the different positioning of the system eigenvalues.* Secondly, for each of the micro-grids in the network, *the conditions that guarantee absolute stability when the system is subject to non-linearities and uncertainties are derived.* Additionally, the study involves the adaptation of the proposed model to real instances in the UK electrical network and the calibration of the nodes' parameters using data of the power capabilities of the micro-grids.

Chapter 4 utilizes the previously presented model for a single micro-grid and subjects it to a normalised leader-follower pricing scheme. As a first result, *the conditions for stability and the transient response of a micro-grid system subject to a price are obtained, where the price is generated exogenously from a Stackelberg game.* The game introduces an incentive problem, which in turn determines the steady-state gain of the open-loop market dynamics. As a second result, *a general feedback rule to obtain the price as a function of the power flow and demand is derived.* Such a rule is based on an ex-ante price formulation. The impact of the parameters on the transient dynamics of the micro-grid system is studied.

Chapter 5 further improves on the Stackelberg game with incentive strategies, where the profit functions of the players are more appropriately defined and tuned, *the analysis is extended to a more realistic model of a low-voltage resistive network system, while the steady-state gain for the consumer response is calculated directly in the game by employing the derived profit functions.* The incentive strategy is included

as means for a personalised price function. The system dynamics incorporates a droop-control structure for each unit in the micro-grid, *a stability analysis of the integrated system is performed, including an extension for the case when implementing bounded droop control that leads to simplified stability conditions*. Another core novelty is that, to the best of our knowledge, *this is the first time that a droop-controlled resistive micro-grid is subjected directly to a game-theoretic pricing scheme*, thus paving the way for the application of game theory-based intelligent demand-side management in future distribution systems.

Chapter 6 takes the resistive micro-grid model studied in Chapter 5 and proposes for it *a novel pricing scheme, in a coalitional game framework, where there are multiple competing retailers in a micro-grid*. A stability analysis is carried out covering the coalitions formed by our proposed game and algorithm. Following with the leader-follower structure of the previous chapters, *the existence of the equilibrium points in the game is demonstrated, namely the guaranteed existence of a consumption value given an announced price with a potential subsidy*. Finally, the advantages of the scheme are numerically demonstrated; the ways in which the profits of the consumers improve in comparison to a single retailer scenario is shown.

Chapter 7 provides a summary of the results achieved in the thesis and proposes several possible directions for future work.

Chapter 2

Literature Review

In this chapter, the previous work that motivates the current research is presented. The literature review is separated into subsections that focus on particular disciplines that have been touched upon, such as the different models and equations used for the micro-grid system, consumer and supplier models, and the utilised concepts from game theory. The tools used for the analysis are also mentioned.

2.1 Network Models

The basis of the micro-grid models analysed in this study rests on the power flow and frequency dynamics (1.1). When such micro-grids are interconnected in a network topology an equivalence can be made to an averaging system based on the form of a Laplacian matrix. We focus our research on the stability analysis of networks comprised of such micro-grid systems and the role of the parameters in the transient and convergence of their response. The main result of the exponential stability of linear systems composed by a row-stochastic matrix (the Laplacian matrix is a case of these), its properties, the conditions for stability and the relation with the zero eigenvector was first introduced in [10]. The paper explains in a generalized way how such systems are constructed and provides a detailed demonstration of the ways in which synchronization is achieved. The majority of the graph theory tools, analysis and main characteristics of network systems are resourcefully and concisely explained in [5], mainly the properties of the Laplacian matrix, its derivation from a network graph and the role of the algebraic connectivity or Fiedler eigenvalue. All the concepts of graph theory used in this work

are also explained in [5]. In [11] an example related to the Kuramoto oscillator is mentioned, these results are explained more extensively in [5]. The role of the Laplacian in the swing dynamics and the analogy with the Kuramoto coupled oscillator model is likewise studied in [5], where the latter denotes the angle θ dynamics of a node in a network as

$$\dot{\theta}_i = \omega_i - \sum_{j=1}^n a_{ij} \sin(\theta_i - \theta_j), \quad i \in \{1, \dots, n\}, \quad (2.1)$$

where θ_i is the node angle, ω_i is the phase and a_{ij} is the weight of the edge connecting nodes i and j . The approximation based on the swing dynamics (1.1) and the link with the Laplacian for small phase angles is discussed in [11], we use this approximation in the micro-grid model. In [11] there are also discussions regarding the role of the second smallest eigenvalue of the network, the eigenvector of the Laplacian and how these kind of systems accomplish synchronization.

In [12] an analysis of synchronization for networks of inverters is performed, the results on the rate of frequency convergence are related directly to the algebraic connectivity that is defined by the network topology, in our study we show a similar result when the network has heterogeneous parameters for the agents. Our current study is inspired by the previous contribution [4], where a stability analysis of micro-grids together with the study of the effects of damping and inertia for homogeneous micro-grids was conducted. Part of the present studies differs from [4] in the sense that one of our objectives is to take the heterogeneity between micro-grids. Another aspect that differentiates our work is our intention to bridge the market layer to the physical layer of the micro-grid network.

2.2 Modelling for Networks of AC Micro-Grids

The first of the micro-grid models used in the present work are derived from the swing equation (1.1). Such an equation is known to represent, to decent approximation, the dynamics of generators in electricity grids. As shown above, the swing equation is characterized by its inertia and damping parameters. This power grid model is frequently used, such as in [2], [3], [13], [14], and [15]. Although the swing equation is well-known and established, it ignores non-linear dynamics such as the mechanical rotational loss due to friction in the generators [16], such considerations are out of the

scope of this study and these terms are approximated by the damping and inertia coefficients as in other conventional approaches. The model is employed in [15] as means to implement a droop controller that we will mention later. The equivalent model for the connection between two micro-grids is based on the reduction shown in [17]. We also use the power flow model introduced in [18] under the assumption that all generators in a micro-grid are operating synchronously. This model also has the form of a consensus protocol which is thoroughly analysed in [13] and mentioned as an example in [5] and [11].

Another instance of using the power flow equation to describe the power transfer between two areas and linearising for small angles is derived in [19] and also employed in the micro-grid model in [3]. Transient analysis on coupled homogeneous oscillators and the relation between damping and inertial coefficients is investigated in [2] and [13]. These works also describe the conditions that these coefficients must fulfill in the form of a perturbation parameter. Subsequent work in [20] shows the micro-grid network model as a correspondence of the Kuramoto coupled oscillator, the network model is subject to a frequency droop controller. The results regarding synchronization are also related to algebraic connectivity. The role of the damping parameters in a network of electrical generators is discussed in [21]; here it is explained that damping is not considered during the modelling of electrical systems but is produced as a result of physical phenomena such as changing loads and control loops. The model mentioned above implemented to a network of interconnected oscillators and the influence of disturbances is also utilized in [3] though is focused in using game-theory to represent disturbances. A study of the power flow and demand response in a distributed system of micro-grids similar to the present one is carried out in [22], as main difference, we provide a stability analysis. The basis of the present work is in the same spirit as [4], where a stability analysis of micro-grids together with the study of the effects of damping and inertia for homogeneous micro-grids was conducted. The present research differs from [4] as we add the market layer to the physical layer of the micro-grid. From the latter, and by taking into account heterogeneity in the network, a brief analysis of the influence of the parameters on a micro-grid, along with a simplified version of the model used in the present work is found in [23]. It is worth mentioning that some of the models studied are input/output systems interconnected through diffusive coupling as in [24, 25], we

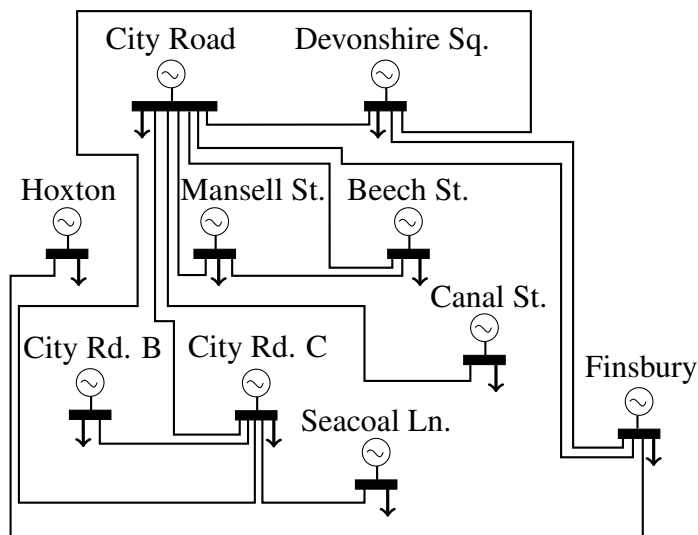


Figure 2.1: One-line diagram derived from part of the London City Road Network as in [1]

differentiate our work by focusing on the case for agents with heterogeneous parameters.

2.3 Line Diagrams and Parameter Approximation

From the interconnected micro-grid models, a one-line diagram can be derived, these kind of diagrams describe the ways in which different micro-grids are connected and how the power is interchanged between them. We borrow from [4] the idea of converting the one-line diagram of an electrical micro-grid network into a dynamic network and extend the approach to heterogeneous networks. The examples of existing UK electrical network topologies and parameters in this thesis are obtained from [1]. In such document, there are detailed diagrams for the 33 kV electrical network for the London city road region in the United Kingdom. The diagrams presented served as a reference for instances of existing electrical network topologies and some of their parameters. A representation of the above is shown in Fig. 2.1. Parameter approximation for electrical networks and their use in the swing equations is studied in [2] and references therein, the book also contains detailed analysis about the units in which the damping of an electrical generator is measured as well as the procedure to obtain it. We used such methods to approximate the data that was not available from [1] to fully adapt the one-line diagram to our model.

2.4 Analysis of Linear and Non-Linear Systems

Since this research project deals with complex network systems that can have matrix representations of high order, we recur to various concepts to analyse their stability. The Gershgorin disc theorem is a tool we use to bind the possible values of the eigenvalues of a square matrix in the complex plane. The theorem was first introduced in [26]. It consists in computing areas in which the eigenvalues of our system's matrix can be located, these areas are obtained from the values of each of its rows. We use this as means to show the transient dynamics of the system's response, how the damping and inertia values change the eigenvalue location and to find the rate of convergence of such response. The method in the present study where we isolate the uncertainty in the feedback loop of the system is explained in [27]. Such method consists on introducing a non-linearity in the feedback loop. This physically represents that the power and frequency measurements in our micro-grid system are subject to disturbances. The conditions obtained from [13] are also employed for the non-linearity sector calculation. From [27] we also use the conditions for absolute stability, these include the conditions for positive definiteness and showing that the system's model is Hurwitz. The Routh-Hurwitz criteria for obtaining the stability conditions for higher-order systems has been studied and used as a tool for our closed-loop system configuration, numerous texts explain the procedure and reasoning behind such criteria, a comprehensive explanation can be found in [28]. The stability analysis of our droop controlled resistive network configuration is performed via Jacobian linearization approximation around an equilibrium point. A concise explanation and method to perform such analysis is presented in [29].

2.5 Consumer-Supplier Models and Ex-Ante Price

To derive the pricing schemes that are presented in this research we have to first characterize the agents involved in the problem, which in our case is suppliers and consumers of electricity. The supplier and consumer models that are analysed in this work were first proposed in [6]. The main characteristic of such models is that both the supplier and the consumers are considered to be price-taking, profit-maximizing agents. These models are widely used in other works related to shiftable demand such as [3] and [30].

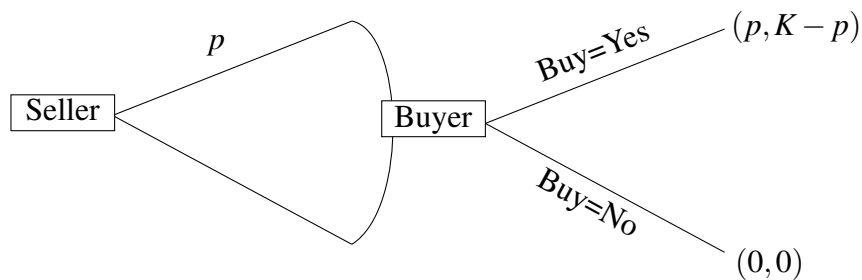


Figure 2.2: Following game where a seller announces an item of price p , value K to the buyer and no value to the seller. The buyer can decide to buy or not to buy, choosing the latter yields a payoff of 0 to both players. The seller has to consider the buyer's responses while formulating p .

Additionally from [6], the standard characteristics of both cost and utility functions for supplier and consumer respectively are employed, namely, both are monotonically increasing and convex and concave respectively. The formulation used in the current study for the ex-ante price is also introduced in [6], such price can be calculated from the derivative of the supplier's cost function evaluated at the value of an estimated supply which is in turn obtained from a recorded previous demand. As part of the formulation of the ex-ante price, the supplier's cost function must be defined, we refer to the cost for electricity generation mentioned in [31]. Such cost has been experimentally validated for thermal generators in [32] and is otherwise generally accepted as a sound approximation as seen in [33], [34] and [35].

2.6 Stackelberg Game and Incentive Strategies

The pricing schemes presented here are formulated using game-theoretic concepts and models. The basic concepts of game theory that are used in this work are explained in [8], such as the definition of equilibrium and strategy, Nash equilibrium, the Bertrand and Cournot models and mainly the formulation of the Stackelberg game model. A Stackelberg game is a two-player extensive game in which a "leader" chooses an action based on the possible rational response of its "follower", who in turn, informed of the leader's choice, chooses an action. We have selected to base our schemes on such a game since it fits a common market dynamics that is simple and easy to relate, understand and is the only one that allows to capture the hierarchical structure that takes place in the electricity market. A simple example of this is shown in Fig. 2.2.

The variation of the Stackelberg game via an introduction of an incentive strategy was first presented in [36]. The main difference with the classic Stackelberg game is that the leader in the game announces a function or ‘incentive’ which depends on the follower’s own response, that is, instead of just a single decision, the follower now has a space of decisions. This variation is used in our study since the leader-follower dynamic fits the one of the system operator-consumer in a dynamic pricing scenario. In our current study, we use a linear function of the power consumed by the follower to represent the incentive strategy. A literature review was performed in order to find out what kind of incentive strategies are employed when this kind of game is used. On [37] fundamental results about mean-payoff games are shown, the paper uses a vector notation to include all followers and refers to it as strategy profiles for all followers; in the examples only proportional strategy profiles are employed. In [38] and [39] the formulation of linear-quadratic games with non-cooperative followers is presented. In the first, linear strategies are explicitly and exclusively used for their purpose. In the latter, linear strategies are used as an example, though it is not discarded that other types of functions can be employed. Examples of the Stackelberg game with incentive strategies are examined in [40] and [41]. In [40] a way to control road traffic flow is presented, two results are shown, the first uses a linear strategy, the second uses a non-linear example comprised of a linear function and then an exponential one for certain domains. A very interesting example of how a game of counter-terrorism would be modelled using the Stackelberg game is presented in [41]. In the example linear and quadratic functions are employed, it is mentioned explicitly that they are formulated that way for the sake of tractability and simplicity. Our justification of choosing a linear function for the incentive strategy comes from the analogy that commonly in the literature the price of energy to the consumer is chosen proportionally to the total demand from all the users [31]. Other examples of this practice are found in [3], [42] and [43]. For practicality sake, the linear price function and generation cost function used in this study have been based and adapted on the ones from [30]. Although incentive strategies on micro-grids have been previously studied in [3], they are implemented as a reward to the consumer when participating in an on-line pricing scheme. Another reward scheme is formulated in [22], the paper discusses a way to adjust the power consumption by trading the one generated and stored by the user. Opposed to [3] and [22], the pricing

scheme we have derived outputs a personalised price to each consumer.

2.7 Demand Response and Load Modelling

Even though is not widely used, the shift in demand response from electricity consumers given an input can be approximated to the response of a first-order system. The demand dynamics employed in this research employ such approximation as means to streamline the systems we propose. The first-order approximation for electricity demand was introduced in [44]; other examples of this for households and businesses can be found in [45] and [46]. The justification of this comes from the reasoning that the majority of the energy consumed by these kinds of buildings comes from heating/air conditioning systems, these types of devices possess the mentioned behaviour. The conventional way to model dynamic loads in electrical systems was first introduced in [47], in this paper it is mentioned that, depending on the type of load to simulate, a series of parameters must be selected to be substituted in a non-linear differential equation. The method for load modelling mentioned above is generally used in power systems literature, such as [15] and [48]. A comprehensive set of explanations about how to model static and dynamic loads, how to select the parameter values for each type of load (i.e. motors, incandescent lights), and how to linearise the equations in [47] is presented in [49] and references therein.

2.8 Stackelberg Game and Micro-Grids

New articles have been emerging that propose the use of the Stackelberg game for on-line pricing in micro-grids. The survey in [50] presents a summary of the potential of applying game-theoretic models to address significant and open problems in areas that relate to the smart-grid paradigm. Examples of the use of the Stackelberg equilibrium for demand management problems are found in [51–56], where [51] and [52] focus mainly on electric vehicle charge management and [53] demonstrates its feasibility numerically. The existence of equilibrium points using game-theoretic approaches including the Stackelberg one is demonstrated in [54] and [55]; in [56] the Stackelberg approach is used in conjunction with evolutionary algorithms for on-line pricing

schemes. In [57] algorithms that use the same kind of game are proposed, the inputs to their proposal include the economic factors and the power and voltage regulations. However, there is no analysis of the stability of the electrical system by introducing the pricing scheme. Another proposal where the game is used is found in [58], the paper demonstrates the existence of an equilibrium price for both leaders and followers in the system, however, the stability analysis together with the physical system integration is also not performed. From the above, although the use of the Stackelberg equilibrium in demand-side management for micro-grids is not an uncommon proposition, to the best of our knowledge, the majority of works that make use of it do not take into account the stability of the physical systems where such schemes are applied [51]- [58]. The main difference between our current study and the papers mentioned above is the implementation of the incentive strategy as means to formulate the price. We can also see that there exists an open challenge in bridging the market layer with the physical layer of the micro-grid system when employing a game-theoretic approach for dynamic pricing.

2.9 Resistive Network Model

In an effort to implement our derived pricing schemes on other types and scales of micro-grid systems, we employ the representation of their equivalent resistive networks. The resistive network model is a modification of the AC micro-grid model, the change comes from the fact that in low voltage configurations, the inductive element of the transmission lines between the elements of the micro-grid network is less dominant than the resistive part. This in consequence matches the model of the DC micro-grid while maintaining AC. An example of the elements of the transmission lines is illustrated in Fig. 2.3. The power representation for each unit in the micro-grid network is given by (1.2).

Such a model has an equivalence to the system's conductance matrix [59], its properties and its interpretation as a loopy Laplacian matrix are explained in [60]. The conductance matrix is frequently employed in the modelling of energy pricing schemes such as stochastic dynamic pricing [61], power balance-based optimization methods [62], day-ahead frequency-based electricity markets [63], among others. An analysis for the conditions for stability in droop controlled micro-grids connected in a network topology is

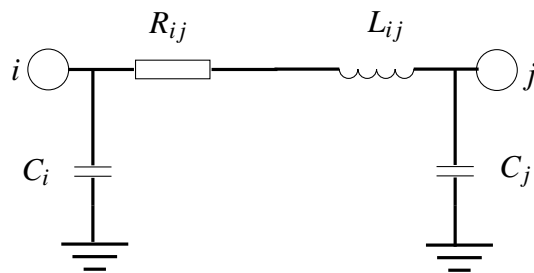


Figure 2.3: Equivalent model of a transmission line between nodes i and j in a micro-grid network.

carried out in [64], the results are useful for inductance dominant networks, the cases for resistive networks are addressed briefly by indicating the changes that should be made to adapt the model. The derivation of the resistive network equations is thoroughly explained in [65]; the book also provides a survey on the state of the art in micro-grid control, which are based on the distributed cooperative control of multi-agent systems, as well as primary techniques for both AC and DC control. In [66] a study about the relationship between the distance of a generator to a load and the power contribution to the latter is decreased when implementing Power/voltage droop controllers. The authors in [66] also demonstrate that the power modification that accompanies such controllers is beneficial as it leads to lower power losses. An examination of the behaviour of DC circuits is performed in [48], the paper makes use of the power equations we are using, such equations express the power in each node in a resistive network of interconnected power devices. The results in the paper deal with the interplay of the network topology and also the definition of a nominal voltage level for the circuit. A variation of the droop controller for resistive low-voltage networks is presented in [67], a procedure for the selection of the gains for the controller is explained and numerical results for a network system subject to disturbances are provided. The resistive network power dynamics have also an equivalence to a non-linear consensus algorithm as mentioned in [68]. Where a Lyapunov function analysis is performed and results on the convergence of the response to a consensus is demonstrated. A subsequent study of the non-linear consensus algorithm is presented in [69], in the paper, the convergence of the algorithm while it is adapted to power networks is analysed. An extended analysis of the same kind of non-linear consensus protocols was originally introduced with examples in [70] where the analysis for the general case and applications to unmanned aerial vehicles for such algorithms is presented. The resistive network model we use in the later parts of our

study is also widely considered when designing droop controllers [71]. Additionally, to the best of our knowledge, the present study marks the first time the conductance matrix is used as means to derive a coalitional game-based pricing scheme.

2.10 Droop Controller

As briefly touched in Chapter 1, to model the voltage dynamics of a micro-grid we utilise droop control. This type of controller is used in AC power generators, it consists of balancing the frequency of the elements of a micro-grid by regulating the power output. Droop controller modeling for micro-grid systems remains an open problem in engineering. Even though the main focus of our investigation is not the design of such controllers, we make use of the one proposed in [72]. Such paper shows results on voltage and frequency synchronization, it also demonstrates stability conditions to integrate distributed generators into power networks. Because of the nature of the resistive network dynamics, we employ the P-V droop control variation, which balances power and voltage similarly to the more common frequency-reactive power configuration. An example slope for the P-V droop is illustrated in Fig. 2.4, from it, the voltage expression for unit i in a micro-grid can be given as

$$V_i = V_{max} - k(P_i - P_{ref}), \quad (2.2)$$

where V_i is the unit voltage, P_i the unit power, V_{max} and P_{ref} are rated reference values for voltage and power respectively and k is a scalar gain based on a selected percentile deviation for the voltage. In the UK, in a micro-grid with low-voltage configuration V_{max} would be around 230V. This static expression (2.2) can be implemented in a dynamic form as in [64], where it is stated that if the measurement of the power is calculated through a low-pass filter, the latter is the one that brings it into such form.

Droop controllers have been implemented in resistive networks previously in [71], however the one proposed in the paper is of quadratic nature different to the simplified linear one we are using. In [71] a stability analysis is performed for a network of loads and generators subject to their proposed controller. As will be explained later, we employ the resistive network dynamics and subject it to droop control [72]; which in turn has been modified to have bounded outputs [73]. The latter is necessary since the node

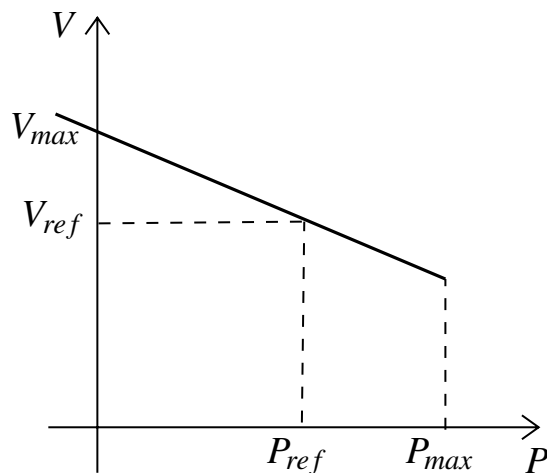


Figure 2.4: P-V droop control slope example.

voltages should remain within specified limits from the rated voltage. The expressions for the bounded droop controller used in this work are based on the bounded integral control theory from [74]. Bounded integral control maintains the well-established integral control concept with guaranteed bounds without any saturation units that complicate the analysis and that can lead to integrator windup.

2.11 Coalitional Games in Micro-Grids

In the last of our derived pricing schemes we propose the use of coalitional game theory as means to encourage competition and collaboration among players by leveraging the connectivity of cyber-physical systems. Coalitional games study the ways in which players can “ally” and cooperate in order to improve their welfare. The fundamentals about coalitional game theory are studied in detail in the tutorial [9], along with applications to communications. A review of the use of coalitional games with a justification for their use in power networks is carried out in [7], where the types of cooperation applicable to electrical systems are explained, including the ways in which these and the behavior of the agents involved can be modeled in a game-theoretic fashion.

The use and formulation of cooperative coalitional games in micro-grids was first introduced in [75], where the proposed algorithm focuses on reducing power losses and costs by forming coalitions of neighboring micro-grids. Similarly, in [76] the coalitions are formed between micro-grids in a macro station, where their profits are distributed using the Shapley value. A similar approach is used in [77], where a case study with

existing data is performed. A centralized algorithm where the micro-grids trade with the macro station is studied in [78], in this the payoff functions to maximize are dependent on the ordering of the joining micro-grids. A study of the case where greedy prosumers do not align with the micro-grid's decision is presented in [79], there, a balanced game is proposed without the need of calculating the imputation set. The problem formulated in [80] minimizes discomfort, which is modeled as a non-linear function of the power deficit in the micro-grid. The coalitions can be formed between macro stations, such as in [81], where it is numerically shown the ways in which the price is affected by them. A game where local micro-grids cooperate without the participation of a main grid is presented in [82], this is done by assuming a known non-flexible demand. In [83] the introduction of auction theory is used to define the pairing of micro-grids that buy and sell. The game proposed in [84] divides the players between consumers and the micro-grid itself, where the latter outputs its payoff function to the consumers; additionally, the calculations for an imputation set is omitted. The same author also proposes the use of evolutionary game theory in conjunction with coalitions [85], where the price is a quadratic function of the consumption. An interesting bidding system for cooperating prosumers is presented in [86], however constraints on power capacity and losses are ignored.

From the above, it can be seen that the use of coalitional games in the subject of micro-grids is a very recent topic, however, to the best of the authors' knowledge, the majority of the works do not take into account the dynamics of the physical systems where such schemes are applied, such as [75,77,79,81–86] among others. Additionally, with a few exceptions [82,84–86], the coalitional games proposed in the literature do not address the end consumers themselves as players, and none of them present a scheme in where there are multiple retailers to choose.

2.12 Conclusion

Having covered multiple works in different disciplines that, because of the technological resources available today, are increasingly interacting with each other, it is important to get some insight on the ways in which some of their concepts are compatible and what aspects are left to be explored.

Table 2.1: Most important literature by topic.

Topic	Key Literature
Network systems and graph theory	[5, 10, 11]
Micro-grid network modelling	[2–5, 11–13]
Linear and non-linear systems analysis	[13, 26, 27]
Consumer-supplier modelling	[3, 6, 30, 33]
Stackelberg game and incentive strategies	[36, 38, 41]
Stackelberg game in micro-grids	[51, 53, 58]
Resistive networks	[60, 65, 68, 71]
Droop control	[64, 71–73]
Coalitional games	[7, 9, 87, 88]
Coalitional games in micro-grids	[75–77]

Table 2.1 contains the key literature that serves as foundation for this research project, we have selected the most influential works and separated them by field.

One of the open challenges identified that motivate the present study lie mainly in the stability analysis of the micro-grid network model when heterogeneity is present between the agents; and the role of the heterogeneity in terms of the system’s response. Another significant aspect is joining the physical layer of the system to the market layer of the dynamic pricing paradigm, as seen above, the large majority of papers focused in deriving a pricing scheme for the micro-grid system do not take into account the physical system’s equations. An important focus of our study is the implications that arise from connecting those layers and the further studies that this implies, an stability analysis for example. Another significant aspect that differentiates our study from the previous ones is our implementation of the incentive strategy and the multiple retailer scheme in a coalitional game framework, both constitute novel approaches to the field of dynamic pricing schemes for micro-grid systems. We believe that the multiple retailer scenario fits the use of coalitional games and needs to be studied, since this approach matches the current needs of energy trading platforms, such as [89, 90] and recent end-user price comparison tools like [91].

Chapter 3

Stability of a Network of Micro-Grids under Uncertainties

3.1 Introduction

This chapter investigates the dynamics of a network of micro-grids, more specifically the effect of oscillations during the system transient response. A micro-grid is modeled using the swing dynamics and integrating parameters for damping and inertia. The interconnection between micro-grids is modeled via the coupled oscillator archetype and the resulting dynamics is described by a graph-Laplacian matrix. The transient analysis is extended to a number of cases to gain insight on the role of the parameters and the connectivity.

Different to our previous work in [23], here the interplay between the transmission dynamics and the micro-grid dynamics is investigated by obtaining the conditions for stability when the system is subject to uncertainties. This is also a continuation of the study in [4] about the effects of the parameters of homogeneous micro-grids on their transient stability. We now enhance the approach to networks with heterogeneous elements.

Although the presented model is a simplified representation for individual micro-grids, it has been proven to be useful as a tool for the study of smart-grid related subjects, such as demand-side management in [92] and real time pricing [3]. This chapter provides a more in-depth stability analysis and yields some other highlights that might not be entirely practical in nature but are interesting nonetheless.

The parameter heterogeneity that is involved in the present study can be useful in the design of modern power systems, since the impact of inertia is a present challenge [93,94], as more low-inertia systems such as renewables are being commonly integrated into current power networks [95].

This chapter is structured as follows. In Section 3.2 we state the problem and introduce the model. In Sections 3.3 and 3.4 we present our findings. In Section 3.6 we provide numerical examples. Finally in Section 3.7 we provide conclusions and comment on the ways in which this model can be subjected to pricing mechanisms.

3.1.1 Summary and Contributions

Firstly, the relation between the transient stability and consensus dynamics is explored under the assumption that the micro-grids are homogeneous, namely every micro-grid in the network has equal parameters. This study sheds light on the ways in which different damping coefficients influence the frequency and power flow consensus values.

Secondly, stability analysis for the heterogeneous case is performed by estimating the system's eigenvalues based on the Gershgorin disc theorem. The conditions that ensure absolute stability, namely the case in where the measurement of the system's states are subject to non-linearities and uncertainties, are also explored.

Thirdly, simulations are performed using different topologies; emphasizing the ways in which the connectivity of the network affects the time constant of the transient response. Additionally, the present work also involves the adaptation of the proposed model to real instances in the UK electrical network and the calibration of the nodes' parameters using data of the power capabilities of the micro-grids, simulation results also show the system's response when subject to parameter change over time.

3.2 Problem Statement and Model

This chapter mainly addresses the analysis of the transient dynamics of a network system comprised of interconnected micro-grids and the influence of the parameters and topology of the network on the stability. More specifically, the ways in which the heterogeneous parameters in the network influence the eigenvalues of the overall system. Furthermore, we investigate conditions that guarantee absolute stability, that is, the

maximum magnitude of uncertain non-linear parameters that the system can withstand when subject to such uncertainties.

Our approach allows to link the transient response to the connectivity of the equivalent network graph, approximate the position of the eigenvalues and the bounds of the values these can take depending on the different micro-grid parameters, derive conditions for stability, and determine the maximum amplitude of uncertainties in terms of the parameters of each micro-grid.

The dynamic model of a single micro-grid i in a network describes the power flow P_i , which follows the first-order differential equation:

$$\dot{P}_i = \sum_{j \in \mathcal{N}_i} \frac{T_{ij}}{\sigma_i} (f_j - f_i) - \frac{\mu_i}{\sigma_i} P_i, \quad (3.1)$$

where f_i and f_j are the frequencies of micro-grids i and j respectively, T_{ij} is the synchronizing coefficient which represents the maximum power transfer between micro-grids i and j [5] in MVA, where $T_{ij} = |V_i||V_j||Y_{ij}|$ and Y_{ij} is the inverse of the impedance Z_{ij} of the transmission line $\{i, j\}$, Fig. 3.1 shows the equivalent circuit representation for the interconnection of two micro-grids [17], σ_i and μ_i are the transmission inertia and damping coefficients respectively. If micro-grid i is connected to multiple other micro-grids, then the first term is a sum of the adjacent micro-grids \mathcal{N}_i to micro-grid i as will be explained later. The second term helps describe the characteristic response of the power transmission. From (3.1) it can be seen that the power flow depends on the frequency error $f_j - f_i$. A physical interpretation of this is that if $f_i < f_j$ then the power flows from micro-grid j to micro-grid i ; in contrast if $f_i > f_j$ then the power flows from micro-grid i to micro-grid j . The model of micro-grid i also involves the dynamics of frequency f_i represented by the swing equation [3, 92]:

$$\dot{f}_i = -\frac{D_i}{M_i} f_i + \frac{1}{M_i} P_i, \quad (3.2)$$

where D_i and M_i denote the micro-grid swing damping and inertia coefficients respectively. In electrical systems, the damping D_i is obtained as a result of changing loads and control loops [21] and is measured in MJ/rad. M_i is the moment of inertia caused by the rotors of the electric generators in the micro-grid [2, p.438] and is measured in MJ-s/rad. Note that due to the simplification of the micro-grid model, its parameters

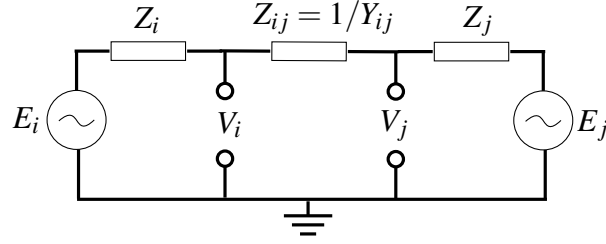


Figure 3.1: Equivalent circuit representing the connection between micro-grids i and j , with shunt conductances $Y_i = 1/Z_i$.

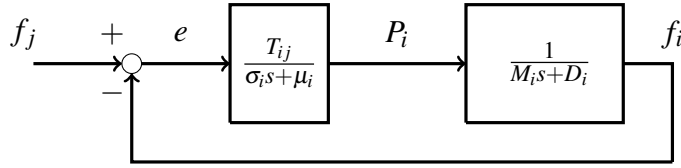


Figure 3.2: System block representation of micro-grid i .

are estimated [2] and contain part of the nonlinear properties [16]. Figure 3.2 shows the system block representation of the system (3.1)-(3.2).

The state space representation of the system is obtained by introducing the state variables $P_i = x_1^{(i)}$, $f_i = x_2^{(i)}$ and taking $f_j = x_2^{(j)}$ as an external input. Model (3.1)-(3.2) is rewritten as:

$$\begin{bmatrix} \dot{x}_1^{(i)} \\ \dot{x}_2^{(i)} \end{bmatrix} = \begin{bmatrix} -\frac{\mu_i}{\sigma_i} & -\frac{T_{ij}}{\sigma_i} \\ \frac{1}{M_i} & -\frac{D_i}{M_i} \end{bmatrix} \begin{bmatrix} x_1^{(i)} \\ x_2^{(i)} \end{bmatrix} + \begin{bmatrix} \frac{T_{ij}}{\sigma_i} \\ 0 \end{bmatrix} x_2^{(j)}. \quad (3.3)$$

A system of interconnected micro-grids can be modelled by a graph like the one shown in Fig. 3.3. Each node represents a micro-grid and each edge the power line that connects two of them; the connectivity of a micro-grid is captured by the degree d_i of the corresponding node, which is equal to its number of connections. In the unweighted and undirected case, d_i is equal to the number of edges that are incident to node i . By extending (3.3) to the case of a system of n micro-grids we obtain the state-space model (3.5). The block matrix that contains the synchronization parameters T_{ij} is linked to the graph-Laplacian matrix, given by

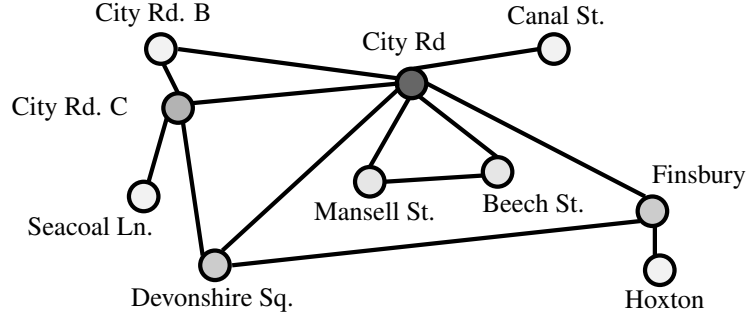


Figure 3.3: Graph topology analogous to the micro-grid network in [1].

$$L := \begin{bmatrix} T_{11} & -T_{12} & \cdots & -T_{1n} \\ -T_{21} & T_{22} & \cdots & -T_{2n} \\ \vdots & \vdots & \ddots & \vdots \\ -T_{n1} & -T_{n2} & \cdots & T_{nn} \end{bmatrix}, \quad (3.4)$$

where the diagonal entries correspond to the sum of the weights of the outgoing edges, while the off-diagonal entries are the weights of the adjacency matrix A of the network. Let us recall that the Laplacian of a graph is expressed as $L = D_{out} - A$, where D_{out} is a diagonal matrix whose elements are the out-degree of the nodes. The Laplacian matrix is then used to represent the system dynamics in matrix form as follows

$$\begin{bmatrix} \dot{x}_1^{(1)} \\ \vdots \\ \dot{x}_1^{(n)} \\ \dot{x}_2^{(1)} \\ \vdots \\ \dot{x}_2^{(n)} \end{bmatrix} = \begin{bmatrix} -\frac{\mu_1}{\sigma_1} & \cdots & 0 & -\frac{T_{11}}{\sigma_1} & \cdots & \frac{T_{1n}}{\sigma_1} \\ 0 & \ddots & 0 & & \ddots & \\ 0 & \cdots & -\frac{\mu_n}{\sigma_n} & \frac{T_{n1}}{\sigma_n} & \cdots & -\frac{T_{nn}}{\sigma_n} \\ \frac{1}{M_1} & \cdots & 0 & -\frac{D_1}{M_1} & \cdots & 0 \\ 0 & \ddots & 0 & 0 & \ddots & 0 \\ 0 & \cdots & \frac{1}{M_n} & 0 & \cdots & -\frac{D_n}{M_n} \end{bmatrix} \begin{bmatrix} x_1^{(1)} \\ \vdots \\ x_1^{(n)} \\ x_2^{(1)} \\ \vdots \\ x_2^{(n)} \end{bmatrix}. \quad (3.5)$$

Let $X_j = [x_j^{(i)}]_{i=1,\dots,n}$ then

$$\begin{bmatrix} \dot{X}_1 \\ \dot{X}_2 \end{bmatrix} = \overbrace{\begin{bmatrix} -diag(\frac{\mu_i}{\sigma_i}) & -diag(\frac{1}{\sigma_i})L \\ diag(\frac{1}{M_i}) & -diag(\frac{D_i}{M_i}) \end{bmatrix}}^A \begin{bmatrix} X_1 \\ X_2 \end{bmatrix}, \quad (3.6)$$

where $diag(D_i/M_i)$ and $diag(\mu_i/\sigma_i)$ denote diagonal matrices with main diagonal entries equal to the damping to inertia ratio and $diag(1/M_i)$ and $diag(1/\sigma_i)$ are diagonal

matrices with main diagonal entries equal to the inverse of the inertial constants M_i and σ_i of each micro-grid i . The state variables X_1 and X_2 are the vectors of power flows P_i and frequencies f_i of each micro-grid i for $i = 1, \dots, n$. Based on the micro-grid network model introduced above, we now leverage the two following derivations to help study its stability.

3.3 Preliminary Derivations

In this section, we review a couple of preliminary results on the determinant of the micro-grid network system and the Gershgorin disc theorem which will be used in the following sections to show the ways in which the eigenvalues are obtained and subsequently the conditions for the system's stability.

3.3.1 Transient Dynamics of the Micro-Grid Network System

The first preliminary derivation is about the transient dynamics of system (3.6). For this purpose, we need to obtain the eigenvalues of matrix \mathbf{A} . For an unweighted, undirected network of heterogeneous micro-grids with inertial coefficients M_i , σ_i and damping coefficients D_i , μ_i , to find the eigenvalues of system (3.6), the roots of $\det(\lambda I - \mathbf{A})$ must be obtained. Taking \mathbf{A} as a square block matrix, its determinant is obtained as

$$\begin{aligned} \det(\lambda I - \mathbf{A}) &= \det \left(\begin{bmatrix} \lambda I + \text{diag}(\frac{\mu_i}{\sigma_i}) & \text{diag}(\frac{1}{\sigma_i})L \\ -\text{diag}(\frac{1}{M_i}) & \lambda I + \text{diag}(\frac{D_i}{M_i}) \end{bmatrix} \right) \\ &= \det \left(\lambda^2 I + \lambda \left(\text{diag}(\frac{D_i}{M_i} + \frac{\mu_i}{\sigma_i}) \right) + \text{diag}(\frac{\mu_i D_i}{\sigma_i M_i}) + \text{diag}(\frac{1}{\sigma_i M_i})L \right). \end{aligned} \quad (3.7)$$

By denoting $\Psi := \text{diag}(\frac{D_i}{M_i})$, $\Phi := \text{diag}(\frac{1}{M_i})$, $\Gamma := \text{diag}(\frac{1}{\sigma_i})$ and $\kappa := \text{diag}(\frac{\mu_i}{\sigma_i})$, the determinant (3.7) is rewritten as

$$\det(\lambda I - \mathbf{A}) = \det(\lambda^2 I + \lambda(\Psi + \kappa) + \kappa\Psi + \Gamma\Phi L). \quad (3.8)$$

System (3.6) is stable if all its eigenvalues λ_i lie in the left-hand-side of the complex plane. The following theorem illustrates the ways in which an estimation of the eigenvalues of matrix \mathbf{A} can be obtained.

3.3.2 Gershgorin Disc Theorem

This theorem is a well known concept used to encircle the possible values of the eigenvalues of a square matrix in the complex plane. Let A_{nn} be a $n \times n$ matrix and let a_{ij} be its ij th entry. For each $i \in 1, \dots, n$ let the radius $R_i = \sum_{j \neq i} |a_{ij}|$ be the sum of the absolute values of the non-diagonal elements in the i th row. Let $\Delta(a_{ii}, R_i)$ be the closed disc centered at a_{ii} with radius R_i . Such disc is called a *Gershgorin disc*.

Theorem 1. *Every eigenvalue λ_i of A_{nn} lies within at least one of the Gershgorin discs $\Delta(a_{ii}, R_i)$.*

Proof. We refer the reader to the original paper by [26] for full details of the proof.

3.4 Stability and Response Analysis

In this section, we present results related to the transient of the system. First, an estimation of the eigenvalues of system (3.6) is provided using the Gershgorin disc theorem. Furthermore, a discussion of the ways in which the eigenvalue that is closest to the origin affects the system's response is presented. Secondly, the eigenvalues are obtained for the case when the damping to inertia ratios are normalised to one and the inertia is either equal to one or has different values for each micro-grid. Thirdly, a procedure to identify regions containing the eigenvalues of the system is shown.

3.4.1 Eigenvalue Location and Response Bounding

In the following, we focus on obtaining an estimation for the eigenvalues of \mathbf{A} taking mainly into account the different damping to inertia ratios of the micro-grids. For the analysis utilizing the Gershgorin disc theorem, two sets of discs are obtained. For the first one, we take $D_i > 0$ and $M_i > 0$ for $i = 1, 2, \dots, m$. Then we obtain a disc $\Delta_i^{(1)}$ in the first set which encloses the position of an eigenvalue λ_i in the complex plane. Let $R^{(1)} = 1/M_i$, then the disc $\Delta_i^{(1)}$ is given by

$$\Delta_i^{(1)}\left(-\frac{D_i}{M_i}, \frac{1}{M_i}\right) = \left\{ \xi : \xi \in \mathbb{C} \mid \left| \xi + \frac{D_i}{M_i} \right| \leq R^{(1)} \right\}. \quad (3.9)$$

Every disc $\Delta_i^{(1)}$ has a radius equal to $R = 1/M_i$ and is centered in $-D_i/M_i$ on the real axis of the complex plane. For the second set of discs denoted by $\Delta_i^{(2)}$, let us set $\mu_i > 0$ for $i = m + 1, m + 2, \dots, n$. Let $R^{(2)} = \sum_{j \in \mathcal{N}_i} |l_{ij}|/\sigma_i$, then we obtain a disc $\Delta_i^{(2)}$ in the second set given by

$$\Delta_i^{(2)}\left(-\frac{\mu_i}{\sigma_i}, \sum_{j \in \mathcal{N}_i} \frac{1}{\sigma_i} |l_{ij}|\right) = \left\{ \xi : \xi \in \mathbb{C} \mid \left| \xi + \frac{\mu_i}{\sigma_i} \right| \leq R^{(2)} \right\}. \quad (3.10)$$

Every disc $\Delta_i^{(2)}$ has a radius equal to $R = \sum_{j \in \mathcal{N}_i} |l_{ij}|/\sigma_i$ and is centered in $-\mu_i/\sigma_i$ on the real axis of the complex plane. Here we denote by $|l_{ij}| = |T_{ij}|$ the absolute value of the ij th element of the Laplacian L . Let us recall that the spectrum of \mathbf{A} is the set of eigenvalues $\{\lambda_1, \lambda_2, \dots, \lambda_n\}$.

Lemma 1. *For the spectrum of matrix \mathbf{A} we have*

$$\text{spec}(\mathbf{A}) \in \bigcup_{i=1}^m \Delta_i^{(1)}\left(-\frac{D_i}{M_i}, \frac{1}{M_i}\right) \cup \bigcup_{i=m}^n \Delta_i^{(2)}\left(-\frac{\mu_i}{\sigma_i}, \sum_{j \in \mathcal{N}_i} \frac{1}{\sigma_i} |l_{ij}|\right). \quad (3.11)$$

Proof. Recalling the Gershgorin disc theorem, all eigenvalues of the system are contained within the union of all areas of the discs. The centre of each disc is situated on each of the diagonal elements of \mathbf{A} in (3.6), the radius of each disc is equal to the sum of the rest of the elements in the matching row. \square

In the following, we present some results in the case where the transmission dynamics is much faster than the swing dynamics. This is an assumption that is commonly found in the literature since it yields the standard swing equation [3, 4, 23] because of the difference in the parameter's magnitude.

Assumption 1. *The transmission damping coefficient μ_i is much larger than the swing damping coefficient D_i , $\mu_i \gg D_i$.*

If Assumption 1 holds, let us then assume without loss of generality that the nodes are ordered decreasingly in the damping to inertia ratio as follows:

$$-\frac{\mu_n}{\sigma_n} < -\frac{\mu_{n-1}}{\sigma_{n-1}} < \dots < -\frac{\mu_{m+2}}{\sigma_{m+2}} < -\frac{\mu_{m+1}}{\sigma_{m+1}} \ll -\frac{D_m}{M_m} < -\frac{D_{m-1}}{M_{m-1}} < \dots < -\frac{D_2}{M_2} < -\frac{D_1}{M_1}. \quad (3.12)$$

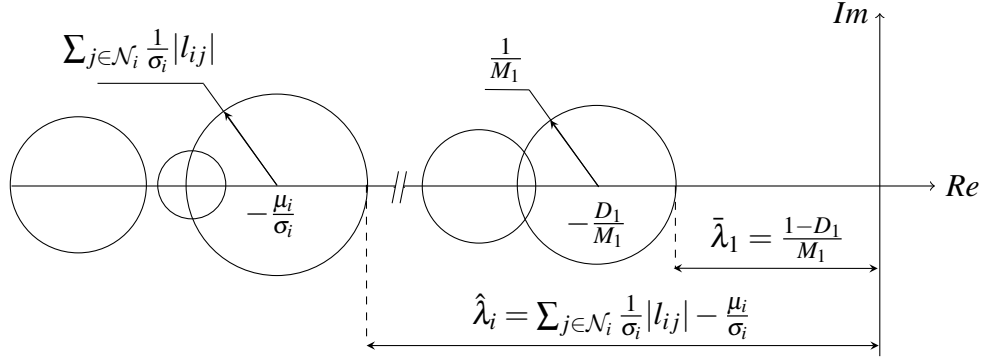


Figure 3.4: Gershgorin disc configuration example.

In other words, the ratio $-D_1/M_1$ corresponds to the micro-grid with the smallest damping to inertia ratio and is the centre to the disc that encircles the smallest eigenvalue λ_1 .

Before presenting the next result, let us define the closest point of each disc to the origin as the upper bound of $\Delta_i^{(1)}$ and $\Delta_i^{(2)}$ respectively as

$$\bar{\lambda}_i := \frac{1-D_i}{M_i}, \quad \hat{\lambda}_i = \sum_{j \in \mathcal{N}_i} \frac{1}{\sigma_i} |l_{ij}| - \frac{\mu_i}{\sigma_i}. \quad (3.13)$$

Figure 3.4 shows a possible configuration of the discs and their upper bounds in the complex plane.

Theorem 2. *System (3.6) is asymptotically stable if for the upper bound of its smallest eigenvalues it holds*

$$\underline{\lambda}_1 := \max_i \{\bar{\lambda}_i, \hat{\lambda}_i\} < 0. \quad (3.14)$$

Furthermore, the rate of convergence satisfies

$$|x(t) - x_{eq}| \leq \Upsilon_{2n} e^{\underline{\lambda}_1 t}, \quad (3.15)$$

where x_{eq} is a generic equilibrium point and Υ_{2n} is an opportune $1 \times 2n$ vector.

Proof. Let any point $\bar{p}_i \in \Delta_i^{(1)}$ and similarly, let $\hat{p}_i \in \Delta_i^{(2)}$ be given, it holds that $\Re[\bar{p}_i] < \bar{\lambda}_i$; $\Re[\hat{p}_i] < \hat{\lambda}_i$. It follows that if condition (3.14) holds true, then $\Re[\bar{p}_i], \Re[\hat{p}_i] < 0$, and therefore, the real part of the eigenvalues is negative.

To proof the result about the rate of convergence, let us assume that \mathbf{A} is diagonalizable. By obtaining all eigenvalues $\{\lambda_1, \dots, \lambda_n\}$ of \mathbf{A} , an eigenvector matrix \mathbf{V} can be computed, as well as its inverse $\mathbf{W} = \mathbf{V}^{-1}$. The modal transformation of \mathbf{A} is obtained

from

$$\mathbf{W}\mathbf{A}\mathbf{V} = \text{diag}(\{\lambda_1, \dots, \lambda_n\}) = \Lambda, \quad (3.16)$$

which results in a diagonal matrix Λ where each of its elements contain an eigenvalue of \mathbf{A} . The response of the system for a given initial state $x(0)$ and zero input is now expressed as

$$x(t) = \mathbf{V}e^{\Lambda t}\mathbf{W}x(0), \quad (3.17)$$

the rate of decay of the smallest eigenvalue λ_1 is dominant for the system's response. Since $\underline{\lambda}_1$ upper bounds the smallest eigenvalue λ_1 , every state of (3.17) is exponentially bounded by $\underline{\lambda}_1$. Namely the system converges to an equilibrium x_{eq} as in (3.15). \square

Remark 1. *In the proof above, although we employ the modal transformation to show the rate of convergence, there can be certain network topologies and micro-grid parameters that can make the system matrix \mathbf{A} non-diagonalizable (i.e. not all of its eigenvalues are unique). However, the rate of decay of the response is still bounded by the smallest eigenvalue, this is true for especial cases of Laplacian-based systems [5, 12, 87].*

From the discs representation in Fig. 3.4 we can see that the radius of each disc $\Delta_i^{(2)}$ depends proportionally on the topology by means of $|l_{ij}|$ of the Laplacian. Therefore, the eigenvalues are tied to the network's connectivity.

From Fig. 3.4 it can also be seen that the imaginary part of the eigenvalues is bounded by the radii of the discs. Namely, the maximal amplitude of the frequency of the oscillations is bounded by the radius. Moreover, without altering the topology, if the inertia coefficients σ_i and M_i increase, the discs are shifted to the left with a reduced radius. Conversely, if decreased, the discs shift to the right and the radii expand, leading to larger and faster oscillations in the transient.

3.4.2 Effect of Inertia on Eigenvalues

In this section, two cases are analyzed. In the first one, the eigenvalues of the system are obtained for the ideal case when all of its parameters are normalised to one. In the second, all inertia coefficients are considered different in order to emphasise the ways

in which such parameters affect the transient. A result for each case is shown below. Let us now state the first assumption.

Assumption 2. *All damping and inertia coefficients in (3.6) are unitary, namely $\mu_i = D_i = 1$, and $\sigma_i = M_i = 1$ for all i , so that $\kappa = \Gamma = \Phi = \Psi = I \in \mathbb{R}^n$.*

This is a strong assumption, however, it is useful for the purpose of isolating the effect of the topology in the network's eigenvalues and subsequently illustrate the rate of convergence towards the consensus value. Such will be relaxed by Assumption 3. Let us denote d_{max} as the maximum degree of all the nodes in the network, namely $d_{max} := \max_i \{d_i\}$ which identifies the node with most connections and its quantity.

Theorem 3. *Let Assumption 2 hold true. Then system (3.6) is stable. Furthermore, the maximal frequency of the oscillations is bounded by*

$$\sqrt{2d_{max}}. \quad (3.18)$$

Proof. From Assumption 2, the determinant (3.8) is rewritten as:

$$\det((\lambda^2 + 2\lambda)I + L + I) = \prod_i^n ((\lambda^2 + 2\lambda)I + \eta_i), \quad (3.19)$$

where η_i denotes the i th eigenvalue of $-(L + I)$. Taking (3.19) equal to zero, the eigenvalues of \mathbf{A} , which we denote by λ_i are then obtained as

$$\lambda_i^+ = \frac{-2 + \sqrt{4 + 4\eta_i}}{2}, \quad \lambda_i^- = \frac{-2 - \sqrt{4 + 4\eta_i}}{2}, \quad \text{for } i = 1, \dots, n. \quad (3.20)$$

From (3.20) and from the fact that by definition $\eta_i \leq -1 \forall i \in \{1, \dots, n\}$, it can be deduced that $\Re(\lambda_i)$ is negative for all eigenvalues, hence the network system is stable.

As discussed in [5], the smallest eigenvalue of $-L$ is lower bounded by $-2d_{max}$. By extension, the lowest bound for the smallest η_i is equal to $-2d_{max} - 1$. From this, we can infer bounds on the argument of the square root of (3.20) which is the imaginary part of the eigenvalues. This in turn establishes that the maximal oscillation frequency of the system's response depends directly on the topology, substituting said bound in (3.20) we get $\sqrt{2d_{max}}$. \square

For the second case, since matrices Φ and Γ are diagonal, $\Gamma\Phi L$ is equal to the

Laplacian L scaled by $1/\sigma_i M_i$ on each row :

$$\Gamma\Phi L = \begin{bmatrix} \frac{l_{11}}{\sigma_1 M_1} & \cdots & \frac{l_{1n}}{\sigma_1 M_1} \\ & \ddots & \\ \frac{l_{n1}}{\sigma_n M_n} & \cdots & \frac{l_{nn}}{\sigma_n M_n} \end{bmatrix} = \begin{bmatrix} \frac{1}{\sigma_1 M_1} l_1 \\ \vdots \\ \frac{1}{\sigma_n M_n} l_n \end{bmatrix}, \quad (3.21)$$

where l_i is the i th row of L . Note that by definition, the eigenvalues of a Laplacian L are non-negative with its smallest eigenvalue equal to zero. Such eigenvalues are non-positive for $-L$. Scaling L by any positive scalar, will not affect the sign of the eigenvalues but these will be compressed or expanded depending on the scalar.

The next result shows that stability is guaranteed under weaker conditions than the ones in Theorem 3 and serves to highlight the effect of the inertia coefficients on the eigenvalues. This can be justified in the sense that, as emphasised by [93, 94] and references therein, a current problem in power systems is the tendency towards adopting generation devices that do not have inherent inertia, resulting on low-inertia micro-grids. Studying the effect of different inertia parameters in the network is pivotal in the stability of the overall system.

Assumption 3. All damping to inertia ratios in (3.6) are unitary, namely $\mu_i/\sigma_i = D_i/M_i = 1$ for all i , so that $\Psi = \kappa = I \in \mathbb{R}^n$.

Let us define σ_{max} and M_{max} as the largest inertia coefficients in the system, namely $\sigma_{max} := \max_i \{\sigma_i\}$, $M_{max} := \max_i \{M_i\}$.

Theorem 4. Let Assumption 3 hold true. Then system (3.6) is stable. Furthermore, the maximum frequency of the oscillations is upper bounded by

$$\sqrt{2M_{max} \frac{d_{max}}{\sigma_{max}}}. \quad (3.22)$$

Proof. With Assumption 3 in mind, the same expression (3.20) can be obtained from the determinant (3.8), substituting η_i with $\hat{\mu}_i$ which is the i th eigenvalue of $-(\Gamma\Phi L + I)$.

The scaling of the Laplacian shifts the discs closer to the origin. Furthermore, introducing the eigenvalues of $-I$ we obtain that all $\hat{\mu}_i < -1$ and therefore all eigenvalues are negative. The bound of the imaginary part of the eigenvalues is obtained by substituting the lowest bound for the smallest $\hat{\mu}_i$ in (3.20) which in this case is $-2d_{max}/\sigma_{max}M_{max} - 1$. \square

3.4.3 Clusterization

In this subsection, we introduce a tool that allows to differentiate and segment the area(s) in the complex plane where the eigenvalues can be located. The union of the area of a number of overlapping discs derived from system (3.6) can be referred to as a *cluster*.

Theorem 5. *The number of clusters is obtained from*

$$\sum_i \mathbb{I} \left[\bigcup_{j=1}^i \Delta_j \cap \bigcup_{j=i+1}^n \Delta_j = \emptyset \right], \quad (3.23)$$

where $\mathbb{I}[\cdot]$ denotes the indicator function, and Δ_j is any disc in the complex plane.

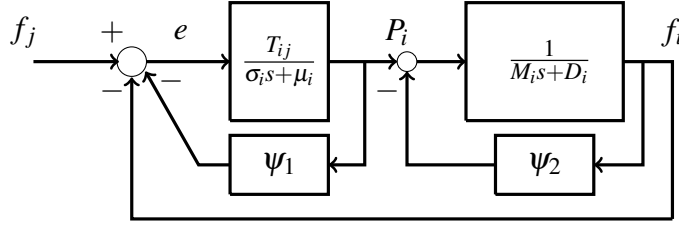
Proof. Depending on the values of D_i and M_i and ordering the discs as in (3.12), there can be an instance where the equality

$$-\frac{1+D_i}{M_i} < \frac{1-D_{i+1}}{M_{i+1}}, \text{ for any } i \in \{1, \dots, m\}, \quad (3.24)$$

is yielded, where the left-hand-side describes the maximum distance of a point in $\Delta_i^{(1)}$ from the origin, and the right-hand-side is the minimum distance of any point in $\Delta_{i+1}^{(1)}$ from the origin, (3.24) means that there is at least a partial overlap between both discs. A similar inequality can be derived for all $\Delta_i^{(2)}$. For the case where two or more discs overlap, suppose there exists a specific value for i denoted by \tilde{i} such that satisfies

$$\bigcup_{j=1}^{\tilde{i}} \Delta_j \cap \bigcup_{j=\tilde{i}+1}^n \Delta_j = \emptyset, \quad (3.25)$$

which is the argument of (3.23). The above condition means that the union of the first \tilde{i} discs $\{\Delta_1, \dots, \Delta_{\tilde{i}}\}$ is disjoint from the union of the last $n - \tilde{i}$ discs $\{\Delta_{\tilde{i}+1}, \dots, \Delta_n\}$. Using the indicator function on (3.25) signals the separation of two clusters, the sum of the times $\mathbb{I}[\cdot]$ yields a positive result equals to the number of clusters in which the eigenvalues are located. \square

Figure 3.5: Micro-grid i subject to disturbances.

3.5 Stability Under Uncertainties

In the following, we extend the analysis to the case where both frequency and power values in each micro-grid are subject to uncertainties ψ_i . Following the proposed method found in [27], we isolate the uncertainty in the feedback loop as illustrated by Fig 3.5 where $\psi_i(\cdot)$ denotes a sector non-linearity. An interpretation of the non-linearity in the feedback loop can be for instance that the power and frequency measurements are subject to disturbances.

For the mentioned case, system (3.3) can then be rewritten as

$$\begin{bmatrix} \dot{x}_1^{(i)} \\ \dot{x}_2^{(i)} \end{bmatrix} = \underbrace{\begin{bmatrix} -\frac{\mu_i}{\sigma_i} & -\frac{T_{ij}}{\sigma_i} \\ \frac{1}{M_i} & -\frac{D_i}{M_i} \end{bmatrix}}_A \begin{bmatrix} x_1^{(i)} \\ x_2^{(i)} \end{bmatrix} + \underbrace{\begin{bmatrix} 1 & 0 \\ 0 & 1 \end{bmatrix}}_B \begin{bmatrix} \psi_1(x_1^{(i)}) \\ \psi_2(x_2^{(i)}) \end{bmatrix} + \underbrace{\begin{bmatrix} \frac{T_{ij}}{\sigma_i} \\ 0 \end{bmatrix}}_U x_2^{(j)}, \quad (3.26)$$

where the non-linearities ψ_i belong to the sector $[K_{min}, K_{max}]$. This implies that the following inequality holds

$$[\psi(x) - K_{min}x]^T [\psi(x) - K_{max}x] \leq 0, \quad (3.27)$$

where $K_{min} = -\gamma_2 I$ and $K_{max} = \gamma_2 I$, γ_2 is a sufficiently small gain that determines the size of the non-linearity sector, and

$$\gamma_1 = \sup_{\omega \in \mathbb{R}} \zeta_{max}[G(j\omega)], \quad (3.28)$$

where $\zeta_{max}[\cdot]$ denotes the maximum singular value of the system's transfer function $G(j\omega)$ and γ_1 its upper bound; both γ_1 and γ_2 serve as means to determine the size of the non-linearity that the system tolerates before becoming unstable. Conceptually, it is assumed that ψ_i satisfies a *sector condition*, namely that ψ_i is at equilibrium at the origin

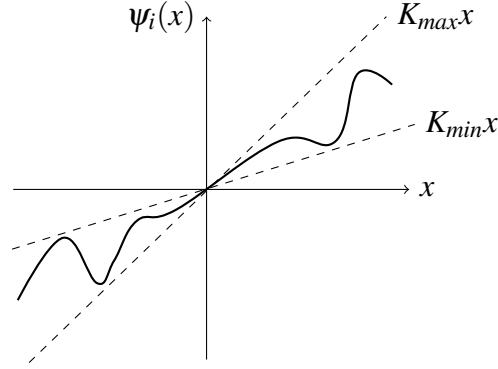


Figure 3.6: Sector definition example (dashed) for non-linearity ψ_i .

and is locally Lipschitz in the system output's domain. Figure 3.6 shows an example of the sector non-linearity and its bounds. The utility of this method is to determine if the origin is asymptotically stable for all non-linearities in the sector, yielding *absolute stability* to the system, this is also referred to as Lure's problem [27]. Although the existence and uniqueness of a solution to the system can potentially be verified through the Lipschitz condition; the presence of uncertainties complicate the analysis, calling for a substantially different approach as touched in [96] and references therein. An advantage of the sector non-linearity method is that to determine stability, as mentioned above, given a positive real system only ψ_i has to be checked to be Lipschitz.

3.5.1 Amplitude of Uncertainty

Let us first point up the system's transfer function $G(s)$ derived from (3.26) as

$$G(s) = \frac{1}{s^2 + \left(\frac{\mu_i}{\sigma_i} + \frac{D_i}{M_i}\right)s + \frac{T_{ij} + D_i \mu_i}{\sigma_i M_i}} \begin{bmatrix} \frac{D_i}{M_i} + s & -\frac{T_{ij}}{\sigma_i} \\ \frac{1}{M_i} & \frac{\mu_i}{\sigma_i} + s \end{bmatrix}. \quad (3.29)$$

In the case where the transmission and swing dynamics have similar parameters, we can obtain a sufficient condition for the maximum size of the non-linearity sector for which absolute stability holds. Such value is equal to the square root of the maximum eigenvalue of the transfer function matrix $G(j\omega)$ multiplied by its conjugate transpose, that is

$$\zeta_{max} = \sqrt{\lambda_{max}[G^T(-j\omega)G(j\omega)]}. \quad (3.30)$$

With the purpose of obtaining such value and for the rest of the analysis, the external input $x_2^{(i)}$ in (3.26) is assumed to be equal to zero. While obtaining an expression of γ_1 , for illustrative purposes, the following assumption can be made:

Assumption 4. *Both swing and transmission damping to inertia ratios, have similar values, such that $D_i/M_i \approx \mu_i/\sigma_i$. Also, we assume $D_i > M_i$, namely, the dynamics are over-damped, as discussed in [13].*

Theorem 6. *Let Assumption 4 hold. Then the maximum amplitude for the non-linearity sector in (3.26) is*

$$\gamma_2 < \frac{1}{\sqrt{M_i^2(D_i^2 + 1)}}. \quad (3.31)$$

Proof. Due to the complexity of the expression for ζ_{max} and for the sake of simplicity, taking δ for shorthand of the polynomial in (3.29), $G(j\omega)$ can be denoted as

$$G(j\omega) = \frac{1}{\delta(j\omega)} \begin{bmatrix} G_{11}(j\omega) & G_{12}(j\omega) \\ G_{21}(j\omega) & G_{22}(j\omega) \end{bmatrix}, \quad (3.32)$$

$G^T(-j\omega)$ can be defined similarly. ζ_{max} comes from the largest eigenvalue of G^*G , where \cdot^* is the conjugate transpose, we can obtain it using the determinant Δ and trace T . Expressions for both are simplified by accounting the following: $G_{12}(j\omega)$ and $G_{21}(j\omega)$ have no imaginary part, taking Assumption 4 as true, it holds that $|G_{11}| = |G_{22}|$. We can also assume the network to be unweighted: $T_{ij} = 1$, yielding $G_{12} = -G_{21}$; $|G_{12}| = |G_{21}|$. Taking $f = |G_{11}|$ and $g = |G_{12}|$ and using $\bar{\cdot}$ to denote the conjugate we obtain

$$T = \frac{2}{\delta\bar{\delta}}(g^2 + f^2), \quad \Delta = \frac{1}{(\delta\bar{\delta})^2}(g^2 + f^2)^2. \quad (3.33)$$

The eigenvalues of G^*G are then obtained from (3.33) as follows

$$\lambda = \frac{2(g^2 + f^2) \pm \sqrt{\frac{4}{(\delta\bar{\delta})^2}(g^2 + f^2)^2 - \frac{4}{(\delta\bar{\delta})^2}(g^2 + f^2)^2}}{2\delta\bar{\delta}} = \frac{g^2 + f^2}{\delta\bar{\delta}}.$$

Then, ζ_{max} is obtained taking the square root as in (3.30)

$$\zeta_{max} = \sqrt{(g^2 + f^2)/\delta\bar{\delta}}. \quad (3.34)$$

Substituting all values and expressions in (3.34), we get

$$\zeta_{max} = \sqrt{\frac{D_i^2}{M_i^2} + \omega^2 + \frac{1}{M_i^2} \left/ \frac{(1 + D_i^2)^2}{M_i^4} + \frac{2(D_i^2 - 1)\omega^2}{M_i^2} + \omega^4 \right.}. \quad (3.35)$$

Substituting (3.35) in (3.28) we get $\gamma_1 = \sup_{\omega \in \mathbb{R}} \zeta_{max}$, which refers to the largest value that (3.35) can get to as ω varies. If Assumption 4 holds, (3.35) is a monotonically decreasing function, with a least upper bound at $\omega = 0$, obtaining $\gamma_1 = \sqrt{M_i^2 / (D_i^2 + 1)}$. Since we know from the small gain theorem [27, p.411] that $\gamma_1 \gamma_2 < 1$, it can be inferred that inequality (3.31) holds. \square

The above gives us a clearer definition of the size of the non-linearity sector as a function of the parameters.

3.5.2 Lyapunov Approach

In the general case where there is no simple analytical expression for the maximum singular value, a numerical Lyapunov stability approach can be carried out. Some other alternatives to corroborate stability include the application of a loop transformation of the system into feedback-connected passive dynamical systems and the utilization of either the Popov or the circle criterion when applicable [4, 27].

Let us propose a candidate Lyapunov function for system (3.26) denoted by V , where $V = x^T P x$.

Theorem 7. *Given a small ε , γ_2 and a symmetric positive definite matrix P that satisfies the Riccati equation:*

$$PA + A^T P + \varepsilon C^T C + \frac{1}{\gamma_2^2} P B B^T P \leq 0, \quad (3.36)$$

then (3.26) is absolutely stable and V is a Lyapunov function.

Proof. The derivative of V along the trajectories of system (3.26) is

$$\dot{V} = x^T (PA + A^T P)x - 2x^T P B \psi. \quad (3.37)$$

\dot{V} is strictly negative if the given \dot{V} plus a small quantity $\gamma_2^2 \psi^T$ is not larger than the

small quadratic function $-\varepsilon x^T Lx$, namely

$$\dot{V} + \gamma_2^2 \psi^T \psi \leq -\varepsilon x^T Lx. \quad (3.38)$$

Then, inequality (3.38) can be expanded as

$$x^T (PA + A^T P)x - 2x^T PB\psi + \gamma_2^2 \psi^T \psi \leq -\varepsilon x^T Lx. \quad (3.39)$$

To validate that (3.39) holds, let us rewrite it using $L = C^T C$ as

$$\begin{bmatrix} x^T & \psi^T \end{bmatrix} \overbrace{\begin{bmatrix} PA + A^T P + \varepsilon C^T C & -PB \\ -B^T P & -\gamma_2^2 I \end{bmatrix}}^{\mathbf{M}} \begin{bmatrix} x \\ \psi \end{bmatrix} \leq 0. \quad (3.40)$$

The negative definiteness of \mathbf{M} can be shown by imposing that its Schur complement is negative. Given that $-\gamma_2 \leq 0$, we take the Schur complement of the block $-\gamma_2^2 I$:

$$\mathbf{M}/[-\gamma_2^2 I] := PA + A^T P + \varepsilon C^T C - (PB(\gamma_2^2 I)^{-1}(-B^T P)),$$

and by setting it to less than or equal to zero, we obtain the Riccati equation (3.36) itself. \square

Other ways in which the linear matrix inequality (3.40) can be solved are via a graphical method or by recurring to a system of algebraic Riccati equations (ARE).

3.6 Numerical Examples

In this section, real instances of power network topologies are simulated. The first one covers the case when the network is considered homogeneous, unweighted and undirected. The second example touches on a different network with a different topology and shows the influence of the connectivity on the response. The third set of simulations contains parameter uncertainties, in such case the network is heterogeneous, weighted and directed.

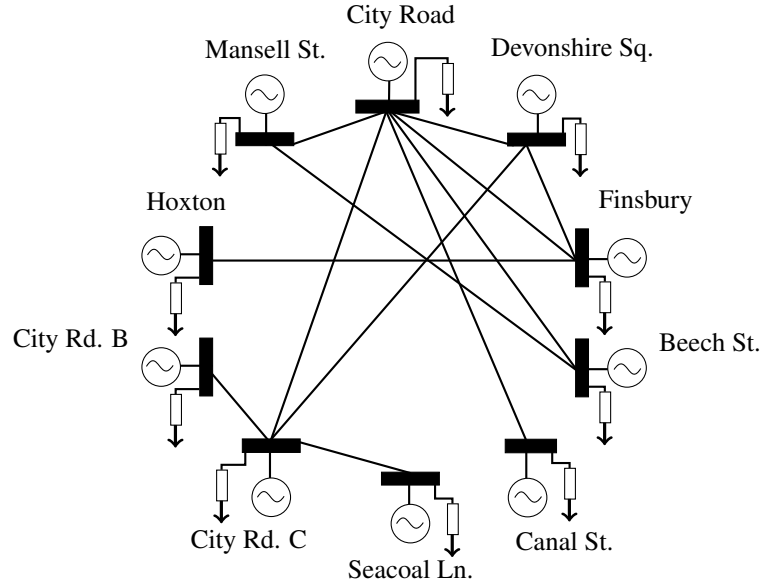


Figure 3.7: Reduced network model based on the one-line diagram of the London City Road Network from [1].

3.6.1 Graph Modeling from Existing Network

Simulations were carried out using data of the London City Road power network as found in [1]. Figure 3.7 shows a simplified diagram extracted from the one-line diagrams in [1], this contains the names of the generators and their respective load buses; from this, a network graph was derived which is the example in Fig. 3.3. The graph was modelled as unweighted and undirected, assuming that the influence between any two nodes is bidirectional. The objective of the first set of simulations is to analyze the transient dynamics and investigate the convergence of the frequency and power to the desired reference. When this occurs, the network achieves synchronization. In the present simulations, all micro-grids are considered homogeneous. The corresponding parameters were selected as follows: number of nodes $n = 10$, inertial constants $M_i = 1$, $\sigma_i = 1$ MJ/rad synchronizing coefficients $T_{ij} = 1$ MVA, number of iterations $N = 1000$, step size $dt = 0.01$ seconds. For illustrative reasons, different damping constants $D_i = 1, 2, 4$ and $\mu_i = 5, 10, 20$ MJ-s/rad are used for different runs. To illustrate the resiliency of the system and as an extreme case study, the initial states of the frequency and power are obtained as random values in the interval $[-0.5, 0.5]$. Frequency and power variables are also reset every 3.3 seconds as a way to simulate periodic extreme disturbances with a value in the vicinity of $\pm 1\%$. The resulting plots have been scaled around 50 Hz and 30 MW for the frequency and power flow respectively to rep-

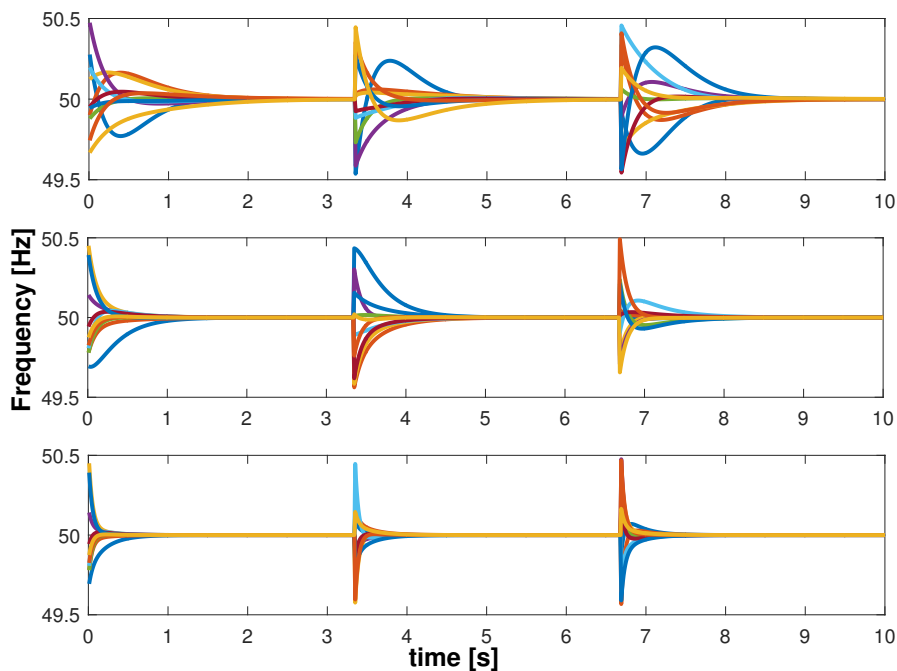


Figure 3.8: State of the micro-grid frequency over time.

resent realistic values. Figure 3.8 shows the frequency response of each micro-grid. It can be seen that the response remains in the range between $[49.5, 50.5]$ Hz and does not exceed in magnitude the desired frequency by more than 1 Hz. Such values have been selected to test an extreme disturbance scenario, the magnitude of the disturbances in a real case would be much lower and handled better by the system. Figure 3.9 displays the power flow of each micro-grid, the values remain in the range of $[29.5, 30.5]$ MW as well. In both plots, different damping values are used from top to bottom. Observe that for larger values both oscillations and settling times are reduced. As mentioned in Section 2.3, we employ some established methods to approximate missing parameters from [1] in the following numerical examples.

3.6.2 Change of Topology

To show that the previous results are scalable, a different section of the London City Road network was selected. The derived undirected unweighted graph is shown in Fig. 3.10. It is worth mentioning that on average this topology has 2.75 connections per node, in contrast to the 2.5 of the previous example. The rest of the parameters are unchanged.

The frequency response is shown in Fig. 3.11. Comparing these results against the

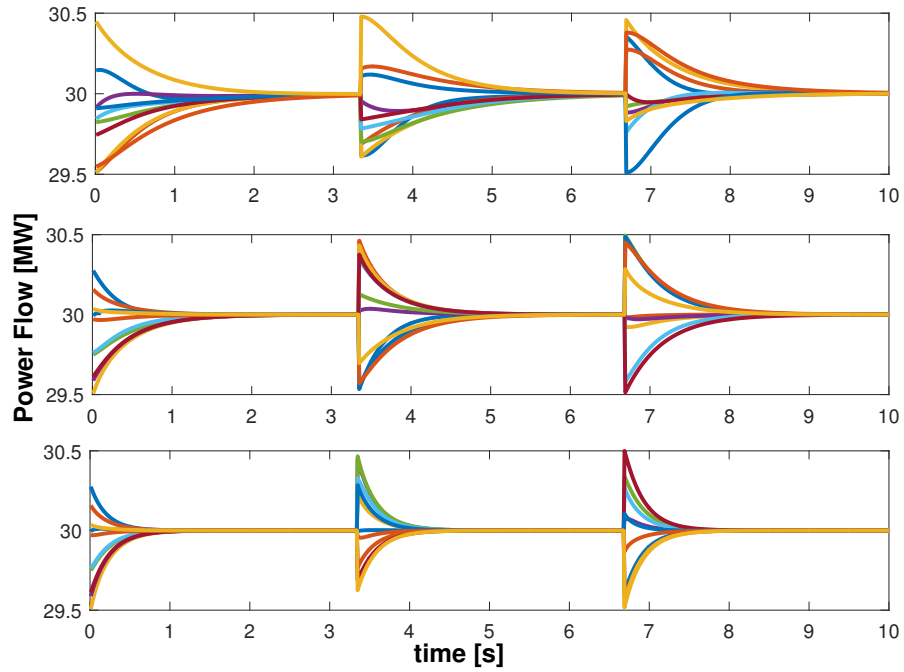


Figure 3.9: State of the power flow in each micro-grid over time.

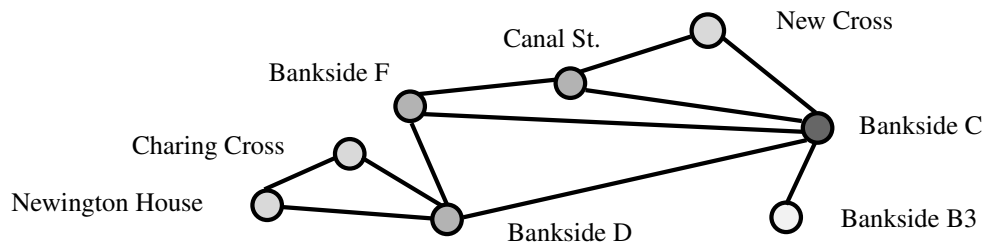


Figure 3.10: Derived graph for a different section of the network in [1].

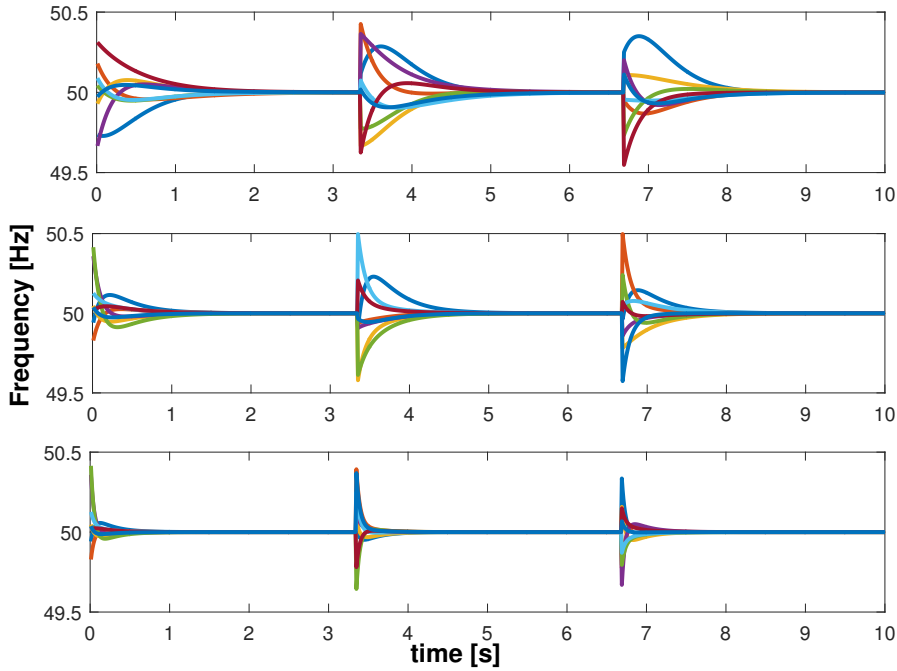


Figure 3.11: Frequency response in a different topology.

previous example, it can be seen that under the second topology the system converges about half a second faster; this is more evident in the top plots where $D_i = 1$ MJ-s/rad, reaffirming our justification for Assumption 2. This implies that a larger connectivity yields a smaller time constant in the overall system. Furthermore, all frequency responses have fewer oscillations with a smaller magnitude during the transient. We omit to show the power flow plot since it has no significant differences from the previous one.

3.6.3 Parameter Varying and Heterogeneity

To account for heterogeneity, we now consider the system shown in Fig. 3.3 where all nodes contain different parameters and the influence from node i to j differs to the one from j to i . The following simulations shed light on the transient response when the synchronizing coefficient T_{ij} , the damping coefficients D_i , μ_i and the inertial coefficient M_i , σ_i are different between micro-grids. First, based on the information in [1], a weighted and directed graph has been derived as shown in Fig. 3.12. The synchronizing coefficients T_{ij} have been selected depending on the power in MVA that flows in and out of each micro-grid as found in [1], i.e. if micro-grid i outputs 60 MVA to micro-grid j , its T_{ij} will vary within the range [59,61] MVA. This range has been introduced with the

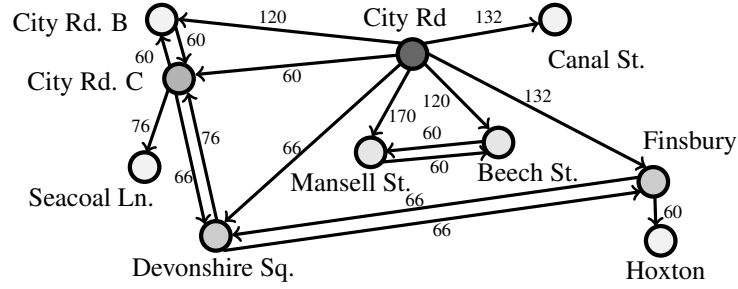


Figure 3.12: Weighted directed graph of the London City Road network [1].

Table 3.1: London City Road Grid Power Capabilities

Number	Name	Capability G_i [MVA]
1	City Road	1440
2	Devonshire Square	180
3	Beech Street	180
4	Mansell Street	190
5	Hoxton	60
6	Finsbury Market	198
7	Canal Street	132
8	City Road C	202
9	Seacoal Lane	76
10	City Road B	120

aim of including uncertainties in the system. Due to the unavailability of data on the exact parameters of the network, approximations were done in accordance with typical data from Westinghouse in [2, p.436]. The inertial coefficients M_i and σ_i depend on the capacity G_i of each micro-grid as in Table 3.1. The constant H_i is assigned randomly from a range of values in $[6, 9]$. For the swing inertia, we take $M_i = G_i H_i / \pi f_i$, where f_i is the nominal frequency, which in this case is 50 Hz. For the damping constant D_i a random value in the interval $[4.5M_i, 5.5M_i]$ is assigned to each micro-grid for the simulation. For illustrative purposes the values of μ_i are chosen as $\mu_i = 15D_i$. As a way to subject the system to non-linearities, the parameters change their value randomly within their assigned range every 0.1 seconds during the simulations. Also, the states are reset every 3.3 seconds as in previous examples.

It can be seen in Fig. 3.13 that the power flow is contained within the acceptable tolerance of 1 MW for the entirety of the simulation. Let us lastly mention that the random change of topology every 0.1 seconds produces barely noticeable oscillations that neither modify the behaviour nor the consensus value. For brevity, we omit to show simulations on the effect of uncertainties that result in an unstable response. However it

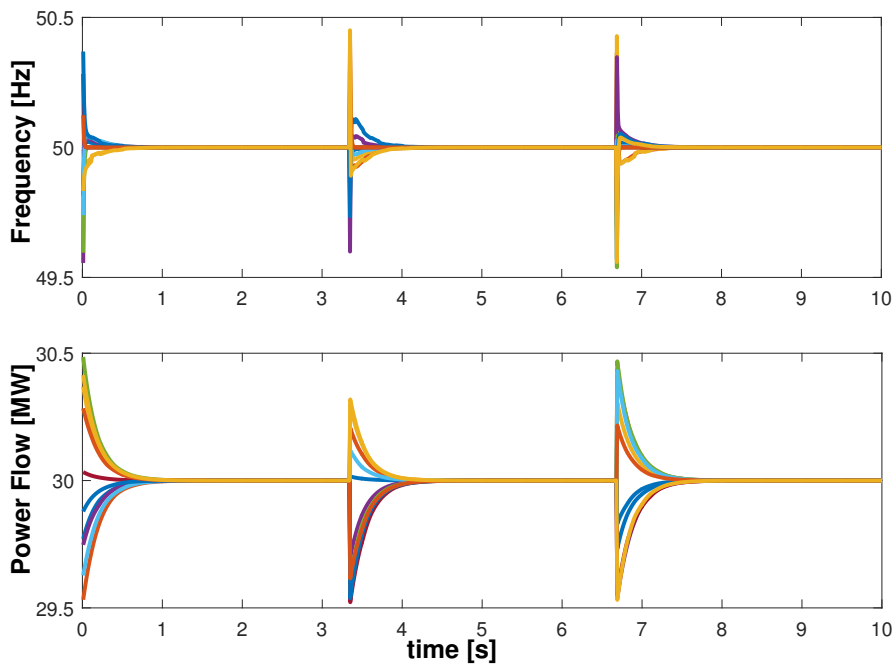


Figure 3.13: Frequency and power flow responses for the directed, weighted and approximated configuration while subject to uncertainties.

is straightforward to choose an uncertainty amplitude value that causes larger measurement variations, namely, an amplitude under which condition (3.31) does not hold for the given inertia and damping parameters.

3.7 Conclusion

As a progression of previous works which are focused on networks of homogeneous micro-grids, we have now extended the analysis to the case where heterogeneity is involved in the form of the different parameters for each micro-grid.

We have investigated the transient stability, and shown the ways in which the heterogeneity of the parameters between micro-grids in the network affects both the response and eigenvalues of the overall system. We mainly focused on the inertial parameters since studying their effect is a current issue in the design of modern power systems.

We obtained a few interesting observations regarding the displacement of the eigenvalues, which depends on the multiple heterogeneous parameters in the network; plus the way of deriving the clusterization of the areas where the eigenvalues might reside in.

We have studied the maximal magnitude of the non-linearities that the system can

accept while remaining stable and expressed it as a function of the parameters.

Finally, we have illustrated the scalability of the model by simulating different topologies and shown the role of connectivity in the network's response.

On the other hand, the uncertainty has been only investigated in this chapter as a sector bounded uncertainty. There exist other kinds of uncertainty and methodologies to examine them and the ways in which they influence the stability of the system [27]. Unfortunately, for this research project we decided to not continue this approach. However, the results shown here provide a good application from the theory presented in [27] and the previous contribution from [4].

Having studied the micro-grid model and its conditions for stability, the next step in this research is the implementation of the on-line pricing mechanisms as will be touched on in the next chapters. Although the uncertainty part is not implemented exactly as touched in this chapter, such analysis sheds light on the resilience of the system and the ways in which the parameters affect the response values. The latter will prove useful when subjecting a single micro-grid to a shift in power consumption, as will be explored in Chapter 4.

Chapter 4

On-line Pricing in a Micro-Grid via a Stackelberg Game with Incentive Strategies

4.1 Introduction

As discussed in Chapter 1, pricing mechanisms on power systems can improve efficiency by shifting the demand. In this chapter, we take the standard form of the micro-grid model as seen in Chapter 3, Assumption 1 and subject it to an on-line pricing scheme derived from a Stackelberg game.

As mentioned in Section 2.6, we chose the Stackelberg game as basis because it enables a market a setup that is easy to relate to: A seller, having some semblance of customer behaviour, announces a price first. Then, the consumer(s) react(s) to such announcement in a way that it maximises its profit. Opposed to other market scenarios and games like auction theory or looking for the Nash or Cournot equilibrium [8, 87], this aspect of hierarchy is only captured by the Stackelberg game.

Such a game accommodates the leader-follower structure of the traditional electricity market, where the consumer reacts to a price that is set by the supplier. The way the game is defined also adapts the underlying rationality of the players where they both try to maximise their profits.

This chapter is organized as follows. In Section 4.2, we introduce the micro-grid and demand response models, and formulate the Stackelberg game. In Section 4.3, we

present the ways in which the game and the physical plant are integrated. In Section 4.4, we provide numerical examples. Finally, in Section 4.5, we provide a brief conclusion.

4.1.1 Main Contributions

As a first finding, conditions for stability are obtained and the transient response of a micro-grid system subject to a price, which is generated exogenously from a Stackelberg game, is studied. The Stackelberg game introduces an incentive problem, which in turn determines the steady-state gain of the open-loop market dynamics. As a second development, a general feedback rule to obtain the price as a function of the power flow and demand is derived. Such a rule is based on an ex-ante price formulation. Stability analysis is performed and the impact of the parameters on the transient dynamics of the micro-grid system is studied. In addition to this, simulations were carried out using both open-loop and closed-loop pricing mechanisms based on data from [2].

4.1.2 Problem Statement

In this chapter we make our first effort on bringing together the market and physical dynamics that are involved in determining the functioning of the micro-grid as a whole. Two configurations are studied in which the market layer is modelled as an open-loop and closed-loop dynamical system respectively. In the first configuration, a Stackelberg game is introduced between the supplier and consumer where the supplier plays an incentive strategy to generate an equilibrium price. In the second, the price is obtained as a feedback function of the power supplied, the demand and an incentive strategy. However, a detailed stability analysis should be conducted on both configurations to ensure their correct operation.

4.2 Micro-Grid and On-Line Pricing Models

In this section, we introduce the dynamic models for the micro-grid and for the on-line pricing mechanism in a unified framework.

4.2.1 Micro-Grid Model

As previously explained in Chapter 3, a micro-grid connected to the main grid can be modelled combining an integrator and the swing dynamics. The first equation is associated with the rate of change of the power flow into the grid as a function of the deviation between the nominal mains frequency and the frequency of the grid [13]. This is given by

$$\dot{P}_{flow} = T(f_{nom} - f), \quad (4.1)$$

where f is the operating frequency of the micro-grid, f_{nom} is the nominal frequency, which is considered to be the frequency of the main grid and T is the synchronizing coefficient which is obtained as the power transferred over the transmission line between the micro-grid and the mains [5]. The second dynamics describe the rate of change of frequency as a function of the current frequency f , the power flow P_{flow} , the generated power from the mains P_{grid} , the nominal consumed power by the loads P_{Lrated} and the shiftable demand response ΔP_L [3]. This second dynamics is given by

$$\dot{f} = -\frac{D}{M}f + \frac{1}{M}(P_{flow} + P_{grid} - P_{Lrated} - \Delta P_L), \quad (4.2)$$

where D denotes the damping coefficient of the micro-grid and M its inertial coefficient, while the dynamics for ΔP_L are explained in the following subsection. The block representation of the market layer and the physical layer of a single micro-grid is shown in Fig. 4.1. There, the input exogenous to the grid represents the price Λ obtained from the on-line open-loop mechanism.

4.2.2 Demand Response

For a given price, the demand response dynamics can be represented as a first-order system [30]

$$\Delta \dot{P}_L = -\frac{1}{\tau}\Delta P_L + \frac{k}{\tau}\Lambda, \quad (4.3)$$

where ΔP_L is the demand, τ the time constant of the market dynamics and Λ is the price multiplied by a DC gain k . The demand is subtracted from the power available in the grid as shown in Fig. 4.1 and represents the quantity of electrical energy that is used by the consumer given the price announced by the supplier. The price Λ is generated from

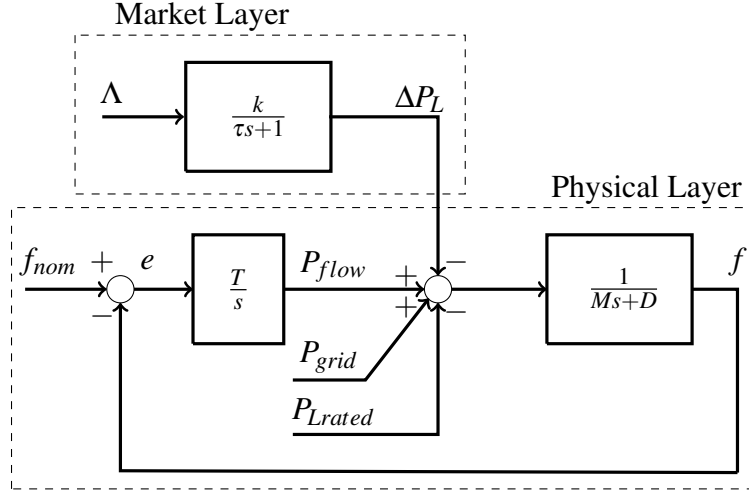


Figure 4.1: Block system of a micro-grid with demand response ΔP_L , power P_{flow} and frequency f subject to exogenous price input Λ .

a Stackelberg game as described in the following section.

4.2.3 Consumer and Supplier Functions

Both the supplier and the consumers are considered to be price-taking, profit-maximizing agents. In particular, the supplier wants to maximize the price and the consumers want to consume as much as possible with the minimum price. The power supplied P_s and power consumed P_c are selected as the quantity that maximizes their profit functions [6]. With some abuse of notation let us denote this as:

$$P_s = \arg \max_x \max_{\Lambda \in [\underline{\Lambda}, \bar{\Lambda}]} \Lambda x - c(x, P_c), \quad (4.4)$$

$$P_c = \arg \max_x \min_{\Lambda \in [\underline{\Lambda}, \bar{\Lambda}]} v(x, \Lambda) - \Lambda x, \quad (4.5)$$

where the value function of the i th consumer in the grid is denoted by $v_i(x, \Lambda)$, which represents the monetary value that the consumer obtains by expending x units of electricity while taking into account the announced price Λ . Analogously, the supplier has a production cost function $c(x, P_c)$. We assume that the value and cost functions are concave and convex, respectively [3, 6].

The simultaneous optimization problems (4.4)-(4.5) serve as a way to describe the game and capture the supplier-consumer tension. The fact that the outcome of (4.4) depends on the output of (4.5) provides some form of constraint; one optimization problem

is subject to the other, which leads to the game-theoretic approach. Other constraints can be taken in to account, we are omitting this for the sake of simplicity. The optimal solutions are unique for every time the game is played, which is done iteratively.

In the maximization problems defined above, we denote by $\bar{\Lambda}$ and $\underline{\Lambda}$ the upper and lower bounds for the price. In other words, we assume that the price Λ lies in the continuous and closed interval $[\underline{\Lambda}, \bar{\Lambda}]$. The corresponding supply and consumption values obtained from (4.4) and (4.5) under the minimum and maximum prices are denoted by $\underline{x}_s, \bar{x}_s$ and $\underline{x}_c, \bar{x}_c$, respectively. This implies that the supply and consumption values x_s and x_c lie in the continuous intervals $[\underline{x}_s, \bar{x}_s]$ and $x[\underline{x}_c, \bar{x}_c]$ respectively. The optimal supply and consumption values \bar{x}_s^* and \bar{x}_c^* can be obtained by taking the derivative of the objective functions in (4.4)-(4.5) and setting them equal to zero. This corresponds to identifying as optimal those points in which the derivative (slope of the curve) is parallel to the price line, as illustrated in Fig. 4.2. From the figure it can be noted that \bar{x}_c corresponds to the maximum consumption given the lowest price $\underline{\Lambda}$, similar conclusions can be drawn for all other bounds.

In order to steer the solutions to an equilibrium, a Stackelberg game is proposed. Let us formally establish the concept of such a game and its equilibrium since we will be using it in the following chapters. This is formalized with the following definitions:

Definition 1 (Player action profile). *Given a universe of players \mathcal{N} , the set \mathcal{H}_i is the set of actions of player i for all $i \in \mathcal{N}$; the set $H := \{h | h = (h_i)_{i \in \mathcal{N}}, h_i \in \mathcal{H}_i, \forall i \in \mathcal{N}\}$ is the set of action profiles, where an action profile is an N -tuple of actions. The function $u_i : H \rightarrow \mathbb{R}$ is the payoff function corresponding to i .*

Definition 2 (Stackelberg equilibrium). *The best response set of player i is defined as $\mathcal{Q}_i(h_{-i}) := \{h_i^* \in \mathcal{H}_i | u_i(h_i^*, h_{-i}) = \max_{h_i \in \mathcal{H}_i} u_i(h_i, h_{-i})\}$.*

An action profile (h_1^S, h_2^S) is a Stackelberg Equilibrium for player 1 if $h_2^S \in \mathcal{Q}_2(h_1^S)$ and

$$u_1(h_1^S, h_2^S) \geq u_1(h_1, h_2), \quad \forall h_1 \in \mathcal{H}_1, h_2 \in \mathcal{Q}_2(h_1). \quad (4.6)$$

From the definitions above, the characteristics of the Stackelberg game are corroborated: The game incorporates a hierarchical structure, where the leader applies his best strategy taking into account the rational reaction of his followers. In turn, the followers output their best response based on the one given by leader.

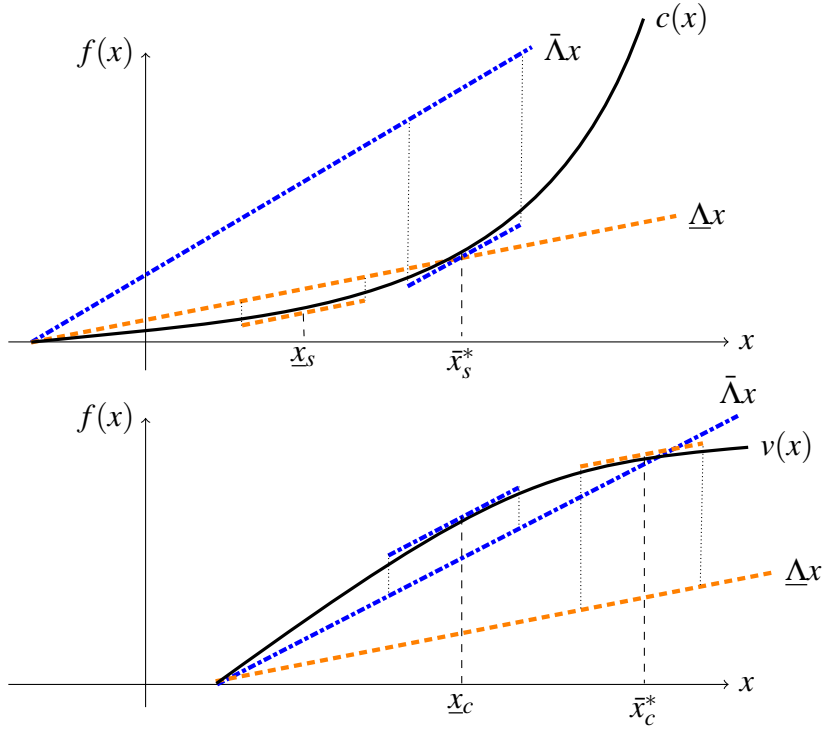


Figure 4.2: Supplier and consumer functions and quantities.

For the case of the supplier and consumer in a single micro-grid, the advantage of formulating such a normalised game is that the incentive strategy no longer depends directly on the cost and value functions, but solely on the Stackelberg equilibrium. Let us define reference points to be employed in the game. Normalizing the optimal solutions to each problem to unitary values, such solutions can be taken equal to

$$(\underline{\Delta}, \bar{x}_c) = (0, 1), \quad (4.7)$$

$$(\bar{\Delta}, \bar{x}_s) = (1, 1), \quad (4.8)$$

for the consumer and for the supplier respectively. The incentive strategy is fully explained in Section 4.3.

4.3 System Integration and Analysis

In this section, the central focus of this chapter is presented. First, for the open-loop configuration, we formulate the Stackelberg game, the incentive problem and determine its optimal solution. Secondly, we perform the stability analysis and obtain the steady-

state gains of the micro-grid model subject to the game-generated price. Thirdly, we show a way to express the price as a function of power and demand and perform both stability and final value analysis on the closed-loop micro-grid model.

4.3.1 Normalized Stackelberg Game Formulation

Assuming that the demand response ΔP_L of the consumers depends on the price Λ set by the supplier, the following Stackelberg game with incentive strategy is proposed. The game provides an incentive strategy and an associated on-line pricing mechanism for the case of open-loop market dynamics. First, denoting the supplier as the *Leader* and the consumers as the *Follower*, we introduce $\pi_L(q_L, q_F)$ and $\pi_F(q_L, q_F)$ as their respective profit functions. Both functions depend on the outputs q_L of the leader and q_F of the follower. The output of the supplier is the price Λ that will minimize its cost and maximize its profits, the output of the follower is the quantity of power ΔP_L that will be shifted from its nominal consumption and maximize its utility from the power while using the minimum price. The incentive problem is formulated in a way such that the leader selects a price as a function of the follower's demand, as given in Definition 2. The following profit functions capture the tension between the supplier and the consumer. Namely the consumer prefers a low price and to consume large quantities of energy, whereas the supplier aims to balance supply and demand. Let (4.7) and (4.8) be the optimal solutions of the optimization problems (4.4) and (4.5) respectively. Then let us propose a profit function π_L for the leader, given by

$$\pi_L = q_L q_F - \frac{1}{2} q_F^2, \quad (4.9)$$

similarly, the profit function π_F for the follower is given by

$$\pi_F = \log q_F + 1 - q_L q_F. \quad (4.10)$$

We refer to *incentive strategy* as the choice that the leader takes depending on the one of the follower. Namely a function $\Gamma(q_F)$. For the sake of tractability, we propose the following assumption, however, without loss of generality, other classes of strategies (functions) can be employed in a similar way as previously discussed in Chapter 2.

Assumption 5. Strategy $\Gamma(q_F)$ is linear and given by

$$q_L = \gamma q_F. \quad (4.11)$$

As also touched in Chapter 2, the above strategy denotes that the output of the leader is proportional to the output of the consumer. This can be interpreted as an *offer* that is announced instead of a price, allowing the consumer choose a price depending on how much it wants to consume.

Theorem 8. Let Assumption 5 hold true. The Stackelberg game yields the following equilibrium point:

$$q_F^* = \gamma^{-\frac{1}{2}}, \quad (4.12)$$

$$q_L^* = \gamma^{\frac{1}{2}}. \quad (4.13)$$

Proof. Let the leader maximize (4.9), and the follower maximize (4.10). Because of the concavity of (4.15), the maximum of the follower is obtained by taking the derivative of its profit function and equating it to zero:

$$\frac{\partial \pi_F}{\partial q_F} = \frac{1}{q_F} - q_L = 0. \quad (4.14)$$

Under the assumption that the leader is playing according to (4.11), then (4.14) can then be rewritten as

$$\frac{1}{q_F} - \gamma q_F = 0. \quad (4.15)$$

The above yields the optimal solution q_F^* as in (4.12). Once the follower has chosen its demand, the leader then obtains the price substituting (4.12) in (4.11), which leads to the equilibrium (4.13). \square

The optimal solutions q_F^* and q_L^* determine the equilibrium of the game. Now the leader has to devise a proper strategy γ to obtain the best equilibrium point. For the supplier, the best equilibrium point, in the normalised case, is the one closest to the optimum (1, 1) as in (4.8). Figure 4.3 illustrates the way in which a different choice for strategy γ produces different quantities of price and demand at the equilibrium. From the figure, it is evident that the output of the leader (the supplier) depends on the quantity

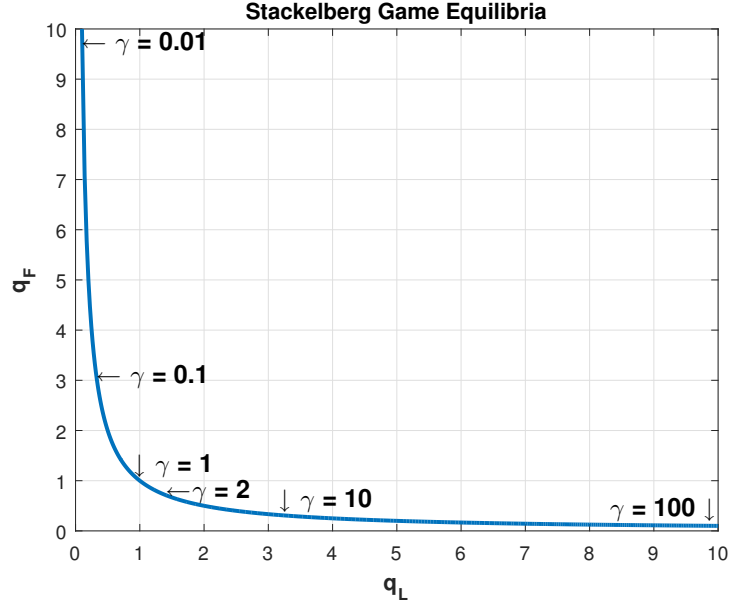


Figure 4.3: Stackelberg equilibrium points as a function of γ .

selected by the follower (consumer). In particular, the higher the price, the lower the consumption.

Remark 2. From the demand response dynamics in (4.3), the following expression can be obtained at steady-state:

$$\Lambda^{ss} = \frac{1}{k} \Delta P_L^{ss}. \quad (4.16)$$

Above, there is a linear relation between the price and the demand, it can be implied that the incentive γ can be treated as a scalar gain, making the choice of the Stackelberg game with a linear $\Gamma(q_F)$ appropriate for the studied case.

4.3.2 Stability of Open-Loop Configuration

Now that we have explained the ways in which the price Λ is obtained, let us analyze the stability of the system subject to such input. From the system configuration illustrated in Fig. 4.1 and equations (4.1)-(4.3) the following state space representation is derived:

$$\begin{bmatrix} \dot{P}_{flow} \\ \dot{f} \\ \dot{\Delta P}_L \end{bmatrix} = \overbrace{\begin{bmatrix} 0 & -T & 0 \\ \frac{1}{M} & -\frac{D}{M} & -\frac{1}{M} \\ 0 & 0 & -\frac{1}{\tau} \end{bmatrix}}^A \begin{bmatrix} P_{flow} \\ f \\ \Delta P_L \end{bmatrix} + \overbrace{\begin{bmatrix} 0 & T & 0 \\ 0 & 0 & \frac{1}{M} \\ \frac{k}{\tau} & 0 & 0 \end{bmatrix}}^B \begin{bmatrix} \Lambda \\ f_{nom} \\ P_{grid} - P_{Lrated} \end{bmatrix}. \quad (4.17)$$

Theorem 9. System (4.17) is stable for all positive values of parameters T , M , D , and τ .

Proof. Consider matrix A in (4.17). The characteristic polynomial of the entire system can be obtained from the denominator of the system's transfer function, which is expressed by the determinant of $sI - A$:

$$|sI - A| = \left| \begin{bmatrix} s & T & 0 \\ -\frac{1}{M} & s + \frac{D}{M} & \frac{1}{M} \\ 0 & 0 & s + \frac{1}{\tau} \end{bmatrix} \right| = s^3 + \left(\frac{D}{M} + \frac{1}{\tau}\right)s^2 + \left(\frac{T}{M} + \frac{D}{\tau M}\right)s + \frac{T}{\tau M}. \quad (4.18)$$

The roots of the above polynomial, namely the eigenvalues of system (4.17) are given as follows:

$$s_1 = -\frac{1}{\tau}, \quad s_{2,3} = \frac{-D \pm \sqrt{D^2 - 4MT}}{2M}. \quad (4.19)$$

For the system to be asymptotically stable, the real part of its eigenvalues must be negative, namely, the eigenvalues must lie on the left-hand-side of the complex plane. From (4.19) the system is stable if the following conditions on the parameters are met:

$$\tau > 0 \text{ and } MT > 0. \quad (4.20)$$

The above conditions are always true given that the parameters are strictly positive. \square

Remark 3. *The transient of the system is characterized by oscillations, when the eigenvalues have a complex part, namely for $D^2 < 4MT$. On the contrary, no oscillations arise when the eigenvalues are real and specifically for $D^2 > 4MT$.*

Since the system is stable as proven in Theorem 9, a steady-state value for a reference step input exists. It is useful to solve for this step value in order to know the response of the power flow and frequency dynamics given a sudden change of price and the consequent consumption. This also allows us to know if the demand will be covered, as will be demonstrated later in the numerical examples.

We can find such steady-state values by setting the derivative on the left-hand-side of (4.17) to zero and employing the final value theorem. The steady-state gain from a step input of magnitude $\Lambda_m = \Lambda$, $f_m = f_{nom}$ or $P_m = P_{grid} - P_{Lrated}$ correspondingly, to

system (4.17) is expressed by:

$$\begin{aligned} P_{flow}^{SS} &= k\Lambda_m + Df_m - P_m, \\ f^{SS} &= f_m, \quad \Delta P_L^{SS} = k\Lambda_m. \end{aligned} \quad (4.21)$$

This is done as follows. From system (4.17) a transfer function matrix can be obtained as $Y(s)/U(s) = C(sI - A)^{-1}B$. Since the feedback in the mentioned system is unitary, matrix C is considered to be an identity matrix I of appropriate dimensions. Substituting matrices A and B we obtain

$$\begin{bmatrix} P_{flow}(s) \\ f(s) \\ \Delta P_L(s) \end{bmatrix} = \begin{bmatrix} G_{11}(s) & G_{12}(s) & G_{13}(s) \\ G_{12}(s) & G_{22}(s) & G_{23}(s) \\ G_{31}(s) & 0 & 0 \end{bmatrix} \begin{bmatrix} \Lambda(s) \\ f_{nom}(s) \\ P_{grid}(s) - P_{Lrated}(s) \end{bmatrix}, \quad (4.22)$$

where

$$\begin{aligned} G_{11}(s) &= \frac{P(s)}{\Lambda(s)} = \frac{kT}{M(\frac{D}{M}s + s^2 + \frac{T}{M})(\tau s + 1)}, \\ G_{12}(s) &= \frac{P(s)}{f_{nom}(s)} = \frac{T(\frac{D}{M} + s)}{\frac{D}{M}s + s^2 + \frac{T}{M}}, \\ G_{13}(s) &= \frac{P(s)}{P_{grid}(s) - P_{Lrated}(s)} = -\frac{T}{M(\frac{D}{M}s + s^2 + \frac{T}{M})}, \\ G_{21}(s) &= \frac{f(s)}{\Lambda(s)} = -\frac{ks}{M(\frac{D}{M}s + s^2 + \frac{T}{M})(\tau s + 1)}, \\ G_{22}(s) &= \frac{f(s)}{f_{nom}(s)} = \frac{\frac{T}{M}}{\frac{D}{M}s + s^2 + \frac{T}{M}}, \\ G_{23}(s) &= \frac{f(s)}{P_{grid}(s) - P_{Lrated}(s)} = \frac{s}{M(\frac{D}{M}s + s^2 + \frac{T}{M})}, \\ G_{31}(s) &= \frac{r(s)}{\Lambda(s)} = \frac{k}{\tau s + 1}. \end{aligned}$$

From the final value theorem, we have that the steady-state gain for a system described by a transfer function $F(s)$ and subjected to an input $U(s)$ can be obtained as

$$\lim_{s \rightarrow 0} sG(s)U(s). \quad (4.23)$$

From (4.23) and (4.22) and assuming a step input of magnitude Λ_m , f_m or P_m we obtain:

$$\begin{aligned} \lim_{s \rightarrow 0} s G_{11}(s) \frac{\Lambda_m}{s} + s G_{12}(s) \frac{f_m}{s} + s G_{13}(s) \frac{P_m}{s} \\ &= \frac{kT}{M \frac{T}{M}} \Lambda_m + \frac{T \frac{D}{M}}{\frac{T}{M}} f_m - \frac{T}{M \frac{T}{M}} P_m, \\ \lim_{s \rightarrow 0} s G_{21}(s) \frac{\Lambda_m}{s} + s G_{22}(s) \frac{f_m}{s} + s G_{23}(s) \frac{P_m}{s} \\ &= -\frac{0}{M \frac{T}{M}} \Lambda_m + \frac{\frac{T}{M}}{\frac{T}{M}} f_m + \frac{0}{M \frac{T}{M}} P_m, \\ \lim_{s \rightarrow 0} s G_{31}(s) \frac{\Lambda_m}{s} &= k \Lambda_m. \end{aligned}$$

Hence, the steady-state values (4.21) are obtained.

In view of the considerations in subsection 4.3.1, the price Λ is the supplier's output from the Stackelberg game and is a function of a selected strategy $\Gamma(q_F)$ that characterizes the equilibrium point in terms of supply and demand as shown in (4.12). This implies that for every possible equilibrium point we obtain a different steady-state value.

4.3.3 Price as a Function of Power and Demand

To determine a way to express the price Λ as a linear function of power and demand while closing the loop of the system in Fig. 4.1, a few concepts must be introduced in the same spirit as in [6].

An ex-ante price $\Lambda(t)$ can be calculated from an estimated supply \hat{s} which is in turn obtained from the total of a previous demand, namely

$$\hat{s}(t) = P_{Lrated}(t) + \Delta P_L(t) \quad (4.24)$$

which essentially represents the balancing of supply and demand. From it and by solving the supplier's cost function in (4.4) we obtain

$$\Lambda(t) = \left. \frac{d}{dx} c(x) \right|_{\hat{s}(t)}. \quad (4.25)$$

A physical interpretation of the above is that the supplier supplies a quantity equal to the demand from a previous period of time. The price is then the one that is optimal for the given supplied quantity. Graphically, the price is identified by the slope of the curve

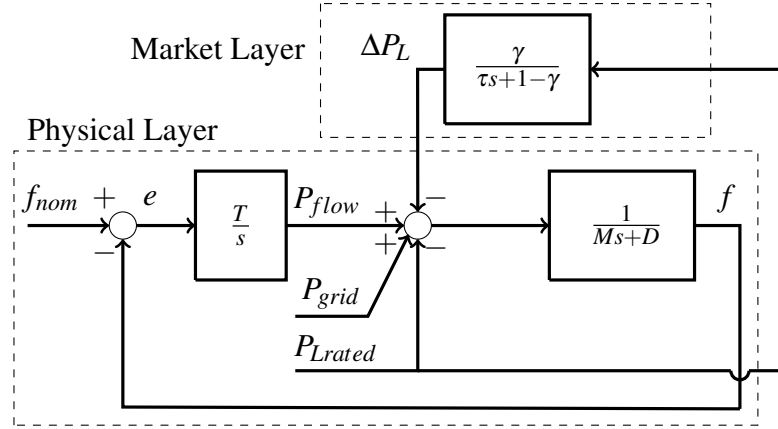


Figure 4.4: Block system of the micro-grid with closed-loop on-line pricing.

representing the cost evaluated in the point corresponding to the supplied quantity. As mentioned in [31], the supplier cost function is the following:

Assumption 6. *The supplier has a cost function $c(x)$ of the form:*

$$c(x) = \alpha \frac{x^2}{2}, \quad (4.26)$$

where x is the quantity of supplied power and α is a scalar value. As mentioned in Chapter 1, such cost function has been validated for thermal generators in [32] and is generally used as a good approximation in the literature as seen in [33], [34] and [35].

Substituting the supply (4.24) and the cost (4.26) into (4.25), the following expression for the ex-ante price is derived:

$$\Lambda(t) = \frac{d}{dx} \alpha \frac{x^2}{2} \Big|_{s(t)} = \alpha x \Big|_{s(t)}. \quad (4.27)$$

We are ready to establish the following result.

Lemma 2. *Let Assumption 6 hold, the price is given by*

$$\Lambda(t) = \alpha(P_{Lrated}(t) + \Delta P_L(t)). \quad (4.28)$$

Now that we have obtained the dependence of price Λ on the sum of the nominal consumed power P_{Lrated} and the demand shift ΔP_L , the block system describing the market dynamics can be rearranged closing the loop as in Fig. 4.4. The system's dynamics

in the case of closed-loop market dynamics can then be written as

$$\begin{aligned}\dot{P}_{flow} &= T(f_{nom} - f), \\ \dot{f} &= -\frac{D}{M}f + \frac{1}{M}(P_{flow} + P_{grid} - P_{Lrated} - \Delta P_L), \\ \Delta \dot{P}_L &= -\frac{1}{\tau}\Delta P_L + \frac{k\alpha}{\tau}(P_{Lrated} + \Delta P_L).\end{aligned}\quad (4.29)$$

We can freely substitute $k\alpha$ with the incentive γ since both are linear relationships to the consumed power and serve as means of shifting the total demand via ΔP_L . The state-space representation of the closed-loop system can be rewritten in matrix form as follows

$$\begin{bmatrix} \dot{P}_{flow} \\ \dot{f} \\ \Delta \dot{P}_L \end{bmatrix} = \overbrace{\begin{bmatrix} 0 & -T & 0 \\ \frac{1}{M} & -\frac{D}{M} & -\frac{1}{M} \\ 0 & 0 & \frac{1}{\tau}(\gamma-1) \end{bmatrix}}^A \begin{bmatrix} P_{flow} \\ f \\ \Delta P_L \end{bmatrix} + \overbrace{\begin{bmatrix} 0 & T & 0 \\ \frac{1}{M} & 0 & -\frac{1}{M} \\ 0 & 0 & \frac{\gamma}{\tau} \end{bmatrix}}^B \begin{bmatrix} P_{grid} \\ f_{nom} \\ P_{Lrated} \end{bmatrix}, \quad (4.30)$$

as in Section 4.3.2, the characteristic polynomial can be obtained from $|sI - A|$, yielding

$$|sI - A| = s^3 + \left(\frac{D}{M} + \frac{1-\gamma}{\tau}\right)s^2 + \left(\frac{T}{M} - \frac{D(\gamma-1)}{\tau M}\right)s - \frac{T(\gamma-1)}{\tau M}. \quad (4.31)$$

We are now ready to enunciate the following result.

Theorem 10. *System (4.30) is stable for all non-negative values of parameters T , M , D and τ . Additionally, the incentive strategy γ must comply with the condition:*

$$0 < \gamma < 1. \quad (4.32)$$

Proof. The role of the system parameters in the conditions for stability is obtained similarly to the analysis demonstrated in Theorem 9. The roots of the characteristic polynomial (4.31) are the following:

$$s_1 = \frac{\gamma-1}{\tau}, \quad s_{2,3} = \frac{-D \pm \sqrt{D^2 - 4MT}}{2M}, \quad (4.33)$$

which yields the condition $MT > 0$ that is always true. To find the conditions for γ , the

Routh-Hurwitz criteria can be applied to (4.31) to obtain the following conditions:

$$\begin{aligned} \frac{D}{M} + \frac{1-\gamma}{\tau} &> 0, \\ \frac{T}{M} - \frac{D(\gamma-1)}{\tau M} &> 0, \\ \left(\frac{D}{M} + \frac{1-\gamma}{\tau}\right) \left(\frac{T}{M} - \frac{D(\gamma-1)}{\tau M}\right) &> -\frac{T(\gamma-1)}{\tau M}. \end{aligned} \quad (4.34)$$

Such conditions together with (4.33) can be reduced to obtain the range of values (4.32) for the incentive strategy. \square

The meaning behind (4.32) is that if the gain is too small this results in a price reduction that will increase the demand, and by trying to maximise their utility function, the consumers will demand power beyond the capabilities of the micro-grid. Therefore, we can conclude that the closed-loop system is stable for certain bounds of γ , as we will illustrate in Section 4.4.2. Hence the supplier must be aware of the consumption historical patterns in the grid and select an appropriate value for the incentive.

Remark 4. *Taking into account the previous statement and the expression of the eigenvalues in (4.33) we can also derive the two following considerations:*

- *The system is stable with complex eigenvalues when $D^2 < 4MT$.*
- *The system is stable with real, distinct and negative eigenvalues when $D^2 > 4MT$.*

As can be seen from the mentioned inequalities, the oscillations in the system's response depend mainly on the value of the damping and inertial parameters D and M , which still holds with the findings in [13] despite our new system configuration. Additionally, we can provide the following observations obtained empirically regarding the role of the system's parameters on the transient of the system. The value of the time constant τ affects directly the settling time of P_{flow} and ΔP_L . The synchronizing coefficient T influences the speed of the oscillations of all states proportionally, and reduces the settling time as well; T also alters the peak values of P_{flow} and ΔP_L . The inertial coefficient M affects oscillation speed on all states and the peak responses of P_{flow} and ΔP_L without affecting their steady-state values. The damping coefficient D directly increases the settling time for larger values while also modifying the steady-state values of P_{flow} and f . The gain γ directly changes the magnitude of P_{flow} and

ΔP_L , increasing the settling time for larger values. The last two observations can be corroborated by the following result.

Similarly to Section 4.3.2, we can apply the final value theorem to (4.30). The steady-state gain from a corresponding step input of magnitude $P_{Gm} = P_{grid}$, $f_m = f_{nom}$ or $P_{Lm} = P_{Lrated}$ to system (4.30) is expressed by:

$$\begin{aligned} P_{flow}^{ss} &= \frac{1}{1-\gamma} P_{Lm} - P_{Gm} + Df_m, \\ f^{ss} &= f_m, \quad \Delta P_L^{ss} = \frac{\gamma}{1-\gamma} P_{Lm}. \end{aligned} \quad (4.35)$$

The above is derived as follows. From system (4.30) a transfer function matrix can be obtained. Since the feedback in the mentioned system is unitary, matrix C is considered to be an identity matrix I of appropriate dimensions. Substituting matrices A and B into $Y(s)/U(s) = C(sI - A)^{-1}B$ we obtain

$$\begin{bmatrix} P_{flow}(s) \\ f(s) \\ \Delta P_d(s) \end{bmatrix} = \begin{bmatrix} G_{11}(s) & G_{12}(s) & G_{13}(s) \\ G_{21}(s) & G_{22}(s) & G_{23}(s) \\ 0 & 0 & G_{33}(s) \end{bmatrix} \begin{bmatrix} P_{grid}(s) \\ f_{nom}(s) \\ P_{Lrated}(s) \end{bmatrix} \quad (4.36)$$

where

$$\begin{aligned} G_{11}(s) &= \frac{P_{flow}(s)}{P_{grid}(s)} = -\frac{T}{s(D+Ms)+T}, \\ G_{12}(s) &= \frac{P_{flow}(s)}{f_{nom}(s)} = \frac{T(D+Ms)}{s(D+Ms)+T}, \\ G_{13}(s) &= \frac{P_{flow}(s)}{P_{Lrated}(s)} = \frac{sT\tau+T}{(-\gamma+s\tau+1)(s(D+Ms)+T)}, \\ G_{21}(s) &= \frac{f(s)}{P_{grid}(s)} = \frac{s}{s(D+Ms)+T}, \\ G_{22}(s) &= \frac{f(s)}{f_{nom}(s)} = \frac{T}{s(D+Ms)+T}, \\ G_{23}(s) &= -\frac{f(s)}{P_{Lrated}(s)} = \frac{\tau s^2+s}{(-\gamma+s\tau+1)(s(D+Ms)+T)}, \\ G_{33}(s) &= \frac{\Delta P_L(s)}{P_{Lrated}(s)} = \frac{\gamma}{\tau s+1-\gamma}. \end{aligned}$$

Applying the final value theorem from (4.23) to (4.36) and assuming a corresponding

step input of magnitude P_{Gm} , f_m or P_{Lm} it yields:

$$\begin{aligned} \lim_{s \rightarrow 0} sG_{11}(s) \frac{P_{Gm}}{s} + sG_{12}(s) \frac{f_m}{s} + sG_{13}(s) \frac{P_{Lm}}{s} \\ = -\frac{T}{T} P_{Gm} + \frac{TD}{T} f_m + \frac{T}{(1-\gamma)T} P_{Lm}, \\ \lim_{s \rightarrow 0} sG_{21}(s) \frac{P_{Gm}}{s} + sG_{22}(s) \frac{f_m}{s} + sG_{23}(s) \frac{P_{Lm}}{s} \\ = -\frac{0}{T} P_{Gm} + \frac{T}{T} f_m + \frac{0}{(1-\gamma)T} P_{Lm}, \\ \lim_{s \rightarrow 0} sG_{31}(s) \frac{P_{Lm}}{s} = \frac{\gamma}{1-\gamma} P_{Lm}. \end{aligned}$$

Hence, the steady-state values (4.35) are obtained.

4.4 Numerical Examples

The parameters were selected based on typical values of a micro-grid with a capacity of 60 MVA that is providing 30 MVA of power to the main grid: $T = 30$ MVA, $M = 0.2$ MJ-s/rad and $D = 1$ MJ/rad in accordance to [2]; the simulation time is 60 seconds, initial state values are selected randomly and the grid is subject to step inputs of $f_{nom} = 50$ Hz, $P_{grid} = 50$ and $P_{Lrated} = 20$ MVA. The time constant for the demand response has been selected as $\tau = 3$ s; two justifications are behind this, the first is to show the results more clearly, the second is that in the future, customers might be able to access real-time prices in a more immediate way (i.e. an automated decision-making system).

4.4.1 Micro-Grid with Exogenous Price Input

In addition to the parameters previously mentioned, the gain is selected as $k = 25$ and the price Λ is a value in the range of $[0, 1]$, in the simulation, only three different values of Λ are selected for illustrative purposes, tractability, and to show the system's response to abrupt changes. Figure 4.5 shows the open-loop configuration response. Note that the demand ΔP_L reacts in accordance with the consumer behaviour discussed in Section 4.2.2. Oscillations arise during the transient of the system, also the sum of powers in the grid $P_{grid} - P_{Lrated} - \Delta P_L$ does not turn negative, meaning that the increase/decrease of demand does not surpass the power available in the grid. Finally, none of the states exceeds the 60 MVA capacity of the micro-grid, it can be seen that the power flow

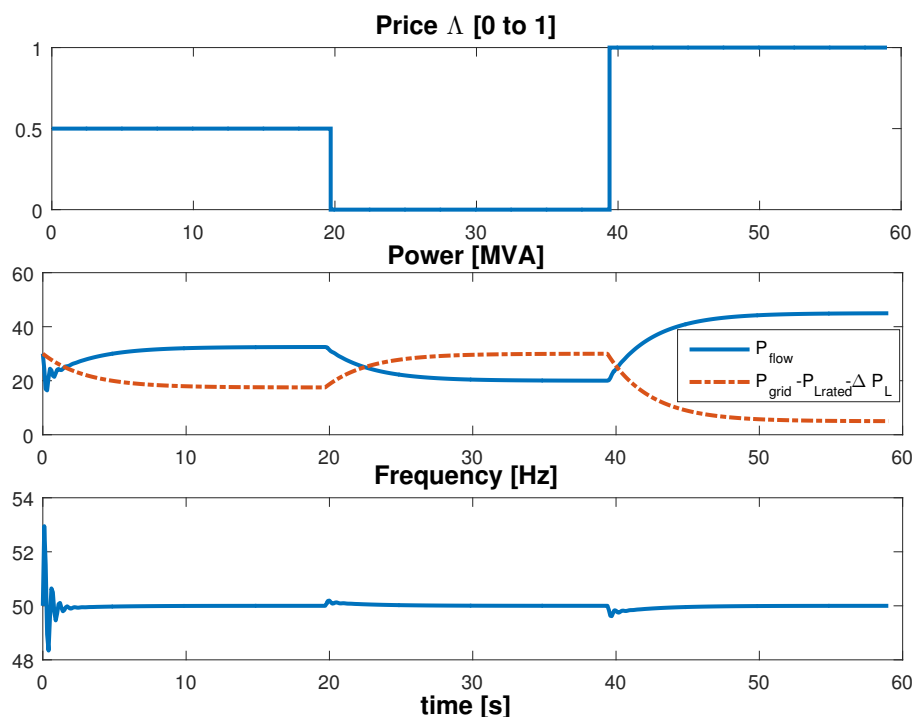


Figure 4.5: Open-loop response of (top) price, (middle) power flow, and (bottom) frequency.

reacts according to the demand shift. As discussed above, choosing larger values for D can attenuate the oscillations but this would, in turn, produce larger power flow values that can surpass the capacity of the grid. Conversely, selecting larger values for k may result in deviations in the frequency state. Figure 4.6 shows the response under the same parameter values with the exception of $D = 2$ MJ/rad, which is sufficiently large to damp the oscillations. Note that when the power flow increases, a larger damping can be chosen but this will in might produce power flow values out of the 60 MVA capacity of the grid. Conversely, selecting larger values for k may result in deviation on the frequency state.

Selecting large values of k can also result in power flow values larger than the capacity of the grid, Fig. 4.7 shows the response of the grid under the same parameter values as for the first example except for $k = 250$. Note that the frequency state deviates largely from the desired 50 Hz. These results show that the response can be asymptotically stable but the parameters must be selected in a way that the demand does not exceed the power available.

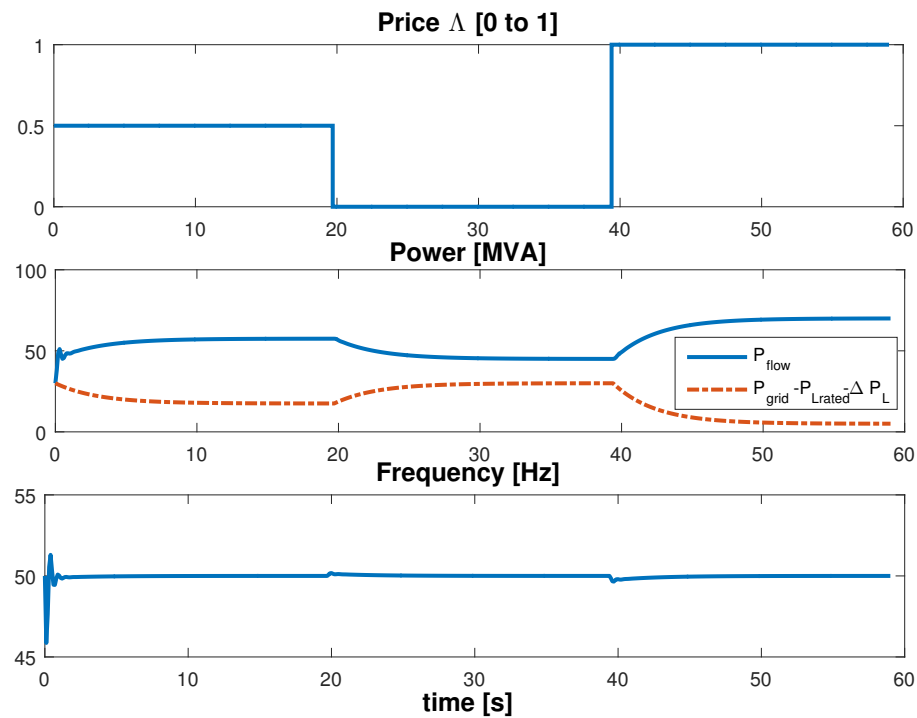


Figure 4.6: Open-loop response of (top) price, (middle) power flow, and (bottom) frequency; by increasing the damping coefficient oscillations are reduced.

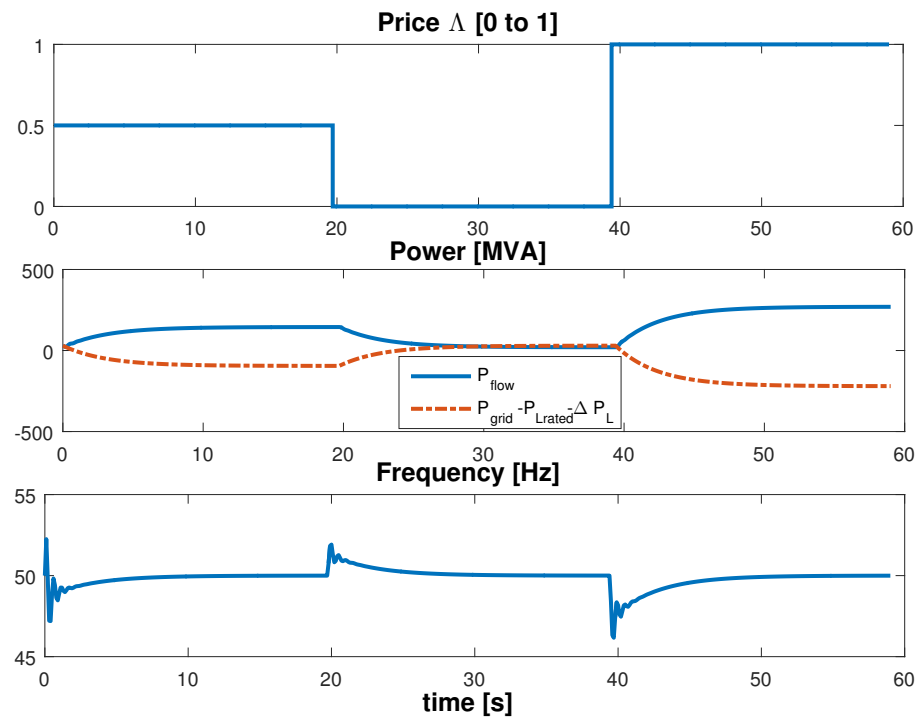


Figure 4.7: Open-loop response of (top) price, (middle) power flow, and (bottom) frequency; by selecting large gain values, the demand exceeds the power available in the grid.

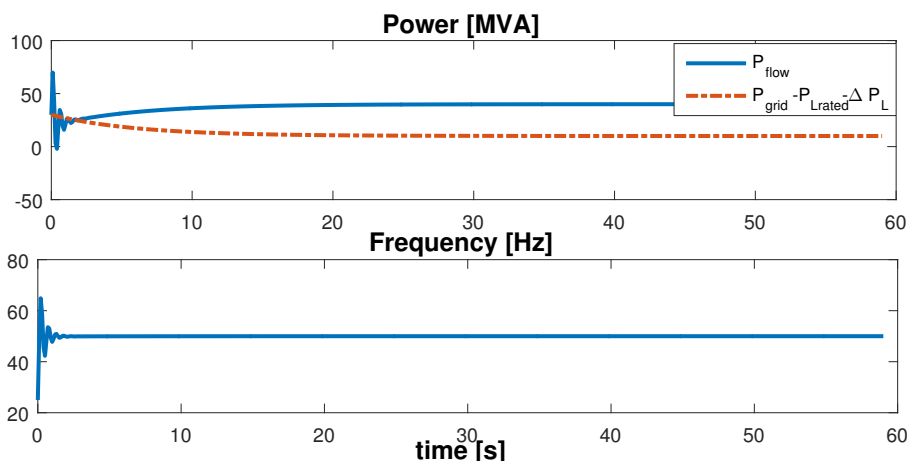


Figure 4.8: Closed-loop response of (top) power flow, and (bottom) frequency.

4.4.2 Micro-Grid with Closed-Loop Market Dynamics

The following set of simulations adopts the same parameters and frequency inputs as in the previous example. In Fig. 4.8 with $\gamma = 0.5$ and $D = 1$ MJ/rad, it can be seen that the power flow can take negative values due to oscillations during the transient. However, the frequency f has the same steady-state value. Also, the demand shifted given the incentive γ is not larger than the power available. As with the open-loop case, increasing the damping D can help to eliminate oscillations at the cost of increasing the power flow. However, as implied in the stability analysis, there exists a sufficiently large value of γ which compromises the stability of the system. In Fig. 4.9 the damping is increased to $D = 2$ MJ/rad to eliminate oscillations and as in the open-loop configuration, there is an increase in the power flow state that can ultimately lead to values exceeding the capacity of the grid. This is illustrated in Fig. 4.10 where $\gamma = 0.8$ and the power available becomes negative due to increased demand, which is physically impossible.

4.5 Conclusion

From the model introduced in Chapter 3, we have explored two ways of implementing on-line pricing mechanics in a single micro-grid, with a novel approach of subjecting the system model to a Stackelberg game with incentive strategies. Furthermore, conditions for stability were found, as well as the role of the grid's time constant, DC gain, inertial, damping and synchronizing coefficients in the transient and steady-state behaviour of both configurations has been studied. More importantly, we brought closer

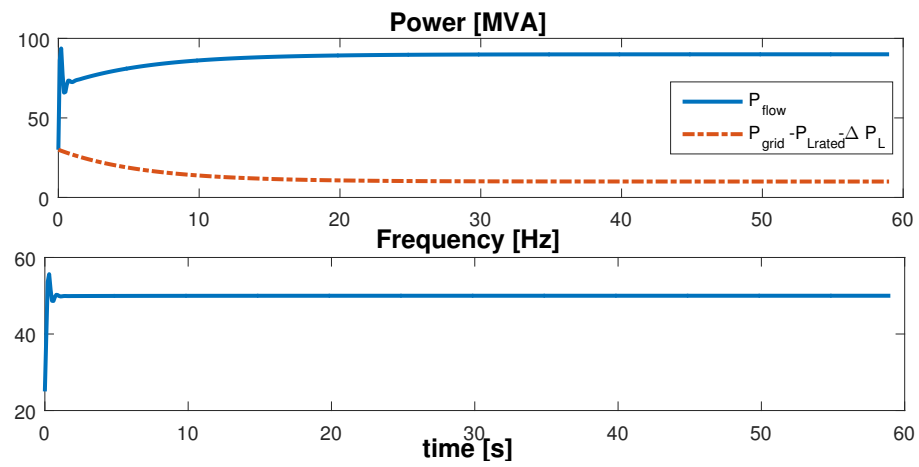


Figure 4.9: Closed-loop response of (top) power flow, and (bottom) frequency; by increasing the damping coefficient oscillations are reduced.

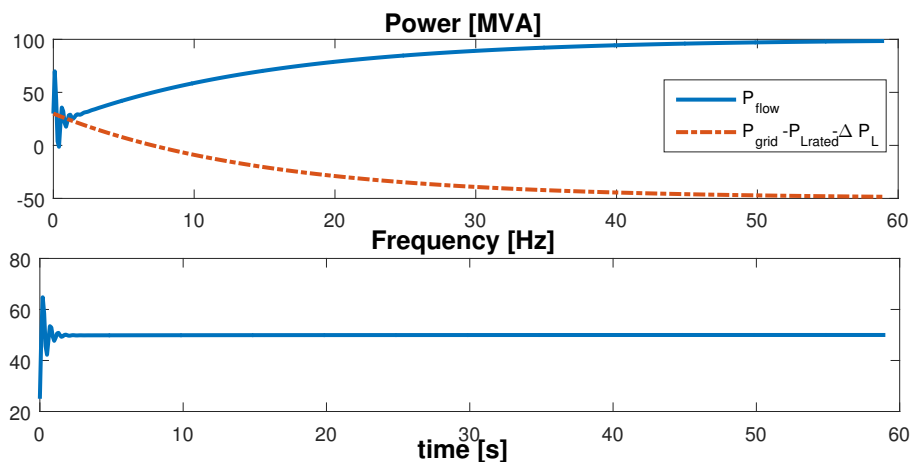


Figure 4.10: Closed-loop response of (top) power flow, and (bottom) frequency; by selecting large gain values, the demand exceeds the power available in the grid.

the market and physical layers in the system by learning the way in which the parameters that are chosen by the supplier, being a price, a gain or incentive, affect the system response. The proposed Stackelberg game will be further explored and refined in the following chapters. Where such is implemented in a more realistic resistive micro-grid model dynamics.

Chapter 5

Personalised Pricing in a Resistive Micro-Grid via a Stackelberg Game with Incentive Strategies

5.1 Introduction

As previously discussed in the chapters above, most literature about dynamic pricing does not touch upon the analysis of the effect and stability of implementing such mechanisms onto a realistic physical electrical system. Having introduced a pricing scheme into the swing equation-based AC micro-grid model in Chapter 4, we now include it with a more realistic low-voltage resistive micro-grid. This enables the profit functions to be defined in a more precise and practical manner. Furthermore, the use of the *incentive strategies* is more notable than in Chapter 4, since the improved adaption of the scheme allows the inclusion of *offers* that result in a personalised price for the consumers in the micro-grid.

5.1.1 Summary and Contributions

As a first result, we present the conditions for stability of the resistive micro-grid model, where the underlying assumption is that every generator and (industrial) load is interfaced with the micro-grid through a power inverter that operates under the P-V droop control (resistive droop), and the loads receive a power reference value given by a pric-

ing scheme. The implementation of the proposed scheme is further simplified by adopting a P-V bounded droop controller. Numerical implementations are carried out, where the strategic competition between the consumer and the follower is shown. Convergence to different equilibrium points for different incentive strategies is also illustrated. A way in which the parameters can be selected for its application is likewise delineated.

5.1.2 Problem Statement

The focus of this chapter consists of the further study of the Stackelberg game with incentive strategies and observe its effect on an industrial low-voltage resistive micro-grid system. Where both the generators and the loads are in grid-forming mode (droop-controlled units), as required in modern power systems, and the load demand is subject to a pricing mechanism from the corresponding leader-follower market structure. We propose and adapt a Stackelberg approach with incentive strategies and a related closed-loop configuration that enables the implementation. However, a detailed analysis for both the system stability and the game operation is necessary to obtain the conditions that ensure the correct operation of the whole integrated system.

5.1.3 Notation Preliminaries

Given the one-dimensional vector $x \in \mathbb{R}^n$ with individual elements $x_i \in \mathbb{R}$, where $i = 1, 2, \dots, n$, we denote $[x] = \text{diag}(x) = \text{diag}(x_i) \in \mathbb{R}^{n \times n}$ as the associated square diagonal matrix with the elements of vector x in the diagonal entries. Let us review the property $[x]^{-1} = [x_i^{-1}]$. Let $\mathbf{0}_{n \times n}$ denote a $n \times n$ matrix with all entries equal to zero, and $\mathbf{1}_{n \times 1}$ be a column vector of n elements with all entries equal to one.

5.2 Micro-Grid Model

In this section, we introduce the dynamic models of both the micro-grid network and the droop controlled units (generators and loads).

5.2.1 Network Model Considerations

Just as in Chapter 3, a network topology is considered. Differently, for this case we consider a single micro-grid that is distributed in a network, the representation is as follows. The micro-grid network is represented by a connected, undirected and weighted graph $\mathcal{G}(\mathcal{V}, \mathcal{E})$, where $\mathcal{V} = \{1, 2, \dots, n\}$ is the set of nodes (vertices). The set of nodes is divided in loads $\mathcal{V}_L = \{1, 2, \dots, l\}$ and generators $\mathcal{V}_G = \{l + 1, l + 2, \dots, n\}$, where $\mathcal{V} = \mathcal{V}_G \cup \mathcal{V}_L$, l is the number of load nodes and n the total number of nodes. The set of edges $\mathcal{E} \subseteq \mathcal{V} \times \mathcal{V}$ is the set of unordered pairs $\{i, j\}$ in consideration of the distribution lines, which are assumed to be resistive. Let $A \in \mathbb{R}^{n \times n}$ denote the adjacency matrix of graph \mathcal{G} , where its ij th element A_{ij} is the corresponding edge represented by a conductance $1/R_{ij}$ between nodes i and j . The set \mathcal{N}_i refers to the neighboring nodes j of node i where $\mathcal{N}_i \in \mathcal{V} : \{i, j\} \in \mathcal{E}$.

5.2.2 Resistive Micro-Grid Model

The micro-grid model under consideration has a low-voltage configuration, also known as a resistive micro-grid. The system is considered as a network of load nodes and generator nodes as shown in Fig. 5.1, where the supplier is considered to be the owner of such generators and each consumer is represented by a load node. Note that the main grid is considered as a generator. The network is assumed to be resistive, namely the impedance of the line, which is usually resistive-inductive, is dominated by the resistive component, hence the reactive power is neglected [67].

The micro-grid is considered to be connected to the main grid that contributes power when the demand is higher than the supply provided by the generators; in the network topology, the main grid is considered as an additional node. However, the results explained here also apply to the case when the micro-grid is islanded.

The power equation of a node i , as a function of its adjacent nodes' voltages in a resistive micro-grid is given by:

$$P_i = V_i^2 \left(\frac{1}{R_{ii}} + \sum_{j \in \mathcal{N}_i} \frac{1}{R_{ij}} \right) - \sum_{j \in \mathcal{N}_i} \frac{V_i V_j}{R_{ij}} \cos \phi_{ij}, \quad (5.1)$$

where V_i is the voltage on node i , P_i is the node power, R_{ij} is the resistance of the line that connects nodes i and j , R_{ii} is the shunt resistance of node i , and ϕ_{ij} is the phase

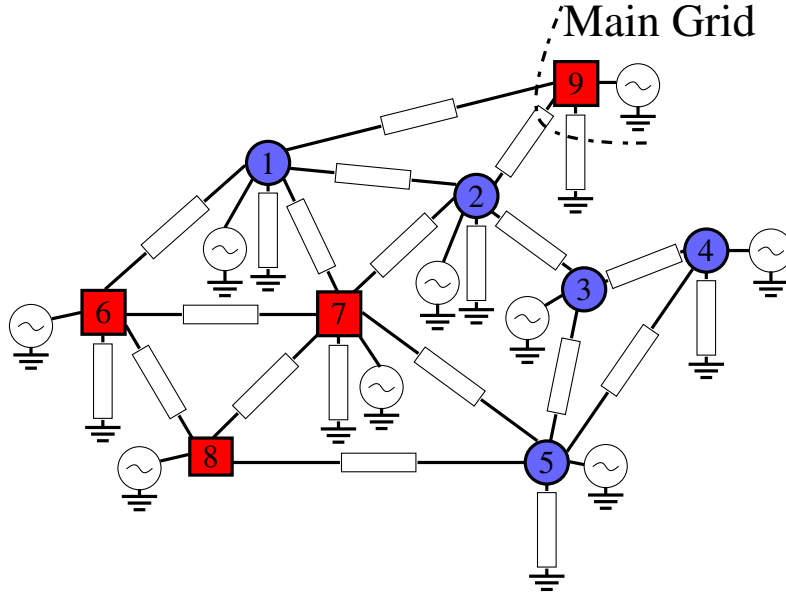


Figure 5.1: Resistive micro-grid in a network representation, comprised by loads ● and generators ■, resistive distribution lines, and shunt conductances.

difference between nodes i and j . Assuming standard decoupling approximation [3,71], namely that the phase ϕ_{ij} has values near to zero, we obtain the following non-linear expression:

$$P_i = V_i^2 \left(\frac{1}{R_{ii}} + \sum_{j \in \mathcal{N}_i} \frac{1}{R_{ij}} \right) - \sum_{j \in \mathcal{N}_i} \frac{V_i V_j}{R_{ij}}. \quad (5.2)$$

The power expression of all the nodes of the network has the non-linear form of

$$P = [V]GV, \quad (5.3)$$

where P and V are vectors containing all the nodes' powers and voltages respectively, and G is the conductance matrix [59] that is derived from the network's Laplacian. Let us briefly explain some of the properties of G in the next subsection.

5.2.3 Definition and Properties of the Conductance Matrix

Let A denote the adjacency matrix of the micro-grid network. The degree matrix of A is defined as $D := [\{\sum_{j=1}^n A_{ij}\}_{i=1}^n]$, while the Laplacian L of A is obtained as $L := D - A$. Note that, although apparent in A , the self-loops in the topology represented by the shunt conductances $A_{ii} = 1/R_{ii} = g_i$ do not appear in L . For this reason, we recur to the conductance matrix G , which has the form of a loopy Laplacian matrix [60] and is

defined as $G := L + [\{A_{ii}\}_{i=1}^n]$. The conductance matrix G has the following properties: its ij th element $g_{ij} = -1/R_{ij}$ and its diagonal elements $g_{ii} = 1/R_{ii} + \sum_{j \in \mathcal{N}_i} 1/R_{ij} = g_i - \sum_{j \in \mathcal{N}_i} g_{ij}$. If there is no connection between two nodes i and j , namely $j \notin \mathcal{N}_i$, then $g_{ij} = 0$. If node i does not contain a shunt conductance, then $g_i = 0$. Note that G as a loopy Laplacian matrix [60], makes the system (5.3) a non-linear consensus algorithm [70].

5.2.4 Additional Model Conventions

It is important to mention that the power injection P_i is positive for generators and negative for loads. The node sequence in the proposed network topology consists of the loads first and then the generators and the main grid, yielding a voltage vector $V = [V_1, V_2, \dots, V_l, V_{l+1}, V_{l+2}, \dots, V_n]^T$, where l is the number of loads in the network, and the n th node corresponds to the main grid. We can freely denote the power contributed by the main grid that the network is connected to as $P_{mg} = P_n$.

5.2.5 P-V Droop Controller

Following the architecture of modern smart-grids [97], it is considered that the micro-grid is dominated by inverter- and rectifier-interfaced units, i.e. both generators and loads, operating under the droop control concept to support the grid. Due to the resistive nature of low-voltage AC micro-grids, the P-V droop controller should be adopted [72]; hence the voltage dynamics for every node take the following form:

$$\tau_v \dot{V} = (V^* \mathbf{1}_{n \times 1} - V) - k(P - P^{set}), \quad (5.4)$$

where $\tau_v = \text{diag}(\tau_{v_i})$ and $k = \text{diag}(k_i)$ are diagonal matrices containing all the nodes' voltage time constants and power droop coefficients respectively, V^* is the rated voltage value and P^{set} a vector representation of the reference power either demanded or generated that is set for each node by a supervisory controller.

The vector P^{set} contains consumption rated values P_i^{Lrated} , $\forall i \in \mathcal{V}_L$. For configurations where the main grid is included, $P_{mg}^{set} = P_{mg}^{Lrated} = 0$ in order to supply any additional demand to the micro-grid or absorb any excess generation. For practicality and to generalize, we are including such node for the remainder of this chapter. Substituting

(5.3) in (5.4), we obtain the dynamics for the resistive network:

$$\dot{V} = -\tau_v^{-1}V - k\tau_v^{-1}[V]GV + \tau_v^{-1}V^*\mathbf{1}_{n \times 1} + k\tau_v^{-1}P^{set}. \quad (5.5)$$

Now we are ready to state our problem formulation.

5.3 Problem Formulation

We will incorporate a Stackelberg game-based pricing scheme, novel in the field of micro-grids. Where we consider the existence of a supplier of electricity and l -consumers. The supplier can be represented by a distribution network operator (DNO) or an independent system operator (ISO) that possesses a distributed set of generators. The set of consumers are represented by the controllable responsive load nodes included in (5.5). The generators take various P^{set} values, obtained by a supervisory controller or a maximum power point tracking algorithm, that concurrently generate different costs to the supplier, triggering a change of price. This in consequence shifts the demand in the consumer load. Such change of P^{set} in the supplier's generators exemplifies a variation of the power outputted by renewable resources.

Following from Chapter 4, both suppliers and consumers are modelled to be price-taking, profit-maximizing agents [3, 6]. We refer to *profit* in monetary terms as the remainder of the earnings minus the costs of generating/consuming power. In order to maximize their profit, the supplier wants to use a price as large as possible and the consumers want to consume as much as they can afford with the announced price. The output of the supplier is the price Λ which is determined by a function $\Gamma(\cdot)$ called an *incentive strategy*, and the output of the consumer is a shift on consumption D_i^{set} , these are selected as the quantities that maximize their profit functions Π_S and Π_C respectively [6]. Let us reserve the full game explanation together with the incentive strategy $\Gamma(\cdot)$ in Section 5.4.2.

We have now defined both the pricing scheme and the micro-grid network dynamics (5.5). We will use the announced price and the decided demand to obtain the stability conditions for the integrated system in a closed-loop configuration, this includes the droop control, load dynamics, and the tension between supplier and consumers.

5.4 System Integration and Stability Analysis

In this section, first we make a brief introduction to the pricing mechanism and explain our proposed variation. Secondly, we explain how the physical model is subjected to the outcome of the price change and obtain the conditions for stability. Thirdly, we formulate in detail the equations involved and demonstrate the existence and expression for the resulting equilibrium points. Finally, we show the influence of such equilibrium points on the dynamics of the physical system.

5.4.1 Consumer and Supplier Functions

Having described the physical dynamics and the problem formulation, let us continue with the game theoretical part of our problem.

The value function of a consumer in the grid is denoted by $v(\cdot)$, which represents the value obtained by utilizing a quantity of electricity. Analogously, the supplier has a production cost function $c(\cdot)$. Following [3, 6], we invoke the following assumption

Assumption 7. *The functions $c(\cdot): \mathbb{R} \rightarrow \mathbb{R}$ and $v(\cdot): \mathbb{R} \rightarrow \mathbb{R}$ are continuous, monotonically increasing. In addition, they are convex and concave respectively.*

For the sake of brevity and with some abuse of notation, let us facilely denote the game and the ways in which outputs Λ and D_i^{set} are calculated:

$$\begin{aligned}\Lambda = \Gamma(\cdot) &= \arg \max_{\Gamma} \Pi_S(\Gamma), \\ &= \arg \max_{\Gamma} \Lambda P_S - c(\Gamma),\end{aligned}\tag{5.6}$$

for the supplier, and

$$\begin{aligned}D_i^{set} &= \arg \max_{D_i^{set}} \Pi_C(D_i^{set}), \\ &= \arg \max_{D_i^{set}} v(D_i^{set}) - \Lambda P_C, \forall i \in \mathcal{V}_L\end{aligned}\tag{5.7}$$

for each consumer, where P_S is the total power supplied by the supplier and P_C the power consumed by a consumer i . The optimal solution is unique for every time the game is played, which is done iteratively. The earnings of the supplier are denoted by the product ΛP_S and the money paid by the consumer as ΛP_C . It can also be seen

from (5.6) that Γ is a functional that has the consumption as parameter and is output from the corresponding optimization problem, this will enable the introduction of offers (as seen in Chapter 4) or a personalized price.

The inclusion of both simultaneous maximization problems motivates the use of game-theoretical concepts such as the Stackelberg game equilibrium, which we will analyze whilst we fully formulate the profit functions of the game in the following section.

5.4.2 Stackelberg Game Formulation

As previously discussed in Chapter 4, the Stackelberg game refers to a hierarchical structure, according to which there is a leader and there are followers (in our case a supplier and consumers respectively). The system setup introduced in this chapter accommodates such a structure where the leader plays first, and the output of the consumer depends on the announced output of the supplier. The supplier in turn has selected its output as the best one from a set.

As introduced in Chapter 4, setting the output of the leader to be a function enables the existence of multiple equilibrium points [36,92]. This allows the follower to decide on an output that aligns with its necessities. This is the main advantage of this variation of the game, where instead of a unique equilibrium point, the follower can select its best response from the multiple options yielded by the announced incentive; all while the game is at an equilibrium.

For the sake of tractability, let us define the incentive strategy $\Gamma(\cdot)$ as the following assumption, however, without loss of generality, other types of strategies/functions can be selected in a similar manner.

Assumption 8. *The incentive strategy $\Gamma(\cdot)$ is a linear function and is given by*

$$\Gamma(P_i^L) := \Lambda_i = \gamma P_i^L, \quad (5.8)$$

where γ is a positive scalar gain. The endogenous variable P_i^L is the power consumed by load i that is being measured the moment before the game is played. Namely, an instant measurement of the system state P_i .

The above can be interpreted as a function for a *personalized* price Λ_i that depends

on how much power each consumer is using, in simpler terms the strategy can represent an *offer* that *incentivizes* consumption, where the offer can take the form of the proposed $\Gamma(\cdot)$ function. This is a sensible assumption since the price would be calculated proportionally to the demand, as is generally utilized in the literature about demand management [31], incentive strategies [42, 92], and dynamic pricing [43].

The gain γ is defined as strictly positive in our setup since a negative value would represent the supplier paying the consumer. For consistency and as in the previous chapter we will refer to γ as *incentive value*.

Let us introduce the quantity P_G which is the total power supplied by the supplier's generators in the network. This does not include the main grid in node n , namely $P_G = \sum_{i \in \mathcal{V}_G \setminus n} P_i$. The power lost in the distribution lines of the network P_{loss} is the remainder of all the power generated minus the sum of measured powers on the nodes. This is calculated as $P_{loss} = \sum_{i \in \mathcal{V}_G} P_i - |\sum_{i \in \mathcal{V}_L} P_i|$.

Remark 5. *For the sake of simplicity we use the above expression to obtain a measure of the power losses, however, the power loss can also be calculated as $P_{loss} = \sum_{i \in \mathcal{V}_G} V_i^2 g_{ii}$; we avoid the use of such expression since it involves the system's state vector.*

As mentioned in Section 5.4.1, from (5.8), the money paid by the consumer i is rewritten as $\gamma P_i^L (D_i^{set} + P_i^{Lrated})$ and the earnings of the supplier as $\gamma \sum_{i \in \mathcal{V}_L} (P_i^L)^2$; both quantities are equal to the price times the respective power consumption/supply. The remaining elements of (5.6) and (5.7) are explained as follows. We define both cost and value functions of the supplier and consumers respectively as

$$c(\cdot) := c(\gamma, P_G, P_{mg}, P_{loss}) = \alpha_G (\gamma P_G)^2 + \alpha_G (\gamma P_{loss})^2 + \alpha_{mg} (\gamma P_{mg})^2, \quad (5.9)$$

$$v(\cdot) := v(D_i^{set}) = \alpha_{Ci} \ln(P_i^{Lrated} + D_i^{set}), \quad (5.10)$$

where it is clear that $c(\cdot)$ and $v(\cdot)$ are convex and concave respectively [6], α_G is a scalar gain directly associated with the cost of running/operating the supplier's own network generators, and α_{mg} is associated with the cost of borrowing power from the main grid. Both positive scalars are selected and derived exogenously according to various factors such as market conditions, time of the year, etc. Analogously, α_{Ci} represents each consumer's own predilection in consuming power. As their names suggest, the cost and value functions represent monetary quantities for the players and the above gains

are used to also adjust such functions' units. All the above yields the maximization problems and profit functions now rewritten as:

$$\begin{aligned} & \arg \max_{\gamma} \gamma \sum_{i \in \mathcal{V}_L} (P_i^L)^2 - c(\gamma, P_G, P_{mg}, P_{loss}), \\ & \arg \max_{D_i^{set}} v(D_i^{set}) - \gamma P_i^L (D_i^{set} + P_i^{Lrated}), \forall i \in \mathcal{V}_L \end{aligned} \quad (5.11)$$

for the supplier and each of the consumers respectively. Where the supplier computes and announces an incentive γ that consequentially results in l output prices Λ_i ; with it, the consumers calculate a power shift D_i^{set} . The existence of the Stackelberg equilibrium points from the game (5.11) is demonstrated as follows.

Theorem 11. *Let Assumption 8 hold and considering the cost and value functions (5.9)-(5.10) in the maximization problem (5.11), the Stackelberg game yields the following equilibrium points as functions of γ :*

$$\Lambda_i^* = \gamma P_i^L, \quad (5.12)$$

$$D_i^{set*} = \frac{\alpha_{Ci}}{\gamma P_i^L} - P_i^{Lrated}. \quad (5.13)$$

Proof. Due to the concavity of (5.10), the follower's maximum is obtained by taking the derivative of Π_C in (5.11) and setting it equal to zero,

$$\frac{\partial \Pi_C}{\partial D_i^{set}} = \alpha_{Ci} \frac{1}{D_i^{set} + P_i^{Lrated}} - \gamma P_i^L = 0. \quad (5.14)$$

The derivative (5.14) yields a function of both player outputs as in a standard Stackelberg game, from (5.8) and solving for D_i^{set} in (5.14) yields the conditions in (5.12)-(5.13). \square

The game is played every determined period of time T_S . The resulting D_i^{set} from the maximization problems (5.11) is then filtered through the first-order system (5.15), feeding back the consumptions as will be explained in Section 5.4.3.

Now that the pricing mechanism has been defined, emphasis will be given to establishing the stability conditions for the physical system, where the input is the shift on consumption D_i^{set} from above.

5.4.3 Closed Loop Configuration

After each consumer i has decided how much to shift its consumption, namely all D_i^{set} values for each load node have been outputted by the game, these are reflected in the micro-grid system by feeding them back into it. Although a decision of how much power a load should be consuming is taken every time step a price is announced, the load introduces a dynamic response. This is captured by a first-order dynamics as follows

$$\tau_i \Delta \dot{P}_i^L = D_i^{set} - \Delta P_i^L, \forall i \in \mathcal{V}_L, \quad (5.15)$$

where $\tau_i \in \mathbb{R}_{>0}$ is the time constant of the system and ΔP_i^L our new consumption shift state. This represents the consumers' response while they shift their consumption before reaching their selected value D_i^{set} [30,92]. From (5.15) it is straightforward to show that at steady-state $\Delta P_i^{L,ss} = D_i^{set}$. Similar demand response modeling is often found in the literature, such as [44–46].

The way in which our system is subjected to the price change comes by integrating the dynamics (5.5)-(5.15). This yields a state vector with the form $[V_1, \dots, V_n, \Delta P_1^L, \dots, \Delta P_n^L]^T$. The added states ΔP_i^L are subtracted to their respective load node powers in the vector P^{set} in (5.5), yielding $P_i^{set} = P_i^{L,rated} - \Delta P_i^L$ if $i \in \mathcal{V}_L$. In other words, the resulting shift of demand given a new price is reflected by modifying the rated load values. For each of the load nodes, the dynamics (5.5) are now modified as follows:

$$\begin{aligned} \dot{V}_i = & -\frac{1}{\tau_{vi}} V_i - \frac{k_i}{\tau_{vi}} V_i^2 g_{ii} - \frac{k_i}{\tau_{vi}} V_i \sum_{j \in \mathcal{N}_i} V_j g_{ij} \\ & + \frac{k_i}{\tau_{vi}} (P_i^{L,rated} - \Delta P_i^L) + \frac{1}{\tau_{vi}} V_i^*, \forall i \in \mathcal{V}_L \end{aligned} \quad (5.16)$$

For the rest of the nodes, namely generator nodes and the main grid node, their dynamics are left unchanged as in (5.5), for the sake of completeness, let us write their dynamics as

$$\begin{aligned} \dot{V}_i = & -\frac{1}{\tau_{vi}} V_i - \frac{k_i}{\tau_{vi}} V_i^2 g_{ii} - \frac{k_i}{\tau_{vi}} V_i \sum_{j \in \mathcal{N}_i} V_j g_{ij} \\ & + \frac{k_i}{\tau_{vi}} P_i^{set} + \frac{1}{\tau_{vi}} V_i^*, \forall i \in \mathcal{V}_G. \end{aligned} \quad (5.17)$$

Now that we have the full dynamics of the system subject to the change of demand due

to an announced price, we can perform a stability analysis.

5.4.4 Closed-Loop Stability

Due to the non-linear nature of (5.15)-(5.17), in the sequel we recur to the method of linearizing around an equilibrium, this provides local stability results.

Calculating the Jacobian of (5.15)-(5.17) we analyze the system under the assumption of the existence of an equilibrium point; we follow the methodology for resistive networks as in [71] and references therein. We also resort to [98, Theorem 1] which states that a non-linear circuit system is to be studied near the equilibrium via linearization for $V \in \mathbb{R}_{>0}$; which is true for our case. Hence, let us state our equilibrium as follows:

Assumption 9. *For constant inputs $D_i^{set} \forall i \in \mathcal{V}_L$ and $P_i^{set} \forall i \in \mathcal{V}_G$ with $P_{mg}^{set} = 0$, there exists an equilibrium point $[\bar{V}_1, \dots, \bar{V}_n, \Delta \bar{P}_1^L, \dots, \Delta \bar{P}_1^L]^T$ for system (5.15)-(5.17), where $\bar{V}_i \in \mathbb{R}_{>0}$ and $\Delta \bar{P}_i^L \in \mathbb{R}$.*

Although the droop control model is standard, the above assumption might seem initially as strong. We utilize it for simplicity as means to approximate the position of the system eigenvalues. This assumption will be relaxed in Section 5.4.5, Assumption 10. We should mention that in a practical scenario, the droop controller has to be designed in a way such that it outputs positive voltage values [20, 64]. Additionally, the fact that the output voltages are at an equilibrium larger than zero, implies that the system operates correctly. We demonstrate stability from the existence of the equilibrium with the Jacobian.

Theorem 12. *Let Assumption 9 hold and given a shift on consumption ΔP_i^L in each load node, system (5.15)-(5.17) is asymptotically stable at the equilibrium point if*

$$\begin{aligned} -1 - k_i \left(2 \frac{\bar{V}_i}{R_{ii}} + \sum_{j \in \mathcal{N}_i} \frac{\bar{V}_i - \bar{V}_j}{R_{ij}} \right) &< 0, \text{ for } i \in \mathcal{V}_G, \\ -1 - k_i \left(2 \frac{\bar{V}_i}{R_{ii}} + \sum_{j \in \mathcal{N}_i} \frac{\bar{V}_i - \bar{V}_j}{R_{ij}} - 1 \right) &< 0, \text{ for } i \in \mathcal{V}_L. \end{aligned} \quad (5.18)$$

Proof. Calculating the Jacobian of system (5.16)-(5.15) with respect to the states V_i and

ΔP_i^L , yields the following $(n+l) \times (n+l)$ matrix

$$J = \begin{bmatrix} J^V & -k\tau_v^{-1} \\ \mathbf{0}_{(n-l) \times l} & \\ \mathbf{0}_{l \times n} & -\tau^{-1} \end{bmatrix}, \quad (5.19)$$

where $\tau = \text{diag}(\tau_i)$ is an $l \times l$ matrix, and J^V is the $n \times n$ matrix corresponding to the Jacobian of the open loop voltage dynamics (5.5) with respect to the state vector V :

$$J^V = -\tau_v^{-1} - k\tau_v^{-1}([\bar{V}]G + [G\bar{V}]), \quad (5.20)$$

which is comprised of diagonal elements

$$J_{ii}^V = -\frac{1}{\tau_{vi}} - 2\frac{k_i}{\tau_{vi}}\bar{V}_i g_{ii} - \frac{k_i}{\tau_{vi}} \sum_{j \in \mathcal{N}_i} \bar{V}_j g_{ij}, \quad (5.21)$$

and non-diagonal elements

$$J_{ij}^V = -\frac{k_i}{\tau_{vi}} \bar{V}_i g_{ij}. \quad (5.22)$$

To obtain the stability conditions, the eigenvalues of our linearized system J should be obtained. However, due to the size of J , the analytic calculation of the eigenvalues is a daunting task. Let us employ the Gershgorin disc theorem to approximate the position of such eigenvalues within the complex plane.

From Assumption 9, a disc Δ_i can be defined for each row i in J , this will encircle the position of the eigenvalue λ_i , such disc is centered at $C_i = J_{ii}$ along the real axis with a radius $R_i = \sum_{j \in \mathcal{N}_i} |J_{ij}|$.

At the equilibrium point, for the i th voltage state of the system, its disc $\Delta_i(C_i, R_i)$ is defined for non-load nodes as

$$\Delta_i\left(-\frac{1}{\tau_{vi}} - 2\frac{k_i}{\tau_{vi}}\bar{V}_i g_{ii} - \frac{k_i}{\tau_{vi}} \sum_{j \in \mathcal{N}_i} \bar{V}_j g_{ij}, \sum_{j \neq i \in \mathcal{N}_i} \left| -\frac{k_i}{\tau_{vi}} \bar{V}_i g_{ij} \right| \right), \text{ for } i \in \mathcal{V}_G, \quad (5.23)$$

and if i is a load node as

$$\Delta_i\left(-\frac{1}{\tau_{vi}} - 2\frac{k_i}{\tau_{vi}}\bar{V}_i g_{ii} - \frac{k_i}{\tau_{vi}} \sum_{j \in \mathcal{N}_i} \bar{V}_j g_{ij}, \sum_{j \in \mathcal{N}_i} \left| -\frac{k_i}{\tau_{vi}} \bar{V}_i g_{ij} \right| + \left| -\frac{k_i}{\tau_{vi}} \right| \right), \text{ for } i \in \mathcal{V}_L. \quad (5.24)$$

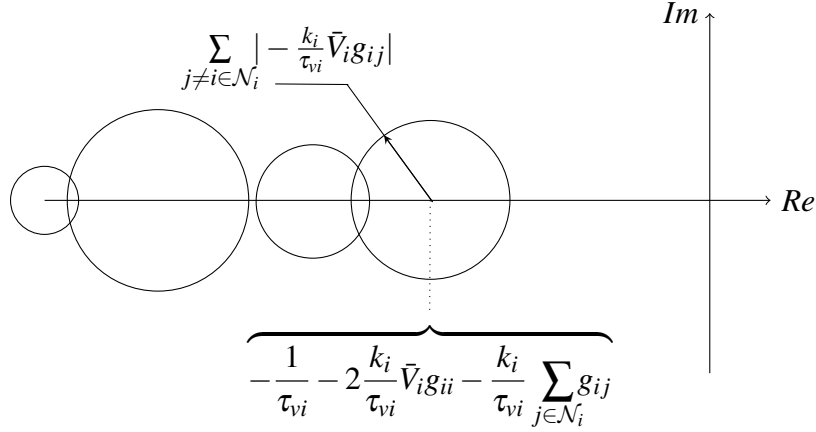


Figure 5.2: Gershgorin disc configuration example, center and radius for the i th disc of J .

Figure 5.2 illustrates a possible configuration of such discs. Taking into account the properties of G mentioned in Section 5.2.3, the expression of $\Delta_i(C_i, R_i)$ is simplified as:

$$\Delta_i\left(-\frac{1}{\tau_{vi}} - 2\frac{k_i}{\tau_{vi}}\bar{V}_i g_{ii} - \frac{k_i}{\tau_{vi}} \sum_{j \in \mathcal{N}_i} \bar{V}_j g_{ij}, \frac{k_i}{\tau_{vi}} \bar{V}_i g_{ii} - \frac{k_i}{\tau_{vi}} \bar{V}_i g_i\right), \text{ if } i \in \mathcal{V}_G \quad (5.25)$$

$$\Delta_i\left(-\frac{1}{\tau_{vi}} - 2\frac{k_i}{\tau_{vi}}\bar{V}_i g_{ii} - \frac{k_i}{\tau_{vi}} \sum_{j \in \mathcal{N}_i} \bar{V}_j g_{ij}, \frac{k_i}{\tau_{vi}} \bar{V}_i g_{ii} - \frac{k_i}{\tau_{vi}} \bar{V}_i g_i + \frac{k_i}{\tau_{vi}}\right), \text{ if } i \in \mathcal{V}_L. \quad (5.26)$$

For the system to be stable, the eigenvalues of the system have to be positioned in the left-hand-side of the complex plane, namely $\Re(\lambda_i) < 0$. To guarantee this, the entirety of all Gershgorin discs should be in the left-hand-side of the complex plane, namely $C_i + R_i < 0$, this yields

$$\begin{aligned} & -\frac{1}{\tau_{vi}} - \frac{k_i}{\tau_{vi}} \bar{V}_i g_{ii} - \frac{k_i}{\tau_{vi}} \sum_{j \in \mathcal{N}_i} \bar{V}_j g_{ij} - \frac{k_i}{\tau_{vi}} \bar{V}_i g_i < 0, \text{ for } i \in \mathcal{V}_G, \quad (5.27) \\ & -\frac{1}{\tau_{vi}} - \frac{k_i}{\tau_{vi}} \bar{V}_i g_{ii} - \frac{k_i}{\tau_{vi}} \sum_{j \in \mathcal{N}_i} \bar{V}_j g_{ij} - \frac{k_i}{\tau_{vi}} \bar{V}_i g_i + \frac{k_i}{\tau_{vi}} < 0, \text{ for } i \in \mathcal{V}_L, \end{aligned}$$

simplifying the expressions above, the two conditions in (5.18) are obtained. Additionally, from J , the ΔP_i^L states yield l stable eigenvalues $\lambda_i = -1/\tau_i$, which is a straightforward result since the time constants are always positive. \square

Remark 6. In the case where all of the node voltages have approximately the same value at the steady-state, i.e. $\bar{V}_i \approx \bar{V}_j$, and the shunt conductances are small enough to

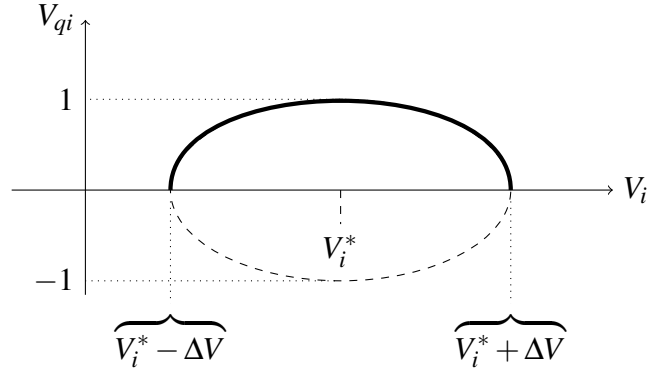


Figure 5.3: Bounded droop controller phase portrait example.

be neglected $1/R_{ii} \approx 0$, condition (5.18) is simplified even further, yielding:

$$k_i < 1 \quad (5.28)$$

this is a stronger assumption to the case studied. However, in practice $k_i = pV_i^*/P_i^{rated} \forall i$, where p is a percentage deviation of the node voltage that corresponds to 100% deviation of the real power, according to the droop control concept. The above result (5.28) yields the inequality $pV^* < P_i^{rated}$, which aligns with the low voltage network assumption.

5.4.5 Implementing a Bounded Droop Control Architecture

It should be highlighted that in a real scenario, it is a requirement that the instantaneous node voltages remain within a given set, usually $V_i \in (V_i^* - \Delta V, V_i^* + \Delta V) \forall t \geq 0$ where ΔV is a deviation value of around 5 to 10 % from the rated voltage, namely $\Delta V = 0.05V^*$. Then, according to [73] we can use the bounded droop controller (BDC) to guarantee such outputs, this is based on the bounded integral control theory from [74]; a characteristic of this is that it still maintains the linear P-V controller approach [72] while generating a bounded output. The above is achieved by introducing a second controller state V_q , hence the voltage dynamics for all the nodes take the following

form:

$$\dot{V} = c\tau_v^{-1}((V^*\mathbf{1}_{n \times 1} - V) - k([V]GV - P^{set}))V_q^2, \quad (5.29)$$

$$\begin{aligned} \dot{V}_q = & -c\tau_v^{-1} \frac{V_q(V - V^*\mathbf{1}_{n \times 1})}{\Delta V^2} (V^*\mathbf{1}_{n \times 1} - V - k([V]GV - P^{set})) \\ & + k^I \left(\frac{(V - V^*\mathbf{1}_{n \times 1})^2}{\Delta V^2} + V_q^2 - \mathbf{1}_{n \times 1} \right) V_q. \end{aligned} \quad (5.30)$$

where V_q is a vector with the same dimensions as V , $c = \text{diag}(c_i)$ and $k^I = \text{diag}(k_i^I)$ are matrices of positive constant gains for the integral control. The yielded state vector has the form $[V_1, \dots, V_n, V_{q1}, \dots, V_{qn}, \Delta P_1^L, \dots, \Delta P_l^L]^T$. With the addition of V_q , it can be seen from (5.29)-(5.30) that the controller is comprised of a non-linear double integrator structure, thus acting as an oscillator [73] and fulfilling the objective of emulating the dynamics of RMS voltage. Figure 5.3 illustrates the ways in which the values of the states V_i and V_{qi} start and remain in the upper part of the ellipse formed by the term $k^I \left(\frac{(V - V^*\mathbf{1}_{n \times 1})^2}{\Delta V^2} + V_q^2 - \mathbf{1}_{n \times 1} \right)$ in (5.30). The above has been previously demonstrated in detail in [74].

The closed-loop configuration of (5.29)-(5.30) for load nodes is now derived as

$$\dot{V}_i = \frac{c_i}{\tau_{vi}} (V_i^* - V_i - k_i(V_i g_{ii} + V_i \sum_{j \in \mathcal{N}_i} V_j g_{ij} - P_i^{set} + \Delta P_i^L)) V_{qi}^2, \forall i \in \mathcal{V}_L, \quad (5.31)$$

$$\begin{aligned} \dot{V}_{qi} = & -\frac{c_i}{\tau_{vi}} \frac{V_{qi}(V_i - V_i^*)}{\Delta V^2} (V_i^* - V_i - k_i(V_i g_{ii} + V_i \sum_{j \in \mathcal{N}_i} V_j g_{ij} - P_i^{set} + \Delta P_i^L)) \\ & + k_i^I \left(\frac{(V_i - V_i^*)^2}{\Delta V^2} + V_{qi}^2 - 1 \right) V_{qi}, \forall i \in \mathcal{V}_L, \end{aligned} \quad (5.32)$$

the equations for generator nodes can be obtained similarly as in Section 5.4.3. The implementation of the BDC into our system dynamics also guarantees the existence of equilibrium points within selected bounds. With the introduction of the bounded voltage dynamics, we can now relax Assumption 9 and present the result that follows.

Assumption 10. For constant inputs $D_i^{set} \forall i \in \mathcal{V}_L$ and $P_i^{set} \forall i \in \mathcal{V}_G$ with $P_{mg}^{set} = 0$, there exists an equilibrium point $[\bar{V}_1, \dots, \bar{V}_n, \bar{V}_{q1}, \dots, \bar{V}_{qn}, \Delta \bar{P}_1^L, \dots, \Delta \bar{P}_l^L]^T$ for system (5.15)-(5.29)-(5.32), where $\Delta \bar{P}_i^L \in \mathbb{R}$, $\bar{V}_i \in \mathbb{R}_{>0}$, $\bar{V}_i \in (V^* - \Delta V, V^* + \Delta V)$ and $\bar{V}_{qi} \in (-1, 1)$.

This enables the system to be stable without depending on the existence of equilibrium points but only on rated and tuned parameters:

Proposition 1. *Let Assumption 10 hold and given a shift on consumption ΔP_i^L in each load node, system (5.15)-(5.29)-(5.32) is asymptotically stable at an equilibrium point if*

$$-1 - k_i \left(2 \frac{V_i^* - \Delta V}{R_{ii}} - 2 \Delta V \sum_{j \in \mathcal{N}_i} \frac{1}{R_{ij}} \right) < 0, \quad \forall i \in \mathcal{V}. \quad (5.33)$$

Proof. Denoting the V_q dynamics (5.30)-(5.32) as $f(V, V_q, \Delta P^L)$ and calculating the Jacobian of system (5.15)-(5.29)-(5.32) with respect to the states V_i , V_{qi} and ΔP_i^L , yields the following $(2n + l) \times (2n + l)$ matrix

$$J^{BDC} = \begin{bmatrix} \Phi J^V & \mathbf{0}_{n \times n} & -\Phi \kappa \\ \frac{\partial f}{\partial V} \Big|_{\bar{V}, \Delta \bar{P}^L} & -[2k_i^I \bar{V}_{qi}^2] & \frac{\partial f}{\partial \Delta P^L} \Big|_{\bar{V}, \Delta \bar{P}^L} \\ \mathbf{0}_{l \times n} & \mathbf{0}_{l \times n} & -\tau^{-1} \end{bmatrix} \quad (5.34)$$

where κ is the $n \times l$ matrix $\kappa = [k\tau_v^{-1}, \mathbf{0}_{(n-l) \times l}]^T$ and Φ is a $n \times n$ matrix $\Phi = [c_i V_{qi}^2]$. For the stability conditions, the eigenvalues λ_i of linearized J^{BDC} are calculated. These are the roots of the polynomial yielded by the determinant

$$|\lambda I - J^{BDC}| = |\lambda I + [2k_i^I V_{qi}^2]| |\lambda I - \Phi J^V| |\lambda I + \tau^{-1}|, \quad (5.35)$$

using the properties of block matrices to (5.35), it is trivial to see that the $n + l$ eigenvalues yielded by both matrices $[2k_i^I V_{qi}^2]$ and τ^{-1} are negative and real due to that all their values are positive. Leaving only to find the eigenvalues of ΦJ^V . We can discard Φ and focus only on J^V since all values of $c_i V_{qi}^2$ are positive as well.

Similarly as in Section 5.4.3, computing the Gershgorin discs $\mathbf{\Delta}_i(C_i, R_i)$ of J^V with $C_i = J_{ii}^V$ and $R_i = \sum_{j \in \mathcal{N}_i} |J_{ij}^V|$, the following condition is yielded by shifting the entirety of disc $\mathbf{\Delta}_i$ to the left-hand-side of the complex plane:

$$-\frac{1}{\tau_{vi}} - \frac{k_i}{\tau_{vi}} \bar{V}_i g_{ii} - \frac{k_i}{\tau_{vi}} \sum_{j \in \mathcal{N}_i} \bar{V}_j g_{ij} - \frac{k_i}{\tau_{vi}} \bar{V}_i g_i < 0, \quad \forall i \in \mathcal{V}. \quad (5.36)$$

Simplifying the expression above, we can substitute \bar{V}_i and \bar{V}_j to the value that yields a disc closer to the origin. The worst-case scenarios for such values are $\bar{V}_i = V_i^* - \Delta V$ and $\bar{V}_j = V_j^* + \Delta V$. By doing this we obtain the sufficient condition (5.33). \square

Note that condition (5.33) can be easily checked since it does not require the calculation of the equilibrium point.

Now that the conditions for the stability of the integrated system have been explained, let us briefly focus on the ways in which the outcome of the game influences the physical system output. After each play of the game, it can be demonstrated that the physical dynamic's equilibrium points depend directly on the game's output values. This can be corroborated as follows.

Remark 7. *The steady-state expression for dynamics (5.15) of node $i \in \mathcal{V}_{\mathcal{L}}$ can be formulated as a function of the Stackelberg equilibrium parameters, namely*

$$V_i^{ss} = f(\gamma, P_i^L, \alpha_{Ci}). \quad (5.37)$$

Once the consumers have decided their consumption and their demand has shifted, the dynamics (5.15) - (5.16) are considered to be at steady-state. From there the following expressions are obtained

$$V_i^{ss} = k_i(P_i^{Lrated} - \Delta P_i^{Lss}) - k_i P_i + V_i^*, \quad (5.38)$$

$$\Delta P_i^{Lss} = D_i^{set}, \quad (5.39)$$

where P_i is shorthand for the static expression (5.2) at the equilibrium point. Substituting (5.13) into (5.39) yields

$$\Delta P_i^{Lss} = \frac{\alpha_{Ci}}{\gamma P_i^L} - P_i^{Lrated}, \quad (5.40)$$

this can be freely substituted into (5.38), resulting in the simplified expression

$$V_i^{ss} = k_i(2P_i^{Lrated} - \frac{\alpha_{Ci}}{\gamma P_i^L}) - k_i P_i + V_i^*, \quad (5.41)$$

which can be presented as the function in (5.37). It is worth mentioning that the steady-state of the system will change value once the game has been played again, this is further exemplified in the numerical examples in the next section. The above derivations can be done similarly for the system subject to the bounded droop control presented in Section 5.4.5.

5.5 Numerical Examples

In this section, we demonstrate two scenarios. In the first, we show how a single load behaves when subject to the incentive strategy, while in the second we show a configuration with two loads, both are implemented using the bounded droop control on Simulink.

In the first scenario the micro-grid consists of the following elements: one load (node 1), two generators (nodes 2 and 3), and the micro-grid is connected to the main grid (node 4). The parameters are selected as follows: droop control time constant $\tau_{vi} = 0.1\text{s}$, load response time constant $\tau_i = 3\text{s}$, nominal voltage $V_i^* = 220\text{V}$, maximum selected voltage deviation $\Delta V = 11\text{V}$, desired power references at each node $P^{set} = [-6.0, 3.5, 2.5, 0]^T \text{kW}$. The integral gains are selected as $k_i^I = 1$, the droop coefficients are calculated in a standard fashion as $k_i = 0.05V_i^*/P_i^{rated}$ for all nodes, where $P^{rated} = [10.0, 7.0, 5.0, 3.0]^T \text{kW}$ is the rated power vector. The network topology is given by the conductances in G , $g_{12} = g_{21} = -5\text{S}$, $g_{13} = g_{31} = -4.167\text{S}$, $g_{14} = g_{41} = -4.545\text{S}$, $g_{23} = g_{32} = -4.347\text{S}$, $g_{24} = g_{42} = -4.761\text{S}$, $g_{34} = g_{43} = -4\text{S}$, and shunt conductances $g_i = 0.6\text{S}$. The value function gain is set to $\alpha_C = 29 \times 10^6 \text{\$/log(W)}$ while the cost function gains have been set to $\alpha_G = 11\text{W}^2/\text{\$}$ and $\alpha_{mg} = 2\text{W}^2/\text{\$}$. These are selected in a way that illustrates that is more costly to use power from the main grid. The initial value of the incentive is set to $\gamma = 0.036 \text{\$/W}^2$. For example purposes, without loss of generality, we have selected the game to be played every $T_S = 60\text{s}$ in which a new γ is calculated. The consumption ΔP_1^{set} is calculated at $T_C = 62\text{s}$, meaning that the incentive is known by the consumer 2 seconds after being announced. To further illustrate the price change, during the simulation we modify the power contributed by the supplier's generators; this is achieved by modifying the generators' set powers to the values $P_2^{set} = 1.9\text{kW}, 0.1\text{kW}, 2.0\text{kW}$ at times $t = 0\text{s}, 1000\text{s},$ and 3000s respectively and $P_3^{set} = 1.5\text{kW}, 0.05\text{kW}, 2.0\text{kW}$ at times $t = 0\text{s}, 2000\text{s},$ and 3000s respectively. The total simulation time is 4000s .

Figure 5.4 shows the node's power plots, it can be seen that there is an incentive change every time the generators shift their value, in consequence, a shift in the load happens depending on how high the incentive is, if the incentive γ increases, the price increases and the consumer reduces its consumption (making it less negative in the plot). It can also be seen that a higher contribution by the main grid leads to a higher

price and vice versa. Finally, the plots show that given a change in the generators, both the incentive and the powers converge towards an equilibrium point. The voltage response stays within acceptable ranges and is mainly affected by the generator shifting as shown in Fig. 5.5, it can be verified that the droop control is successful and there is no deviation

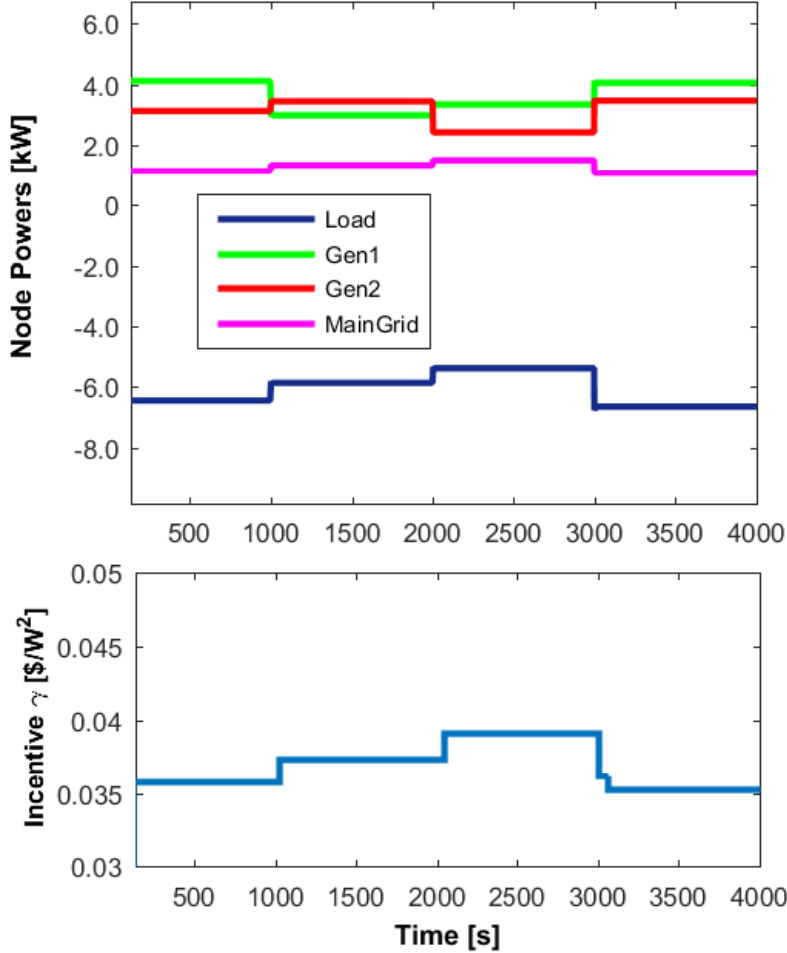


Figure 5.4: Simulation of a network connected to the main grid with one load and two varying generators.

The second scenario consists of two loads (nodes 1 and 2), two generators (nodes 3 and 4), and the main grid (node 5). The new example vectors are selected as $P^{set} = [-3.5, -3.0, 3.5, 2.5, 0]^T$ kW and $P^{rated} = [6.0, 6.0, 7.0, 6.0, 3.0]^T$. The topology is expanded from the previous with the conductances $g_{15} = g_{51} = -3.845$ S, $g_{25} = g_{52} = -3.703$ S, $g_{35} = g_{53} = -3.571$ S, $g_{54} = g_{45} = -3.448$ S. The cost function gains have been re-tuned to $\alpha_G = 9.5$ W²/\\$ and $\alpha_{mg} = 7.5$ W²/\\$, while the value function gains are set to $\alpha_{C1} = 29 \times 10^6$ \\$/log(W) and $\alpha_{C2} = 20 \times 10^6$ \\$/log(W), these have been selected to show two consumers with different interests. The generators' set powers are modified as in the previous simulation: $P_3^{set} = 1.9$ kW, 0.1kW, 2.0kW at times $t = 0$ s, 1000s, and

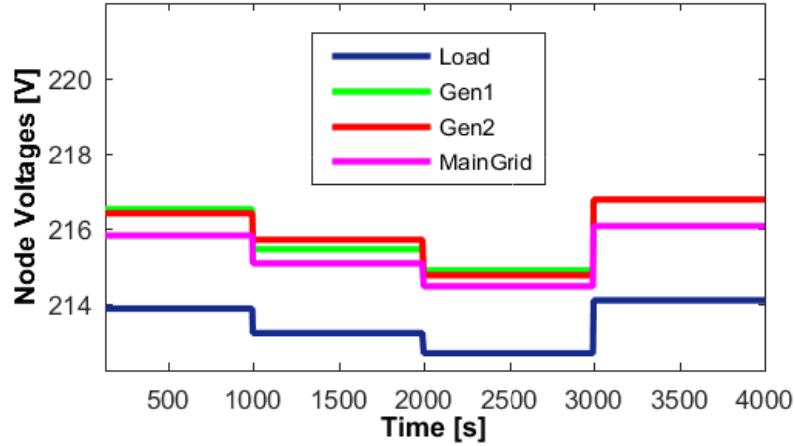


Figure 5.5: Voltage plots for the one load configuration.

3000s respectively and $P_4^{set} = 1.5\text{kW}, 0.05\text{kW}, 2.0\text{kW}$ at times $t = 0\text{s}, 2000\text{s},$ and 3000s respectively. The rest of the parameters are left as in the previous simulation.

Figure 5.6, shows the second power plots. As before, it can be seen that there is convergence towards different equilibrium points for different γ . The different consumer value gains α_{C_i} result in distinct steady-states from their equal rated consumption values. The voltage plots for the second scenario are shown in Fig. 5.7. As expected, the inclusion of another load lowers the voltages overall. However, the 5% deviation from the set voltages is still respected by the droop controller. It is also worth noting that the rational behaviour for both the supplier and the consumer has been captured: When the main grid contributes more power, its higher cost forces the supplier to increase the incentive which results in higher prices; in response, the consumer lowers its load to a point that brings better profit given the current price. The converse case when the contribution from the main grid is low, lowering the price and increasing the loads is also captured in the final part of both simulations.

As a final note, the simulation results for the system without using the bounded droop control are very similar to the ones presented and are not shown here for the sake of brevity. However, it is easy to check that condition (5.18) holds based on the parameters used above.

5.6 Conclusion

The pricing scheme based on the Stackelberg game has been refined. Differently from the normalised version of Chapter 4, it has been adapted to a more realistic setting such

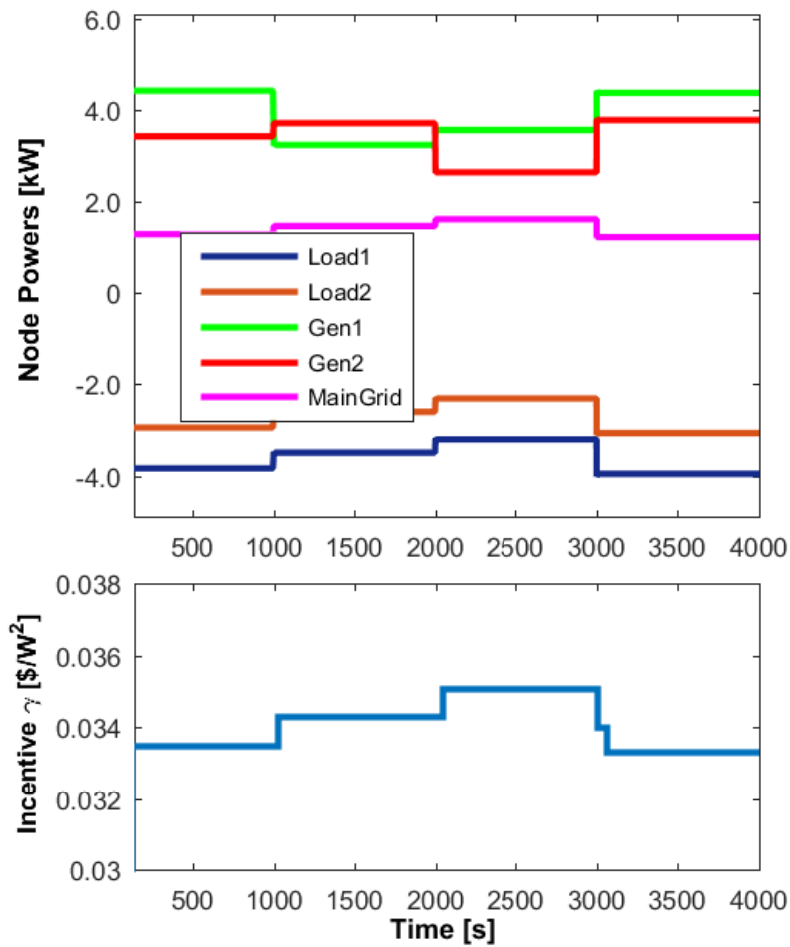


Figure 5.6: Simulation of a network connected to the main grid with two loads and two varying generators.

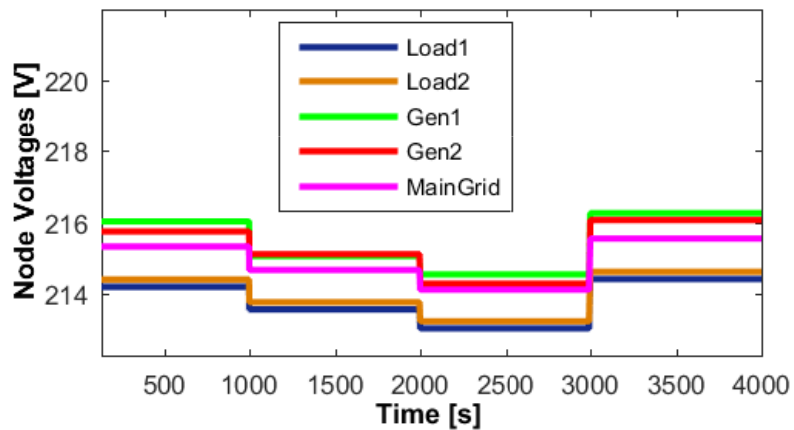


Figure 5.7: Voltage plots for the two load configuration.

as the low-voltage resistive micro-grid, integrating the market and physical components of the problem in a more fluent way. The proposed game and player models successfully capture the rationality of energy consumers. We have demonstrated the asymptotic stability conditions and adapted the parameters and functions for the implementation of the on-line pricing mechanism.

The resistive micro-grid network model introduced in this chapter, together with the derivations related to stability will be utilised for an integration with another pricing scheme based on coalitional games. For such a scheme, the consumer and supplier models presented in this chapter will also prove useful.

Chapter 6

Pricing and Stability via Coalitional Games in a Resistive Micro-Grid

6.1 Introduction

With the advent of the smart-grid paradigm, more ways to distribute power have emerged, bringing recent changes to the electricity market. Here governments and general consumers now seek and switch to better providers and sources of power that enable them to fulfil certain requirements while still being profitable. Such a paradigm has also enabled a higher degree of communication between the consumers themselves and the energy retailers, providing new set-ups where these interact and cooperate to optimize their outputs.

These aspects of switch-ability, cooperation and applicability are the main foci of this chapter, since the majority of works about coalitional game theory applied to smart-grids do not spotlight scenarios where there are multiple electricity retailers for the end-users to choose; let alone the effect of these in the physical system.

Taking the physical system and the analysis introduced in Chapter 5, we now will subject it to a novel pricing scheme where there are multiple retailers, where the Stackelberg equilibrium is also integrated. The problem statement is the following.

6.1.1 Problem Statement and Contributions

We propose a dynamic pricing scheme with multiple electricity providers or *retailers*. These compete to attract the largest number of *consumers* inside a community, which in our case is represented by a micro-grid.

When consumers choose to be provided by a particular retailer, they join the retailer's coalition. This induces a partition on the set of players, which is comprised of non-overlapping coalitions. It is understood that a coalition can accommodate only one retailer since all electricity providers are considered *quarrels*. Another underlying assumption is that both consumers and providers are price-taking rational agents that look forward to increasing their profits. Both evaluate the price of energy in their respective profit functions. The ways in which a retailer gains a consumer is by announcing its price for electricity accompanied by an incentive. The retailers adjust their prices periodically, which in consequence will cause them to lose or gain consumers, and at the same time, adjust the demand and supply of energy in the micro-grid.

Although the competition between retailers would seem fit to apply a non-cooperative game framework, the inclusion of the consumer and its choice of retailer could not be captured by this. In such a game the consumer as a player would be individually competing against the retailers and other consumers. We also aim to capture the ways in which consumers can "ally" to get a better profit by choosing a retailer in common, recalling some form of the classic "cable tv company problem" [87] from graph theory while including a market layer by taking into account profits, connection fees, potential subsidies and costs.

The main contributions of this chapter can be summarized as follows:

- A pricing scheme based on notions from coalitional games is proposed, where there are multiple competing retailers in a micro-grid. To the best of the author's knowledge, this is a novel problem setup in micro-grid literature. This is done in Section 6.2.
- In Section 6.3 a stability analysis is performed covering the coalitions formed by the proposed game and algorithm. The existence of the equilibrium points in the game is also demonstrated, namely the guaranteed existence of a consumption value given a price.

- Section 6.5 focuses on deriving the stability conditions for the physical micro-grid when subject to our pricing scheme. This is the first time in which this kind of scheme is analyzed alongside a resistive low-voltage micro-grid.
- Additionally, the basis for a novel method where a costs-saving game is linked and formulated directly from the existing physical conductance matrix of the grid is introduced.

In Section 6.6 we numerically illustrate the advantages of the scheme; the ways in which the profits of the consumers improve in comparison to a single retailer scenario is shown. Section 6.7 streamlines conclusions of this work.

6.2 System Model, Definition and Preliminaries

In this section, we introduce the ways in which both retailers and consumers are modelled. We review the concept of the Stackelberg game and recall the concepts from graph theory that will be useful for the rest of this study.

6.2.1 Sets and Coalitions Definition

To study the coalitional behaviour of our scheme, we recur to a game-theoretic framework. Let us define the universe of players in the micro-grid as \mathcal{N} which contains N players. This is partitioned into two non-overlapping sets: the set of retailers $\mathcal{R} \subset \mathcal{N}$ and the set of consumers $\mathcal{B} \subset \mathcal{N}$; where $\mathcal{R} \cup \mathcal{B} = \mathcal{N}$. For the sake of simplicity, we assume that $\mathcal{R} \cap \mathcal{B} = \emptyset$, namely a consumer cannot be a retailer and vice versa. Such sets are composed as $\mathcal{R} := \{r_1, \dots, r_p\}$ and $\mathcal{B} := \{b_1, \dots, b_l\}$, where $p + l = N$. Besides this basic partition, we seek a pairing between a retailer and a subset of consumers.

Definition 3 (Retailer's coalition). *A coalition $S_i \subset \mathcal{N}$ is given by assigning k consumers $b_j \in \mathcal{B}$ to a single retailer $r_i \in \mathcal{R}$,*

$$S_i := \{r_i, b_j, \dots, b_k\}, \forall i \in \mathcal{R}, j, k \in \mathcal{B}. \quad (6.1)$$

For the case where a retailer r_i does not succeed to attract any consumer, its coalition is reduced to a singleton $S_i = \{r_i\}$. In the problem, due to the nature of our market setup, there are underlying assumptions that need to be addressed.

Assumption 11. *Each consumer $b_j \in \mathcal{B}$ has to be assigned to one retailer at all times. As a consequence, for the union of all coalitions, it holds*

$$\bigcup_i S_i = \mathcal{N}, \forall i \in \mathcal{R}. \quad (6.2)$$

As a countermeasure, each consumer can decide to have zero consumption. This will be the case according to its profit function, as it will be explained in Section 6.2.2. Coalitions that have more than one retailer or that share consumers are considered infeasible, and this is formalized as follows.

Assumption 12. *The coalitions comply with the conditions:*

1. *Two or more retailers cannot be allocated to the same coalition since they are considered quarrels:*

$$S_i \cap \mathcal{R} \setminus r_i = \emptyset, \forall S_i \in \mathcal{N}. \quad (6.3)$$

2. *Coalitions are non-overlapping, a consumer cannot be assigned to more than one coalition:*

$$S_i \cap S_j = \emptyset, \forall S_i, S_j \in \mathcal{N}. \quad (6.4)$$

With the above, all possible coalitions are guaranteed to be feasible.

6.2.2 Consumer and Retailer Profit Functions

As touched in Chapters 4 and 5, both consumers and retailers are considered to be price-taking rational agents. Both have the objective of maximizing their profits. This is captured by their profit functions $\Pi(\cdot)$, which we will review here for the sake of convenience. Such functions represent the remaining amount of money after producing/consuming electricity and after covering the underlying production/consumption fees. For the retailer r_i this is calculated as

$$\Pi_i = \Lambda_i x - C(x), i \in \mathcal{R}, \quad (6.5)$$

where $C(\cdot)$ is a function that corresponds to the cost of producing x quantity of electricity and Λ_i is the price announced by the retailer which will be applied to its coalition.

Similarly, every consumer b_j that has opted to consume from r_i calculates its profit in accordance to

$$\Pi_j = U(x) - \Lambda_i x, \quad j \in \mathcal{B}, i \in \mathcal{R}, \quad (6.6)$$

where $U(\cdot)$ is the monetary equivalent to the utility from consuming x quantity of electricity. As in Chapter 5, Assumption 7 we assume that such utility and costs functions are monotonically increasing, while being concave and convex respectively [3, 6].

The rationale of both players in the setup of this chapter is represented by two maximization problems, the output of which is the price Λ_i for the retailer and a quantity of power consumption $P_{b_j}^d$ for the consumer; these are obtained as

$$\Lambda_i = \arg \max_{\lambda \in [\underline{\lambda}, \bar{\lambda}]} \lambda \cdot \left(\sum_{b_j \in \mathcal{S}_i} P_{b_j}^d - P_i^{loss} \right) - C(P_i^g), \quad (6.7)$$

$$P_{b_j}^d = \arg \max_{\zeta \in [\underline{\zeta}, \bar{\zeta}]} U(\zeta) - \Lambda_i \zeta, \quad (6.8)$$

where λ and ζ are the maximization argument variables for the retailer's price and power used by each consumer respectively, P_i^g is the power generated by the retailer and P_i^{loss} equals to the power losses incurred by the individual retailer in the micro-grid transmission lines. The latter two terms are measured at the moment of evaluating (6.7). \mathcal{S}_i is the coalition that contains the consumers b_j of retailer r_i ; as explained in Section 6.2.1. In the maximization problems (6.7)-(6.8), it can be seen that the retailer wishes to use the maximum price for bigger profits, and that the consumer wishes to consume accordingly to its needs given the announced price. This scenario can be accommodated in a game with a leader-follower structure. The optimal solution for (6.7)-(6.8) is unique for every time the game is played, which is done iteratively.

The consumer is expected to evaluate all the prices Λ_i announced by all retailers r_i in the micro-grid. This will determine its decision on picking a retailer, namely which coalition to join. By adding consumers to its coalition, the retailer also has to take into account the following constraint:

$$\left| \sum_{b_j \in \mathcal{S}_i} P_{b_j}^d + P_i^{loss} \right| \leq |P_i^g|, \quad (6.9)$$

meaning that the retailer cannot provide power to the consumers beyond its own power

capabilities. The dimensions of the power quantities are used in (6.9) since, as explained in Chapter 5 with the physical model, the convention is to consider generation as a positive value and consumption and losses as negative values.

6.2.3 Stackelberg Game Review

In our demand-side management problem, the consumption is regulated by means of price. Therefore, the ways in which the consumers respond to the retailers' announced price involve a hierarchical structure. This can be represented by a Stackelberg game [87], where among the players there is a *leader*, (in our case the retailers) that play first, and some *followers* (the consumers), that play their best response to the leader's action. In essence, the retailers try to maximize their profits by announcing a price which in turn is formulated as a function from the expected demand, and the consumers consume as much as possible with the given price to also maximize their profits. Such tension between leader and followers is captured by (6.7)-(6.8). When both leader and followers select their optimal outputs, it is said that the game is at an equilibrium, as will be further explained in Section 6.3.6.

6.2.4 Network Systems Review

For convenience, let us review the following concepts, which condense some notions touched previously in Chapters 3, 4 and 5. The topology of the networks described in this chapter is represented by a connected, undirected and weighted graph $\mathcal{G}_i(\mathcal{V}, \mathcal{E})$, where \mathcal{V} is the set of nodes (vertices). The set of edges $\mathcal{E} \subseteq \mathcal{V} \times \mathcal{V}$ is the set of unordered pairs $\{i, j\}$. The out-degree δ_k of a node refers to the number of edges that connect to a certain node k , which in the undirected case is equal to the number of edges that are incident to a specific node. The *minimum spanning tree* of a network refers to the subset of edges that connect all the nodes in the network, with the minimum total edge weight. The adjacency matrix corresponding to a graph \mathcal{G} is denoted by $A \in \mathbb{R}^{n \times n}$, where its ij th element A_{ij} is the corresponding edge that connects nodes i and j . The set \mathcal{A}_i refers to the neighboring nodes j of node i where $\mathcal{V}_i \in \mathcal{A} : \{i, j\} \in \mathcal{E}$. Let the degree matrix of A be defined as $D := [\{\sum_{j=1}^n A_{ij}\}_{i=1}^n]$, while the Laplacian L of A is obtained as $L := D - A$.

In the coalitional game layer of our problem, each provider knows the cost of con-

nection for every consumer in the micro-grid. These can be delineated by a graph; in the set of nodes for the cost network we find a retailer and a number of consumers $\mathcal{V} = \{r_i, b_j, \dots, b_k\}$. The value (weight) of each edge in the corresponding graph represents a cost. These non-physical cost edges vary from consumer to consumer depending on various factors like the physical position relative to each supplier (e.g. one consumer is near a retailer's own generator), plausible power losses or fees from regulatory agencies. It is important to emphasize that the edges in the cost networks do not necessarily represent physical connections or communication links.

In order to get from a supplier to a consumer, a certain *path* can be followed. This path is described by the succession of edges in the network that can be used to reach a consumer. The absence or presence of certain consumers in the provider's network can affect the path and result in higher or lower costs by adding the edge weights; this is explained in Section 6.3.1.

6.2.5 Definition and Properties of the Conductance Matrix

Just as in Chapter 5, for the physical layer of our problem, the system is considered as a network of load nodes and generator nodes, we will review some useful characteristics of the system for ease of reading: The element A_{ij} in the adjacency matrix is the corresponding edge represented by a conductance $1/R_{ij}$ between nodes i and j in consideration of the distribution lines, which are assumed to be resistive. The conductance matrix G is derived from the physical network's Laplacian. However, although apparent in A , the self-loops in the topology represented by the shunt conductances $1/R_{ii}$ of each node do not appear in L . For this reason, we recur to the conductance matrix G , which has the form of a loopy Laplacian matrix [60] and is defined as $G := L + [\{A_{ii}\}_{i=1}^n]$. Such matrix has the following properties: its ij th element $G_{ij} = -1/R_{ij}$ and its diagonal elements $G_{ii} = 1/R_{ii} + \sum_{j \in \mathcal{A}_i} 1/R_{ij}$. If there is no connection between two nodes i and j , namely $j \notin \mathcal{A}_i$, then $G_{ij} = 0$. If node i does not contain a shunt conductance, then $G_{ii} = \sum_{j \in \mathcal{A}_i} 1/R_{ij}$.

6.3 Coalitional Game with Multiple Retailers

In this section, we formally present the rules of the game and the ways in which the coalitions are formed. We also present the algorithm that describes by what means the game is played, along with a stability analysis in the coalitional games sense.

A coalitional game is defined by the tuple $\langle \mathcal{N}, v \rangle$, where $v : 2^{\mathcal{N}} \rightarrow \mathbb{R}$ is a function that assigns a real number to every coalition $S_i \subset \mathcal{N}$. In our case, this is the savings that the consumers in a coalition achieve by choosing the same retailer. To define the value function $v(S_i)$ for any coalition $S_i \subset \mathcal{N}$, the costs inferred by each consumer relative to all available retailers have to be defined as detailed in the sequel.

6.3.1 Cost Definition and Minimum Spanning Tree Problem

Given a coalition S_i , the retailer r_i has knowledge on how much it costs to provide electricity to a consumer b_j in the retailer's coalition, i.e. a connection fee to be paid by the consumer. We refer to it as *direct connection* cost and can be denoted as $c(\{r_i, b_j\})$ which can be represented by the weight of edge (r_i, b_j) . Such cost $c(\{r_i, b_j\})$ is equal to the cost for having $b_j \in \mathcal{B}$ as the only consumer of $r_i \in \mathcal{R}$, namely, with $S_i = \{r_i, b_j\}$, $c(S_i) = c(\{r_i, b_j\})$. The retailer also allocates different *aggregate connection* costs that are enabled depending on the consumers in the coalition, namely the cost for connecting consumer b_j if b_i is already in the coalition; denoted by $c(\{b_i, b_j\})$ and represented in a network as edges connecting consumers. The paths and edges are defined in a way that makes more sense to have consumers join a coalition; resulting in higher savings for the consumers when more consumers join the coalition. However, a consumer has to be able to join whatever retailer it wants in accordance to its individual objectives.

The above can be represented by a graph \mathcal{G}_i , where the nodes are all the players in the coalition and the edges represent the connection costs both direct and aggregates. The existence of the latter is subject to various exogenous factors such as geographical location, high costs, etc. In this chapter, we will refer to this kind of network as *retailer's cost network*. We are now ready to present the definition below.

Definition 4 (Cost of a coalition). *Given a coalition S_i with an associated graph \mathcal{G}_i and characteristic cost function $c : 2^{|S_i|} \rightarrow \mathbb{R}$, the cost $c(S_i)$ is given by the minimum spanning tree of \mathcal{G}_i .*

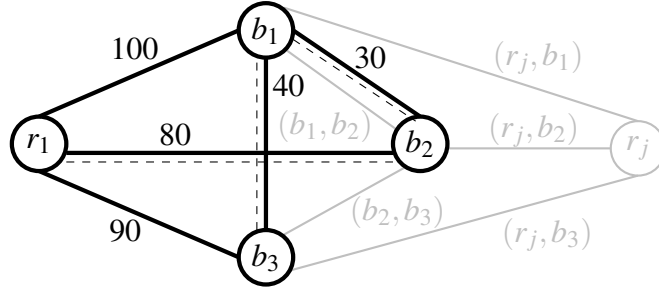


Figure 6.1: Example cost network from retailer r_1 , and its minimum spanning tree (dashed). Other retailers r_j also assign similar costs (gray).

Conceptually, the minimum spanning tree in a weighted and well-connected graph \mathcal{G} contains all the nodes and the minimum possible total edge weight, that is, the smallest possible sum of all weights. Further properties about the cost of the coalition defined above are presented in Sub-section 6.3.5.

Example 1. Let the coalition $S_1 = \{r_1, b_1, b_2, b_3\}$, where the cost network for retailer r_1 is the one in Fig. 1. There exist five different edges $\mathcal{E}_1 = \{(r_1, b_1), (r_1, b_2), (r_1, b_3), (b_1, b_2), (b_1, b_3)\}$.

From the graph, there are seven possible trees that contain all nodes.

$$c(\{(r_1, b_1), (b_1, b_2), (b_1, b_3)\}) = 170$$

$$c(\{(r_1, b_1), (b_1, b_2), (r_1, b_3)\}) = 220$$

$$c(\{(r_1, b_1), (r_1, b_2), (r_1, b_3)\}) = 270$$

$$c(\{(r_1, b_2), (b_1, b_2), (b_1, b_3)\}) = 150$$

$$c(\{(r_1, b_2), (r_1, b_1), (b_1, b_3)\}) = 220$$

$$c(\{(r_1, b_3), (b_1, b_3), (b_1, b_2)\}) = 160$$

$$c(\{(r_1, b_3), (r_1, b_2), (b_1, b_3)\}) = 210$$

The minimum spanning tree is found to be the one containing the edges $\{(r_1, b_2), (b_1, b_2), (b_1, b_3)\}$, yielding the cost of the coalition as:

$$c(S_1) = c(\{r_1, b_1, b_2, b_3\}) = 150. \quad (6.10)$$

With the cost of a coalition, its value function can be obtained by turning the consumer's *minimum cost spanning tree game* [99] into a *costs-saving game*. The value

function of any feasible coalition S_i can be expressed as:

$$v(S_i) = \begin{cases} \sum_{j \in S_i} c(\{r_i, b_j\}) - c(S_i), & \text{if } S_i \text{ is feasible,} \\ 0, & \text{if } r_{i_1}, r_{i_2} \in S_i, \\ 0, & \text{if } r_k \notin S_i \forall k \in \mathcal{R}, \end{cases} \quad (6.11)$$

where the value equals the sum of savings of all individual consumers, that is, the cost for being the only consumer in the coalition minus the cost of the coalition with other consumers.

Having defined the ways in which the savings are obtained through $v(\cdot)$, in order to make sense of the network design and coalition forming, the following straightforward assumption is formulated.

Assumption 13. *Given a coalition S_i consisting of a retailer r_i and two or more consumers b_j , the following condition holds:*

$$v(\{r_i, b_j\}) \leq v(S_i), \forall b_j \in S_i. \quad (6.12)$$

Namely, the savings are larger in a coalition with various consumers than in a coalition containing only a retailer and a single consumer. The purpose of the costs-saving game is to use it as a tool to incentivize consumers for joining a retailer's coalition, by aiding to increase the consumers' profits with such savings.

6.3.2 Savings Imputation via Shapley Value

Given a coalition S_i , the savings produced by the consumers of retailer r_i have to be imputed fairly. We recur to the Shapley value to do so since it is a well-known and standard solution for coalitional game problems [87]. A few concepts have to be established before introducing the Shapley value, such as the marginal value which determines how valuable a player can be when joining a coalition.

Assuming that the consumers enter in a certain sequence σ to an already defined S_i (e.g. $\sigma = \{r_i, b_6, b_8, \dots, b_k\}$), where the ordering number of a buyer b_j is given by $\sigma^{-1}(b_j)$

(in the example, $\sigma^{-1}(b_8) = 3$), the set of predecessors of consumer b_j is defined as

$$\rho_{b_j}^\sigma := \{b_l \in S_i \mid \sigma^{-1}(b_l) < \sigma^{-1}(b_j)\}. \quad (6.13)$$

From this, the marginal value for b_j given an arbitrary sequence σ can be defined as

$$m_{b_j}^\sigma(v) = v(\rho_{b_j}^\sigma \cup \{b_j\}) - v(\rho_{b_j}^\sigma). \quad (6.14)$$

The marginal value for each existing sequence can be stored in vector form as

$$m^\sigma(v) = \{m_{b_j}^\sigma(v), b_j \in S_i\}. \quad (6.15)$$

Finally, the Shapley value is then calculated as the average of the marginal vector over all permutations of sequences, namely

$$\Phi(v) = \frac{1}{k!} \sum_{\sigma} m^\sigma(v), \quad (6.16)$$

where k is the total number of consumers in the coalition. The resulting vector outputs the corresponding portion of savings imputed to each consumer $b_j \in S_i$.

6.3.3 Retailer's Cost Network Derivation

This sub-section is focused on the ways in which the previously introduced cost network is derived from the individual retailer perspective. As mentioned, its edge values and topology represent costs that are dependent on numerous factors both physical such as distance and non-physical such as running costs and the retailer's discretion. Because of these reasons, several methods might arise to determine the weights of the cost network. Here we present a novel and straightforward way to derive the costs based on the micro-grid conductance matrix G [59]; which in a resistive micro-grid, represents the ways in which the transmission lines involve the voltage dynamics. We have selected to derive the cost network from G since it indirectly affects the running and connection costs for the power suppliers by taking into account the power losses. The integration of G into the physical system dynamics will be explained in Section 6.5.1.

The steps for deriving the cost network for a particular retailer r_i are enumerated as

follows:

1. Obtain the adjacency matrix. Given the conductance matrix G of the whole micro-grid, it is straightforward to derive the adjacency matrix A , which contains the conductance values of all connections between the nodes (loads and generators) in the network; its diagonal elements are equal to zero. The ij th element $A_{ij} = A_{ji}$ contains the conductance between nodes i and j . From A , an unweighted adjacency matrix B can also be obtained as follows:

$$B_{ij} = \begin{cases} 1 & \text{if } A_{ij} > 0 \forall i, j \in \mathcal{N} \\ 0 & \text{otherwise} \end{cases}, \quad (6.17)$$

2. Get the direct connection costs. The weight of the edge connecting the retailer to a single consumer $c(\{r_i, b_j\})$ is based on the average value of the path edges from r_i to b_j nodes in \mathcal{G}_A . We employ the properties of the powers of both adjacency matrices [5], namely A^n and B^n , where the element $(B^n)_{ij}$ is equal to the number of walks of length n between nodes i and j . Conversely, $(A^n)_{ij}$ is equal to the products of the edges of such n -length walks. The average product of edges per path can be obtained as the elements of E :

$$E_{ij} = \begin{cases} ((A^n)_{ij}/(B^n)_{ij})^{\frac{1}{n}} & \text{if } (A^n)_{ij} > 0 \forall i, j \in \mathcal{N} \\ 0 & \text{otherwise} \end{cases}, \quad (6.18)$$

where the n -th root of the value is taken to preserve the same units and dimensions given the increasing value of the n powers of A_{ij} . To calculate the costs, the retailer has to define two monetary quantities: γ and ξ , where γ is a scalar to adjust the conductance value to a monetary cost and ξ is a scalar equal to a fixed fee that will increase the cost proportionally to the number of edges in the walk from retailer to consumer. The cost $c(\{r_i, b_j\})$ is then found as given below in an iterative way, depending on the values of n and E_{ij} , $\forall i \in \mathcal{R}, j \in \mathcal{B}$, starting with $n = 1$:

$$c(\{r_i, b_j\}) = \gamma E_{ij} + n\xi, \text{ if } E_{ij} > 0, \forall i \in \mathcal{R}, j \in \mathcal{B}. \quad (6.19)$$

Once a direct cost is assigned, n is to be increased by one $n = n + 1$ and b_j is

discarded for the next iteration so its direct connection cost is not re-calculated. This step is to be repeated until all direct costs $c(\{r_i, b_j\})$ have been assigned a value.

3. Get the aggregate connection costs. This step is straightforward since these are coupled to the connections between consumer nodes. The edges $c(\{b_i, b_j\})$ can be calculated from A as:

$$c(\{b_i, b_j\}) = \begin{cases} \gamma A_{b_i b_j} + \omega \xi, & \text{if } A_{b_i b_j} > 0 \\ 0 & \text{otherwise} \end{cases}, \quad (6.20)$$

where ω is a scalar to differentiate between direct and aggregate fees if the retailer desires to do so.

After completing the above steps, retailer r_i has defined the connection costs and consequently, the weights for graph \mathcal{G}_i for its utilization in the minimum spanning tree problem explained in Section 6.3.1.

6.3.4 Price, Consumption and Coalition Forming

In this section, the individual retailer's cost function $C(\cdot)$ and every consumer utility function $U(\cdot)$ are defined, their link with the supplier cost networks is introduced and the ways in which these lead to the formation of the coalitions is explained.

As explained in Section 6.2.2, the cost and utility functions are monotonically increasing and convex and concave respectively. To comply with this we have chosen the quadratic term $(\Lambda_i P_i^s)^2$ for $C(\cdot)$ and the radical term $(P_{b_j}^d)^{\frac{1}{6}}$ for $U(\cdot)$ in the same spirit as introduced in Chapters 4 and 5.

Both functions output a monetary value, hence the terms discussed in the following have to be included in the cost/utility of each player. The coalitional game is connected to these functions by including the term $v(S_i)$ directly into the cost of the retailer, which is equal to the consumer savings that will be rewarded back via imputation. The consumers also include the individual base payment $-c(\{r_i, b_j\})$ into their profit function since it has to be paid regardless of the prospective savings. The retailers also announce the value of a *potential subsidy* $\kappa_{r_i} \delta_{b_j}^{r_i}$ to the consumer. Where $\delta_{b_j}^{r_i}$ is the degree of the node represented by b_j in the cost network relative to r_i . The scalar κ_{r_i} is a positive

constant to adjust the potential subsidy proportionally to the number of connections in the cost network. The subsidy term is an equivalent to the Bahnzaf power index employed in cooperative games which dictates how pivotal is a players' presence in a coalition [100]. A form of the subsidy term is also used in [3] as an incentive tool. The potential subsidy is announced by the retailer to the consumer as means to incentivize the latter to join the retailer's coalition, since in minimum spanning tree games the players with more connections in the cost network can potentially hold more value [87], enabling the consumer to consequently increase its own profits. The actual resulting subsidy is calculated after the coalition is formed; its value is equal to each consumer's Shapley value $\Phi(v)$ imputation.

Having introduced the above, and similarly to Chapter 5, we have defined the cost and utility functions for retailers and consumers respectively as:

$$C(P_i^g, S_i) = \alpha_{r_i} \cdot (\Lambda_i P_i^g)^2 + v(S_i), \quad \forall i \in \mathcal{R}, \quad (6.21)$$

$$U(P_{b_j}^d) = \alpha_{b_j} \cdot (P_{b_j}^d)^{\frac{1}{6}} + \kappa_{r_i} \delta_{b_j}^{r_i} - c(\{r_i, b_j\}), \quad \forall r_i \in \mathcal{R}, b_j \in \mathcal{B}, \quad (6.22)$$

where the constant α_{r_i} is a scalar associated to the production cost of the generated power corresponding to retailer r_i . Analogously, α_{b_j} represents each consumer's predilection to consume power. Regarding the first term in (6.22); although any radical (or concave function for that matter) can be used, we have chosen a sixth root for the sake of simplicity and ease of tuning during the simulations. The inclusion of (6.21)-(6.22) to the profit functions defined in (6.7)-(6.8), yields the maximization problems:

$$\Lambda_i = \arg \max_{\lambda \in [\underline{\lambda}, \bar{\lambda}]} \lambda \cdot \left(\sum_{b_j \in S_i} P_{b_j}^d - P_i^{loss} \right) + \sum_{j \in S_i} c(\{r_i, b_j\}) - \alpha_{r_i} \cdot (\lambda P_i^g)^2 - v(S_i), \quad (6.23)$$

$$P_{b_j}^d = \arg \max_{\zeta \in [\underline{\zeta}, \bar{\zeta}]} \alpha_{b_j} \cdot (\zeta)^{\frac{1}{6}} + \kappa_{r_i} \delta_{b_j}^{r_i} - c(\{r_i, b_j\}) - \Lambda_i \zeta, \quad (6.24)$$

for each $r_i \in \mathcal{R}$ and $b_j \in \mathcal{B}$ respectively.

The process of consumer b_j selecting a coalition S_i is done by evaluating all prices $\Lambda_i \forall i \in \mathcal{R}$, base payments $c(\{r_i, b_j\}) \forall i \in \mathcal{R}$ and the value of the potential subsidies $\kappa_{r_i} \delta_{b_j}^{r_i}$ announced by all the retailers into its profit function as in (6.24) and then taking

the one that yields the largest profit:

$$S_i \leftarrow S_i \cup \{b_j\} \iff i = \arg \max_i \{ \Pi_{b_j}(\Lambda_i, \kappa_i \delta_{b_j}^{r_i}, c(\{r_i, b_j\})) \}, i \in \mathcal{R} \}. \quad (6.25)$$

The consumption is then optimized in (6.24) with the consumer outputting the demanded quantity of power $P_{b_j}^d$ whilst announcing it back to the retailer. In the case where the constraint (6.9) does not hold for S_i , retailer r_i will have to reject the consumers that generate the least profit in its coalition until the constraint is fulfilled, leaving the rejected consumers to re-evaluate (6.25) without the former selected retailer. Once the coalitions are formed, namely all consumers have been allocated a retailer; the value of the savings of the consumers in the coalition is obtained by calculating the Shapley value $\Phi(v)$ as explained in Section 6.3.2 and paid back to each consumer in the coalition. This whole process is repeated every fixed period of time $T = t_f - t_0$ in the interval $[t_0, t_f]$, allowing the price to be changed by the retailers. The sequence of all the steps in the game is presented in Algorithm 1.

Algorithm 1: Coalition Forming and Savings Imputation

- 1 **Initial State**
 - 2 Any $b_j \in \mathcal{B}$ is assigned to an initial S_i .
 - 3 Any $r_i \in \mathcal{R}$ starts with initial P_i^g , fixed κ_{r_i} and Λ_i .
 - 4 Any $b_j \in \mathcal{B}$ starts with initial $P_{b_j}^d$.
 - 5 **repeat**
 - 6 Any $r_i \in \mathcal{R}$ measure $\sum_{b_j \in S_i} P_{b_j}^d$ and evaluate (6.23);
 - 7 Any $r_i \in \mathcal{R}$ output Λ_i and $\kappa_{r_i} \delta_{b_j}^{r_i}$ to all b_j ;
 - 8 Any $b_j \in \mathcal{B}$ evaluate all Λ_i and $\kappa_{r_i} \delta_{b_j}^{r_i}$ into (6.24);
 - 9 $\forall b_j \in \mathcal{B}$ select coalition S_i and announce $P_{b_j}^d$ to $r_i \in S_i$;
 - 10 **if** (6.9) does not hold for $r_i \in S_i$
 - 11 **repeat**
 - 12 $r_i \in S_i$ rejects $b_j \in S_i$ with the lowest $P_{b_j}^d$;
 - 13 **until** (6.9) holds for r_i ;
 - 14 Rejected b_j by r_i evaluate Λ_l and $\kappa_{r_l} \delta_{b_j}^{r_l}$ into (6.24) $\forall l \in \mathcal{R} \setminus r_i$;
 - 15 Rejected b_j select another coalition $S_l \forall l \in \mathcal{R} \setminus r_i$;
 - 16 **end if**
 - 17 Any $r_i \in S_i$ calculates $v(S_i)$ and $\Phi(v)$;
 - 18 Any $r_i \in S_i$ outputs $\Phi(v)$ to each b_j ;
 - 19 Any $b_j \in S_i$ consume $P_{b_j}^d$;
 - 20 Wait for a period of time for next play;
 - 21 **end repeat**
-

6.3.5 Properties and Stability of the Coalitional Game

In this section, we enumerate and demonstrate the ways in which our game introduced above yields stable coalitions and at the same time encourages competition between the retailers. We also briefly analyse the existence of its equilibrium point.

The core of a coalitional game (\mathcal{N}, v) represents a key concept when analysing the equilibrium of such games. A pay-off vector is an element $a \in \mathbb{R}^{|\mathcal{N}|}$ such that $a_i \in \mathbb{R}$ represents the gains of player $i \in \mathcal{N}$. The core is defined as:

Definition 5 (Core). For a coalitional game (\mathcal{N}, v) , the core \mathcal{C} is a subset of $\mathbb{R}^{|\mathcal{N}|}$ such that $\mathcal{C} = \{a \in \mathbb{R}^{|\mathcal{N}|} : \sum_{i \in S} a_i \geq v(S), \forall S \subset \mathcal{N}\}$.

Let us investigate first the existence of a solution for the *minimum cost spanning tree game* (MCST) we introduced in Section 6.3.1. Namely the existence of a non-empty core given a retailer's coalition S_j . Non-emptiness of the core is a known property of convex games [101]. Although the convexity of the game cannot be proven directly, we recur to the concept of *permutationally convex games* (PC) originally introduced in [99], where it is demonstrated that all PC games possess a non-empty core and both MCST and convex games are PC. Let us introduce some general concepts in the following.

Definition 6 (Convex game). Let $N = \{1, 2, \dots, n\}$ be an arbitrary set of players and $c : 2^N \rightarrow \mathbb{R}$ a characteristic cost function where $c(\emptyset) = 0$. A cost cooperative game $\langle N, c \rangle$ is convex if

$$c(S \cup T) + c(S \cap T) \leq c(S) + c(T) \quad \forall S, T \subseteq N. \quad (6.26)$$

To demonstrate the analogy between PC and convex games, let us first note that c satisfies

$$c(S \cup \{i\}) - c(S) \leq c(T) + c(T \cup \{i\}) \quad (6.27)$$

for all $i \in N, T \subseteq S \subseteq N \setminus i$. This means that the cost of connecting node i is reduced when is included in an existing larger set of players. Following the general example, let us denote the node corresponding to the retailer as 0. Finding the minimum spanning tree in a graph induces a partial order $i \succ j$, namely for $i, j \in N$ we say that $i \succ j$ if node j is in the unique path connecting node i to 0. The one immediate predecessor of i can

be denoted as $j(i) \in \{0, 1, 2, \dots, i-1\}$. Let us also denote $[0] = \emptyset$ and $[k] = \{1, 2, \dots, k\}$. We can now present the following generalization that yields from (6.27).

Definition 7 (Permutationally convex game). *A game $\langle N, c \rangle$ is convex if there exist a labeling of players, say $1, 2, \dots, n$, such that*

$$c([k] \cup S) - c([k]) \leq c([j] \cup S) - c([j]) \quad (6.28)$$

for all $S \subseteq N \setminus [k]$ and $k \succ j$. Namely, the costs are reduced further when sequentially adding more players in a labelling. Any labelling satisfying (6.28) is a *permutationally convex order*. We are now ready to present the following result:

Theorem 13. *Given a retailer's coalition S_i , with a respective cost network described by the graph \mathcal{G}_i , the resulting minimum cost spanning tree game is permutationally convex.*

Proof. Let us denote $[b_j] = \{b_1, b_2, b_j - 1\}$, with $b_k \succ b_j$ in the minimum spanning tree and in consequence $b_j(b_k) \in \{r_i, b_1, b_2, \dots, b_k - 1\} \forall i \in S_i \cap \mathcal{R}, j, k \in S_i \cap \mathcal{B}$. With some abuse of notation, let $c([b_j])$ and $c([b_k])$ denote the costs associated to the corresponding labeled subsets of consumers $[b_j]$ and $[b_k]$. From (6.28), it is straightforward to determine that

$$c([b_k]) \leq c([b_j]) \text{ if } b_k \succ b_j. \quad (6.29)$$

Given that smaller costs are obtained by including nodes in the unique path of the minimum spanning tree, satisfying (6.29), it can be said that the induced order is PC, hence, the MCST game of S_i is PC. \square

From the relations and analogies above, we can state the following.

Theorem 14. *Given a retailer's coalition S_i with a number of consumers b_j , the respective minimum cost spanning tree game has a non-empty core.*

Proof. We refer to the proof of [99, Theorem 1]. \square

Remark 8. *If the reader wishes further details on the derivations regarding the core non-emptiness of PC games; we highly encourage the reader to revise the seminal study in [99]. Additionally, the properties of a generalization for minimum spanning tree*

games are studied in [102], along with methods for finding its cost allocation and examples that illustrate its application.

Regarding the multiple retailer game described in Section 6.3.4 and with the purpose of showing that competition among retailers brings them greater payoffs, we can demonstrate that the game is subadditive [86]. Subadditivity is established in the following theorem.

Theorem 15. *The coalitional game with multiple energy retailers $\langle \mathcal{N}, v \rangle$ with value function v is subadditive, namely*

$$v(S_i \cup S_j) \leq v(S_i) + v(S_j), \quad \forall i, j \in \mathcal{R}. \quad (6.30)$$

Proof. From Assumption 12, it is straightforward to determine that $v(S_i \cup S_j) = 0$. Furthermore, as explained in Section 6.3.1, the value of a coalition $v(S_i)$ is given by the minimum spanning tree that connects the retailer to its consumers in the coalition via the cost network, yielding the savings/subsidies; the worst-case scenario for the value of any coalition is $v(S_i) = 0$, always yielding that $v(S_i) \geq 0$, hence (6.30) holds. \square

Subadditivity is not sufficient to demonstrate the stability of the game or the satisfaction of the coalition members [86]. A stabilizing allocation can be guaranteed by proving that the game is balanced. To do this, we first need to introduce the following consequential property of our game:

Theorem 16. *The coalitional game with multiple energy retailers $\langle \mathcal{N}, v \rangle$ is concave, namely, for any $S_i, S_j \subseteq \mathcal{N}$,*

$$v(S_i \cup S_j) + v(S_i \cap S_j) \leq v(S_i) + v(S_j), \quad \forall i, j \in \mathcal{R}. \quad (6.31)$$

Proof. As consequence of (6.3) and (6.4) in Assumption 12, it is true that $v(S_i \cup S_j) = 0$ and $v(S_i \cap S_j) = v(\emptyset) = 0$. Also, as in our previous demonstration; for any coalition $v(S_i) \geq 0$, thus (6.31) holds. \square

A property of all N -player concave games is that they are balanced [103], meaning that for any concave game, there exists an equilibrium point. Therefore, we can state the following theorem:

Theorem 17. *The coalitional game with multiple energy retailers $\langle \mathcal{N}, v \rangle$ is balanced.*

Proof. We refer to the proof of [103, Theorem 1] for this demonstration. \square

Remark 9. *Given the properties of subadditivity and concavity, we refer to [104] and references therein, where additionally to the study in [103], the sufficient conditions for a subadditive game to be balanced are enumerated and explained in detail.*

In the following, we provide a complimentary analysis for the stability of the game's coalitions, where we investigate consumer satisfaction and the ways in which this is guaranteed.

From the game proposed, Theorem 15 and Assumption 12 it can be inferred that the value of the grand coalition $v(\mathcal{N}) = 0$ since the grand coalition, by definition, would include all competing retailers. This, in consequence, renders conventional cooperative game stability and balance analysis [86, 87] unusable. We recur to the notion of stable partitions first introduced in [88], more specifically \mathbb{D}_{hp} -stability, where the *defection function* $\mathbb{D}(S_i)$ is defined in a way that it outputs collections of players that can leave the coalition S_i to form *homogeneous partitions*. A coalition is \mathbb{D} -stable when no group of players is interested in leaving the coalition.

Definition 8 (\mathbb{D}_{hp} stability). *A coalition $S_i = \{r_i, b_j, \dots, b_k\}$ is \mathbb{D}_{hp} -stable if the following conditions are satisfied:*

1. *given a collection $\{P_{i_1}, \dots, P_{i_L}\}$ resulting from an arbitrary partition of S_i , such that $\cup_{j=1}^L P_{i_j} = S_i$:*

$$v(S_i) \geq \sum_{j=1}^L v(P_{i_j}), \quad \forall i \in \mathcal{R}, \quad (6.32)$$

2. *given the coalitions S_i in the subset $\mathcal{T} \subseteq \{1, \dots, K\}$, where $i \in \mathcal{T}$ and $K \leq p$:*

$$\sum_{i \in \mathcal{T}} v(S_i) \geq v\left(\bigcup_{i \in \mathcal{T}} S_i\right), \quad (6.33)$$

Theorem 18. *Given the coalitional game with multiple energy retailers $\langle \mathcal{N}, v \rangle$. The coalitions S_i formed by such are \mathbb{D}_{hp} stable.*

Proof. For a fixed $r_i \in \mathcal{R}$ and associated coalition $S_i \subset \mathcal{N}$, consider a collection $\{P_{i_1}, \dots, P_{i_L}\}$. It follows that $r_i \in P_{i_j}$ for some $i_j \in \{1, \dots, L\}$ which implies $v(P_{i_j}) \geq 0$, and $v(P_{i_k}) = 0$

for the rest. The cost associated with P_{i_j} satisfies $c(S_i) \geq c(P_{i_j})$ since the minimum spanning tree of P_{i_j} is contained in the one corresponding to S_i . Condition (6.32) follows directly from

$$v(S_i) - v(P_{i_j}) \geq c(S_i) - c(P_{i_j})$$

since $c(\{r_i, b_{i_k}\}) > 0$ for all $i_k \in S_i \setminus P_{i_j}$.

For the second condition, it can be inferred from (6.3)-(6.4) that $v(\cup_{i \in \mathcal{T}} S_i) = 0$. From the value formulation for a coalition (6.10)-(6.11), it is true that $v(S_i) \geq 0$. From the above, it is trivial that condition (6.33) holds. □

6.3.6 Stackelberg Equilibrium

Having fully formulated both the profit functions and the maximization problems involved in our proposed game, we are now ready to present the following result that guarantees the existence of a Stackelberg equilibrium.

Theorem 19. *There exists an equilibrium point $(\Lambda_i^*, P_{b_j}^{d*}) \in \mathbb{R}^2, \forall r_i, b_j \in S_i$ for the Stackelberg game (6.23)-(6.24).*

Proof. Let a retailer r_i and a consumer b_j be in the same coalition, where they maximize the profit functions in (6.23) and (6.24) respectively. The maximum of both profits can be obtained by taking the derivative of both functions and equaling to zero:

$$\frac{\partial \Pi_{r_i}}{\partial \Lambda_i} = P_{b_j}^d - P_i^{loss} - 2\alpha_{r_i} P_i^{g^2} \Lambda_i = 0, \quad (6.34)$$

$$\frac{\partial \Pi_{b_j}}{\partial P_{b_j}^d} = \frac{\alpha_{b_j}}{6} (P_{b_j}^d)^{-\frac{5}{6}} - \Lambda_i = 0, \quad (6.35)$$

which follows the procedure to obtain the equilibrium point in a two-player Stackelberg game [87, 92]. From (6.35) an expression for the consumer's demand as a function of the price is obtained

$$P_{b_j}^d = \frac{1}{6\sqrt[5]{6}} \left(\frac{\Lambda_i}{\alpha_{b_j}} \right)^{-\frac{6}{5}}. \quad (6.36)$$

Substituting (6.36) in (6.34), yields the following expression:

$$\frac{1}{6\sqrt[5]{6}} \frac{\Lambda_i^{-\frac{6}{5}}}{\alpha_{b_j}} - 2\alpha_{r_i} P_i^{g^2} \Lambda_i - P_i^{loss} = 0. \quad (6.37)$$

Solving for Λ_i while substituting the respective values of the parameters in (6.37), equals a real positive value which corresponds to Λ_i^* . Substituting it into (6.36) results in $P_{b_j}^{d*}$, thus yielding both equilibrium values. \square

The existence and convergence towards a Stackelberg equilibrium for our game is further illustrated with the numerical results in Section 6.5.

6.4 Risk Sharing and Reduction of Statistical Dispersion

In this section, we provide a brief insight into the statistical implications for the consumers when considering their demand to be a random variable. Motivated by [105], here we consider the statistical properties of the consumer demand in order to demonstrate that coalition forming entails lower risks.

In the game, there is an implied risk for the consumers when selecting a supplier; such can result in the consumer not meeting the expected profit, i.e. the yielded subsidy is lower than the potential one announced by the retailer. As demonstrated above, consumers are induced to form a coalition to jointly increase the subsidy, leading to an increase in the collective profit by sharing their risk.

For the sake of simplicity, let us consider the consumer's α_{b_j} to be a random variable $\alpha_{b_j}(t) \sim N(\mu, \sigma^2)$. This a sensible assumption since the demand depends on various factors such as the time of day, the different usage tasks, etc. Then, because of the maximization problem (6.24), the resulting consumption $P_{b_j}^d$ for each consumer can be consequentially modeled as a stochastic process $P_{b_j}^d(t) \in [0, D_{b_j}]$, which truncates the normal distribution of the original random variables. Where D_{b_j} is the upper limit of consumption by b_j . The vector-valued random process can be denoted as $P^d(t) = [P_{b_1}^d(t), \dots, P_{b_l}^d(t)]^T$. The cumulative distribution function (CDF) at each time t is given by

$$\Phi(P^d; t) = \mathbb{P}\{P^d(t) \leq P^d\}, \quad (6.38)$$

which signifies the probability of the random process $P^d(t)$ taking a value less than or equal to P^d . The distribution $\Phi(P^d; t)$ is supported on a compact subset $\prod_{b_j} [0, D_{b_j}] \subseteq \mathbb{R}_{\geq 0}^l$.

As already mentioned, the power consumption of a coalition $S_i \subseteq \mathcal{N}$ would be then represented by a sum of stochastic processes:

$$P_{S_i}^d(t) = \sum_{b_j \in S_i} P_{b_j}^d(t), \quad i \in \mathcal{R} \cap S_i, \quad j \in \mathcal{B} \cap S_i. \quad (6.39)$$

The corresponding random process is denoted by $\mathbf{P}_{S_i}^d = \{P_{S_i}^d(t) < P^d\}$ with support $[0, \sum_{b_j \in S_i} D_{b_j}]$. From this, the time averaged CDF is

$$F_{S_i}(P^d) = \frac{1}{T} \int_{t_0}^{t_f} \Phi_{S_i}(P^d, t) dt. \quad (6.40)$$

Let $F_{S_i}^{-1} : [0, 1] \rightarrow [0, \sum_{b_j \in S_i} D_{b_j}]$ be the associated quantile function. For any $p \in [0, 1]$, the p -quantile of F_{S_i} is $F_{S_i}^{-1}(p) = \inf\{x \in [0, 1] | F_{S_i}(x) \geq p\}$.

Let us define the total consumer profit given a price Λ_i as the function:

$$\Pi_{S_i}(P^d, \Lambda_i) = \sum_{b_j \in S_i} \Pi_{b_j}(P_{b_j}^d, \Lambda_i), \quad (6.41)$$

where $\Pi_{b_j}(P_{b_j}^d, \Lambda_i)$ is the individual consumer's profit function from (6.24). Π_{S_i} includes the subsidies to distribute. Taking Π_{S_i} as dependent on the stochastic process $\mathbf{P}_{S_i}^d$, the expected consumer profit can be defined as

$$J_{S_i}(\Lambda_i) = \mathbb{E} \Pi_{S_i}(\mathbf{P}_{S_i}^d, \Lambda_i). \quad (6.42)$$

Let us also define the individual profit for a consumer b_j as $\Pi_{b_j}^0$ specifically for the case where it does not want to cooperate with other consumers as if it were the only client of a retailer r_i . In such profit, the resulting subsidy is equal to zero since there are no other consumers to generate savings with, namely, its coalition is reduced to $S_i = \{r_i, b_j\}$.

The following result demonstrates that risk-sharing through coalition leads to an increase in profit *almost surely*.

Lemma 3. *Given a price Λ_i announced by r_i , and an associated coalition S_i with a*

number of consumers b_j , we have almost surely that:

$$\Pi_{S_i}(\mathbf{P}_{S_i}^d, \Lambda_i) \geq \sum_{b_j \in S_i} \Pi_{b_j}^0(\mathbf{P}_{b_j}^d, \Lambda_i). \quad (6.43)$$

Proof. By the properties of the sum of random variables [106] and of homogeneity and superadditivity of functions of stochastic processes [105]; the condition (6.43) is fulfilled as a direct consequence of (6.12), where the value of a coalition is always greater or equal than the value of a single consumer with a retailer. \square

The above establishes that coalitions always bring larger collective profits for the consumers. In a tangible manner, the savings obtained and their benefit can be referenced to the attenuation of statistical dispersion from aggregation. This has been described in detail in [107], where the optimal expected profit directly depends on the deviation of the coalitional value-at-risk (CVaR) [108] or *coalitional shortfall deviation*. This is formalized as follows.

For any $q \in (0, 1)$, the CVaR deviation of $\mathbf{P}_{S_i}^d \sim F_{S_i}$ is defined as

$$\mathcal{D}_q(\mathbf{P}_{S_i}^d) := \mathbb{E}[\mathbf{P}_{S_i}^d] - \mathbb{E}[\mathbf{P}_{S_i}^d | \mathbf{P}_{S_i}^d \leq F_{S_i}^{-1}(q)]. \quad (6.44)$$

Such deviation measures the difference between the expected value and the probability of q being near the bounds of the probability distribution. Then, the reduction of dispersion that is induced by consumers joining a coalition S_i and aggregating their demand can be represented as:

$$\Delta_{S_i} := \sum_{b_j \in S_i} \mathcal{D}_q(\mathbf{P}_{b_j}^d) - \mathcal{D}_q(\mathbf{P}_{S_i}^d). \quad (6.45)$$

It is straightforward to show that $\Delta_{S_i} \geq 0$ for all coalitions $S_i \subseteq \mathcal{N}$. As a consequence, the advantages arising from aggregation are attributable to the reduction in dispersion as measured by CVaR. Namely, the aggregation will improve the expected profit as much as the statistical dispersion of the aggregate consumption is reduced.

6.5 Implementation with Physical Dynamics

To illustrate the effect of our proposed pricing scheme in the physical micro-grid, in this section we derive a way to couple the physical dynamics and the game. A stability

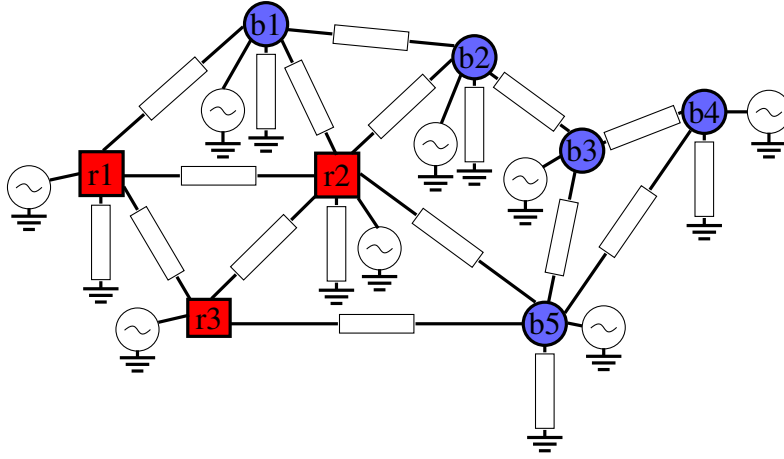


Figure 6.2: Resistive micro-grid in a network representation, comprised by loads/consumers \bullet and generators/retailers \blacksquare , resistive distribution lines, and shunt conductances.

analysis of the integrated system is also formulated. The derivations obtained here are a more refined version of the ones presented in Chapter 5, for completeness and to show the improvement of the dynamics equation we present them in the sequel.

6.5.1 Micro-Grid and Demand Dynamics

As previously shown, due to the relatively small scale of the market setup of our problem, the model taken into consideration is of a low-voltage configuration. This is otherwise known as a resistive micro-grid model, by cause of the resistive dominance over the inductance in the micro-grid's transmission lines, consequently neglecting the reactive power [67]. Such a system is considered as a network of p generator nodes and l load nodes (retailers and consumers respectively); as shown in Fig. 6.2. Here the weighted edges connecting the nodes are equivalent to resistive transmission lines. For this study, we focus on an islanded micro-grid since it is better suited for our multiple retailer scheme. However, a scenario where there is a main grid that supplies power additional to the generators/retailers in the micro-grid can also be accommodated in the present model by adding an additional generator node as the main grid.

For the sake of completeness and clarity, let us briefly enumerate and explain the dynamics of the physical system, which consists of a bounded P-V droop and demand response.

We consider the case where each generator and consumer is providing grid support by operating under P-V droop control. Opposed to the conventional droop control [72],

here we propose an improved version of the bounded droop controller (BDC), which results in a simplified structure compared to [74] and maintains the voltage of each node within a required bound around the rated value at all times. As it is shown in the sequel, this is important to obtain analytic stability conditions for the closed-loop system. In this framework, the voltage dynamics of each node under the proposed bounded droop control take the form:

$$\dot{V} = c\tau_v^{-1} \left((V^* \mathbf{1}_{n \times 1} - V) - k([V]GV - P^{set}) \right) \left(\mathbf{1}_{n \times 1} - \frac{(V - V^* \mathbf{1}_{n \times 1})^2}{\Delta V^2} \right), \quad (6.46)$$

where V is a vector containing the ordered voltages of the loads and the generators $V = [V_{b_1}, V_{b_2}, \dots, V_{b_l}, V_{r_1}, V_{r_2}, \dots, V_{r_p}]^T \forall b_i \in \mathcal{B}, r_i \in \mathcal{R}$. The square diagonal matrix $[V] = \text{diag}(V)$ contains the elements of vector V . The diagonal matrices $\tau_v = \text{diag}(\tau_{vi})$ and $k = \text{diag}(k_i)$ contain all the nodes' voltage time constants and power droop coefficients respectively, $c = \text{diag}(c_i)$ contains positive constant gains for the integral control. The matrix G is the conductance matrix. The value of V^* is the rated voltage and ΔV is a positive value to define the desired voltage bounds which is employed in the quadratic terms in the dynamics that enable the voltage outputs to be bounded [73, 74]. Let us briefly demonstrate that the voltage values always remain within the desired bounds.

Lemma 4. *Let all the nodes in the system be subject to the dynamics (6.46), with initial conditions $V_i(0) \in (V^* - \Delta V, V^* + \Delta V)$, $\forall i \in \mathcal{N}$. Then for all the voltage values we have*

$$V_i(t) \in (V^* - \Delta V, V^* + \Delta V), \forall i \in \mathcal{N} \quad (6.47)$$

at all times $t > 0$.

Proof. The proof follows from contradiction. Consider a trajectory for $V_i(t)$ that violates the bound (6.47), i.e. there exists a time T where $V_i(T) = V^* + \Delta V$ or $V_i(T) = V^* - \Delta V$. Then from (6.46), we get $\dot{V}_i(T) = 0$ and therefore $V_i(t) = V_i(T) \forall t \geq T$, hence, it remains at the limit of the bound and does not violate it. \square

The vector P^{set} contains the reference value of the power that is demanded or generated by each node and is set via a supervisory controller. Its values are defined for generators/retailers as $P_i^{set} = P_{r_i}^{Lrated}, \forall i \in \mathcal{R}$ and is a constant; this is changed for the load/consumer nodes to include their demand response as $P_i^{set} = P_i^L, \forall i \in \mathcal{B}$. Where P_i^L is

the corresponding demand response which is given by the first-order dynamics [30, 92] as follows

$$\tau_i \dot{P}_i^L = P_{b_i}^d - P_i^L, \forall i \in \mathcal{B}, \quad (6.48)$$

where $\tau_i \in \mathbb{R}_{>0}$ is the time constant of the response and the input $P_{b_i}^d$ is the desired power demand from the consumers' maximization problem (6.24). Hence, coupling the game and the physical dynamics yields the following state vector with the form $[V_{b_1}, \dots, V_{b_l}, V_{r_1}, \dots, V_{r_p}, P_{b_1}^L, \dots, P_{b_l}^L]^T \forall b_i \in \mathcal{B}, r_i \in \mathcal{R}$. Now that we have defined the dynamics and explained the ways in which the physical layer of our problem is coupled with the market layer, we are ready to demonstrate under which conditions the stability of the physical system is guaranteed.

6.5.2 Physical Stability Analysis

In this sub-section, a stability analysis very similar to the one presented previously in Chapter 5 is presented, it has been left here for the sake of completeness.

The BDC implemented into the voltage dynamics guarantees the existence of an equilibrium point within the given bounds. We now present the assumption below:

Assumption 14. *For constant inputs $P_i^L \forall i \in \mathcal{B}$ and $P_i^{set} \forall i \in \mathcal{R}$, there exists an equilibrium point $[\bar{V}_{b_1}, \dots, \bar{V}_{b_l}, \bar{V}_{r_1}, \dots, \bar{V}_{r_p}, \bar{P}_{b_1}^L, \dots, \bar{P}_{b_l}^L]^T$ for system (6.46)-(6.48), where $\bar{P}_{b_i}^L \in \mathbb{R}, \forall i \in \mathcal{B}, \bar{V}_i \in \mathbb{R}_{>0}, \forall i \in \mathcal{N}, \bar{V}_i \in (V^* - \Delta V, V^* + \Delta V), \forall i \in \mathcal{N}$.*

From the above, the conditions for stability do not depend on the equilibrium points and only do on the parameters to tune. This leads to the following proposition.

Proposition 2. *Let Assumption 14 hold and let a shift on consumption P_i^L in each load node be given, then system (6.46)-(6.48) is asymptotically stable at the equilibrium point if*

$$-1 - k_i \left(2 \frac{V_i^* - \Delta V}{R_{ii}} - 2 \Delta V \sum_{j \in \mathcal{A}_i} \frac{1}{R_{ij}} \right) < 0, \forall i \in \mathcal{N}. \quad (6.49)$$

Proof. Calculating the Jacobian of system (6.46)-(6.48) with respect to the states V_i and ΔP_i^L yields the following $(N + l) \times (N + l)$ matrix

$$J^{BDC} = \begin{bmatrix} \Upsilon J^V & -\Upsilon \kappa \\ \mathbf{0}_{l \times N} & -\tau^{-1} \end{bmatrix}, \quad (6.50)$$

where $\Upsilon = \text{diag}(v_i)$ is an $N \times N$ matrix containing small positive scalars as a result of substituting the equilibrium voltage values \bar{V}_i into the term $v_i = (1 - (\bar{V}_i - V^*)^2 / \Delta V^2) \forall i \in \mathcal{N}$. $\tau = \text{diag}(\tau_i)$ is an $l \times l$ matrix and κ is the $N \times l$ matrix $\kappa = [k\tau_v^{-1}, \mathbf{0}_{(N-l) \times l}]^T$. J^V is the $N \times N$ matrix corresponding to the Jacobian of the voltage dynamics (6.46) in an open-loop configuration with respect to the state vector V [72], namely:

$$J^V = -\tau_v^{-1} - k\tau_v^{-1}([\bar{V}]G + [G\bar{V}]). \quad (6.51)$$

Correspondingly, (6.51) is comprised of diagonal elements

$$J_{ii}^V = -\frac{1}{\tau_{vi}} - 2\frac{k_i}{\tau_{vi}}\bar{V}_i G_{ii} - \frac{k_i}{\tau_{vi}} \sum_{j \in \mathcal{N}_i} \bar{V}_j G_{ij}, \forall i \in \mathcal{N}, \quad (6.52)$$

and non-diagonal elements

$$J_{ij}^V = -\frac{k_i}{\tau_{vi}}\bar{V}_i G_{ij}, \forall i, j \in \mathcal{N}. \quad (6.53)$$

To obtain the stability conditions, the eigenvalues λ_i of J^{BDC} are to be calculated. These correspond to the roots of the resulting polynomial of the determinant

$$|\lambda I - J^{BDC}| = |\lambda I - \Upsilon J^V| |\lambda I + \tau^{-1}|. \quad (6.54)$$

By the properties of block matrices, it is trivial to see that the eigenvalues of τ^{-1} are negative and real due to all the time constants being positive. We are left only with finding the eigenvalues of ΥJ^V . We can focus only on J^V since all values of v_i of Υ are also positive.

Given the complexity to analytically obtain the eigenvalues of J^V due to its potential size, we can compute the Gershgorin discs [26] $\Delta_i(C_i, R_i)$ with their center $C_i = J_{ii}^V$ and radius $R_i = \sum_{j \in \mathcal{N}_i} |J_{ij}^V|$ which enclose the position of any eigenvalue λ_i in the complex plane. We can guarantee stability by shifting all the discs Δ_i to the left-hand-side of the

complex plane. The following condition results from such a shift:

$$-\frac{1}{\tau_{vi}} - \frac{k_i}{\tau_{vi}} \bar{V}_i G_{ii} - \frac{k_i}{\tau_{vi}} \sum_{j \in \mathcal{A}_i} \bar{V}_j G_{ij} - \frac{k_i}{\tau_{vi}} \frac{\bar{V}_i}{R_{ii}} < 0, \forall i \in \mathcal{N}. \quad (6.55)$$

Simplifying the expression above, and substituting \bar{V}_i and \bar{V}_j to the value that yields a disc closer to the origin for which in the worst-case scenario we have $\bar{V}_i = V_i^* - \Delta V$ and $\bar{V}_j = V_j^* + \Delta V$, the sufficient condition for stability (6.49) is obtained. \square

It is straightforward to check the stability condition (6.49), since calculating the equilibrium points of the whole system is not required.

6.6 Numerical Examples

6.6.1 Coalition Formation and Profit Calculation

In order to show the ways in which retailers calculate new prices according to the demand as well as how consumers react to a change of prices in the micro-grid, we have formulated two scenarios. The first consists of a micro-grid that contains five consumers $\mathcal{B} = \{b_1, b_2, b_3, b_4, b_5\}$ that are supplied with power by only one retailer $\mathcal{R} = \{r_1\}$. The second consists of the same consumers supplied by two additional retailers $\mathcal{R} = \{r_1, r_2, r_3\}$. The parameters for all the players are listed in Table 6.1. The cost networks for the different retailers are defined as in Fig. 6.3. In the simulations, the game is played every certain amount of time; we show the response along ten time periods. We have simulated both scenarios at the same time to illustrate the difference in the players' responses.

From Fig. 6.4, which shows the price and consumption in each retailer's coalition, it can be seen that the rationality of the players has been captured, namely that the consumers tend to consume more (less) given a lower (higher) price, and that the retailers tend to lower (raise) their price when the consumption is low (high). This is more clearly evident in the single retailer scenario, where it is also demonstrated that the game eventually converges to a Stackelberg equilibrium [87, 92].

Additionally, Fig. 6.4 shows that there are instances where the game yields zero consumption to certain coalitions. This is the result of the consumers choosing the

Table 6.1: Parameters for Retailers and Consumers.

Retailer	α_{r_i}	κ_{r_i}	$\underline{\lambda}_i$	$\bar{\lambda}_i$	P_i^g
r_1	$1e-4 \text{ \$}^{\frac{1}{2}}$	65 \$	0.01 \$/W	4 \$/W	30 kW
r_2	$7e-5 \text{ \$}^{\frac{1}{2}}$	64 \$	0.01 \$/W	2 \$/W	30 kW
r_3	$5e-5 \text{ \$}^{\frac{1}{2}}$	63 \$	0.01 \$/W	3.5 \$/W	30 kW

Consumer	α_{b_j}	$P_{b_j}^{d_{rated}}$	$\underline{\zeta}_{b_j}$	$\bar{\zeta}_{b_j}$
b_1	1800 W^6	3 kW	0 kW	6 kW
b_2	150 W^6	3.5 kW	0 kW	7 kW
b_3	140 W^6	2.8 kW	0 kW	5.6 kW
b_4	100 W^6	4 kW	0 kW	8 kW
b_5	1600 W^6	1.5 kW	0 kW	3 kW

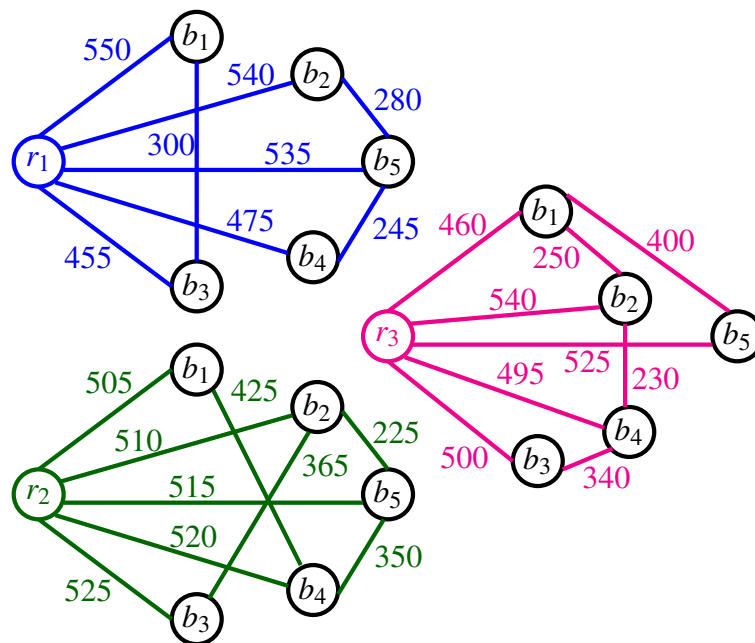


Figure 6.3: Cost networks defined by each retailer for the same set of consumers.

coalition that maximizes their profit (i.e. taking the lowest price), leaving some retailers without consumers for a period of time.

The individual consumptions are captured in Fig. 6.5, from which it is clear that all the consumers are able to consume more in the multiple retailer scenario where the consumption converges above the rated values for all consumers, even with those that do not prioritize consumption as much (lower α_{b_j}). This behaviour is further justified by looking at the individual profits of the consumers in Fig. 6.6. Here it can be seen that the profits are larger for the consumers in the multiple retailer scenario. An exemplary contrast is shown for b_4 , which has a very low consumption in the first scenario but

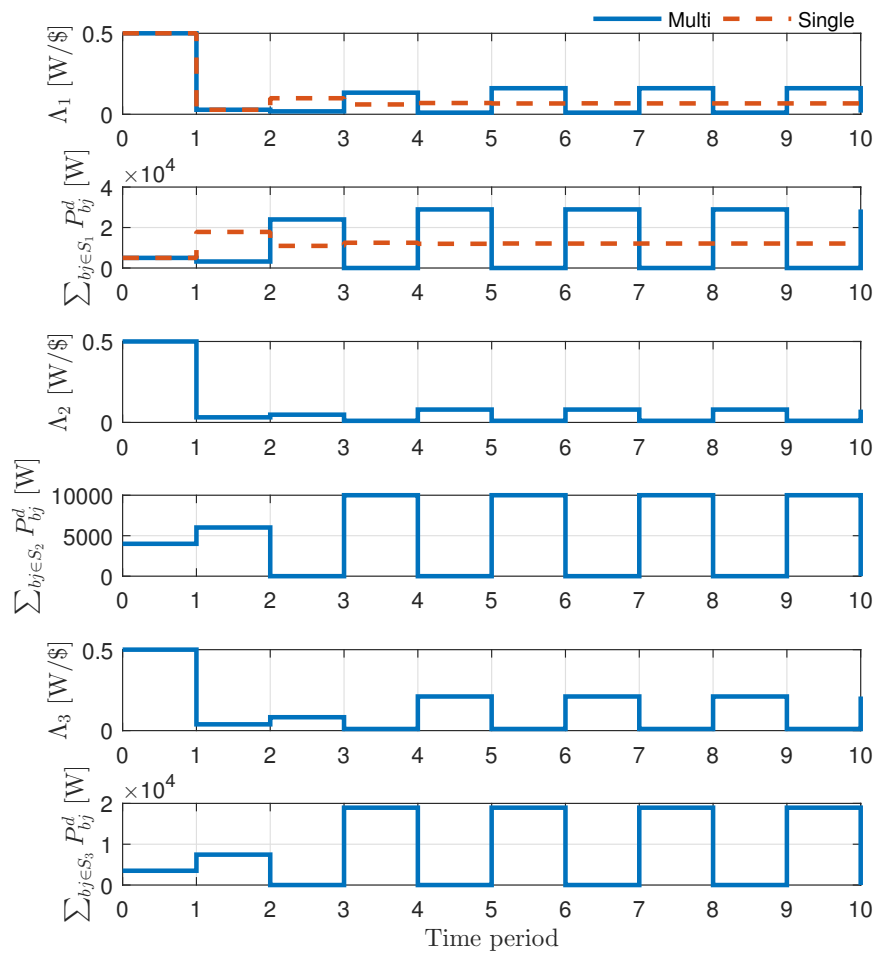


Figure 6.4: Price and coalition consumption responses over time.

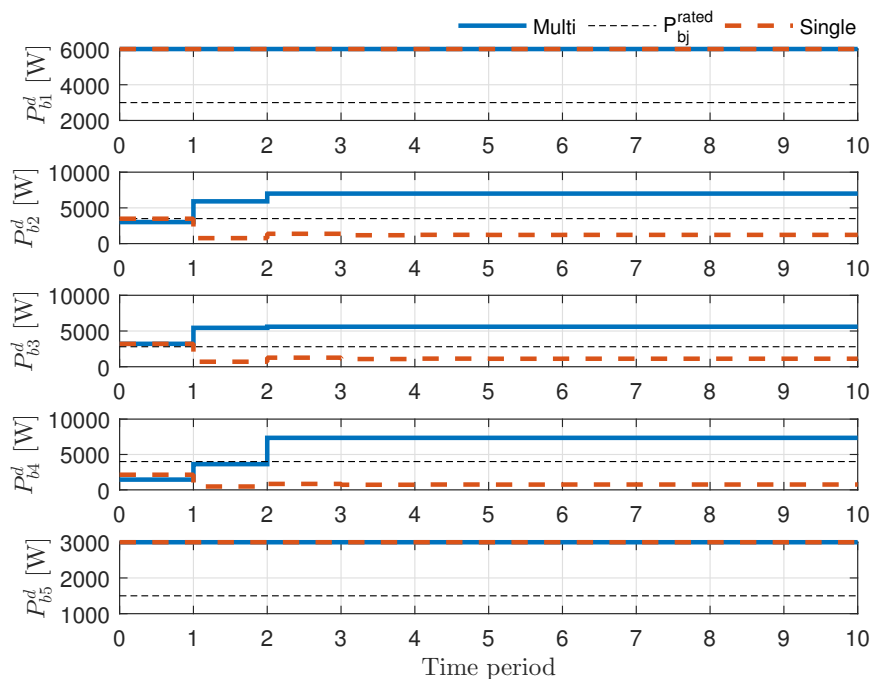


Figure 6.5: Consumers' individual power demand over time.

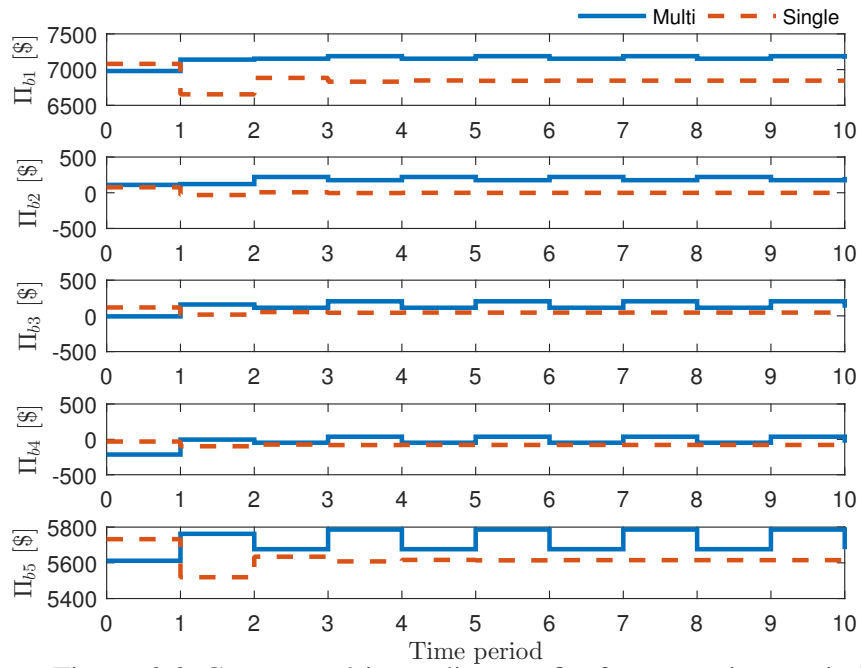


Figure 6.6: Consumers' immediate profits for every time period.

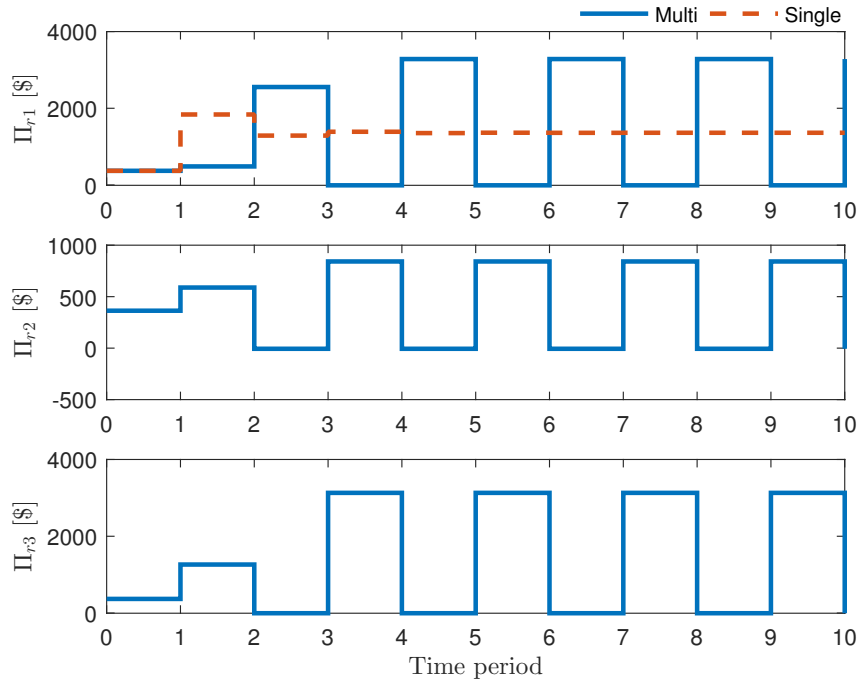


Figure 6.7: Retailers' immediate profits for every time period.

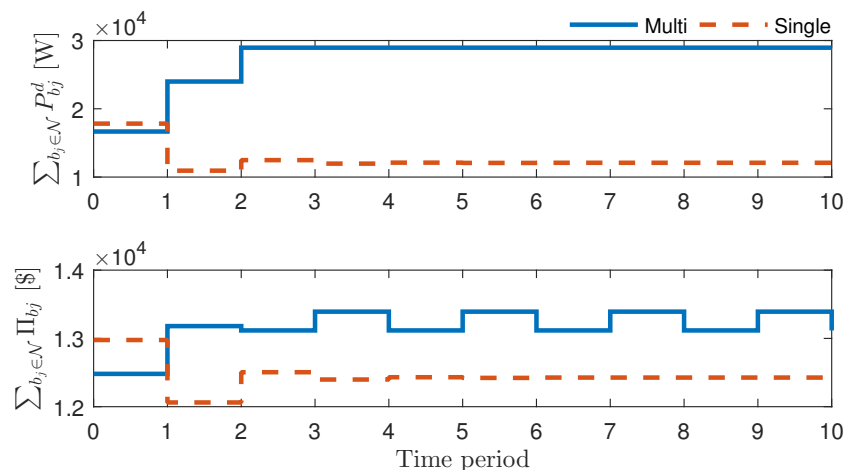


Figure 6.8: Total consumption and profits from all consumers in the problem.

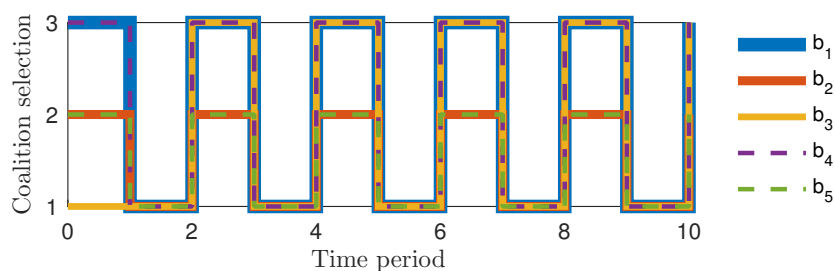


Figure 6.9: Consumers' coalition selection over time.

with negative profits caused by the fact that it has to be connected to the only available retailer and has to cover the connection fee; this is alleviated in the second scenario where its consumption is much larger, yielding positive profits. However, as expected, the profits for r_1 are reduced comparing the first scenario to the second as shown in Fig. 6.7. As mentioned, the lack of customers can yield negative profits due to the running costs, as captured by r_2 's profit. Nonetheless, the advantage of the multiple retailer scheme is clear. This is evident from Fig. 6.8, whereby comparing the total sum of profits yielded by all consumers in the problem, the one in the multiple retailer case is significantly larger.

The decision made by each consumer regarding which coalition to join in the second scenario is distinctly delineated by the plots in Fig. 6.9, where the consumers do not stay fixated with one retailer in their effort to take the one that gains them the largest profit.

From Fig. 6.11 it can be seen that the negative power values (consumptions) for each consumer node approximately coincide with the demand magnitudes previously shown in the previous example in Fig. 6.5, confirming that the rationality of the consumers is captured accordingly to the theoretical example. The small deviations from previous simulations reside on various factors such as power losses and the nature of the P-V droop controller; where the power is regulated to maintain the voltage values within the desired values. The latter is corroborated in Fig. 6.12, where the voltage values are contained within the defined equilibrium bounds, the dynamics are also corroborated by the voltage changes incurred due to the shifts in power/demand.

As in the previous example, the dynamics of the game and preferences of the consumers are illustrated in Fig. 6.13, where the coalitions with lower prices have the highest consumptions and each price changes according to the measured coalition consumption. That is, given a low (high) consumption, the price decreases (increases) in the following time period. The individual consumer preference and retailer switching is captured in Fig. 6.14.

Although the consumers' coalition switching from Fig. 6.9 and Fig. 6.14 appears to not converge to a definitive selection, this can be easily alleviated by introducing *consumer retention schemes* such as disconnection or early contract exit fees to mention some examples. The results shown serve to emphasize the price-taking rationality of both leader and followers.

6.7 Conclusion

The definitions and the algorithm for the pricing scheme have been established and the stability of the game and its induced coalitions have been demonstrated. We have

$$G = \begin{bmatrix} 19.16 & -5.0 & 0 & 0 & 0 & -3.33 & -5.55 & -5.26 \\ -5.0 & 20.79 & -4.34 & 0 & 0 & 0 & -5.88 & -5.55 \\ 0 & -4.34 & 8.35 & -4.0 & 0 & 0 & 0 & 0 \\ 0 & 0 & -4.00 & 7.45 & -3.45 & 0 & 0 & 0 \\ 0 & 0 & 0 & -3.45 & 6.78 & 0 & -3.33 & 0 \\ -3.33 & 0 & 0 & 0 & 0 & 7.33 & -4.0 & 0 \\ -5.55 & -5.88 & 0 & 0 & -3.33 & -4.0 & 18.78 & 0 \\ -5.26 & -5.55 & 0 & 0 & 0 & 0 & 0 & 10.81 \end{bmatrix} \quad (6.56)$$

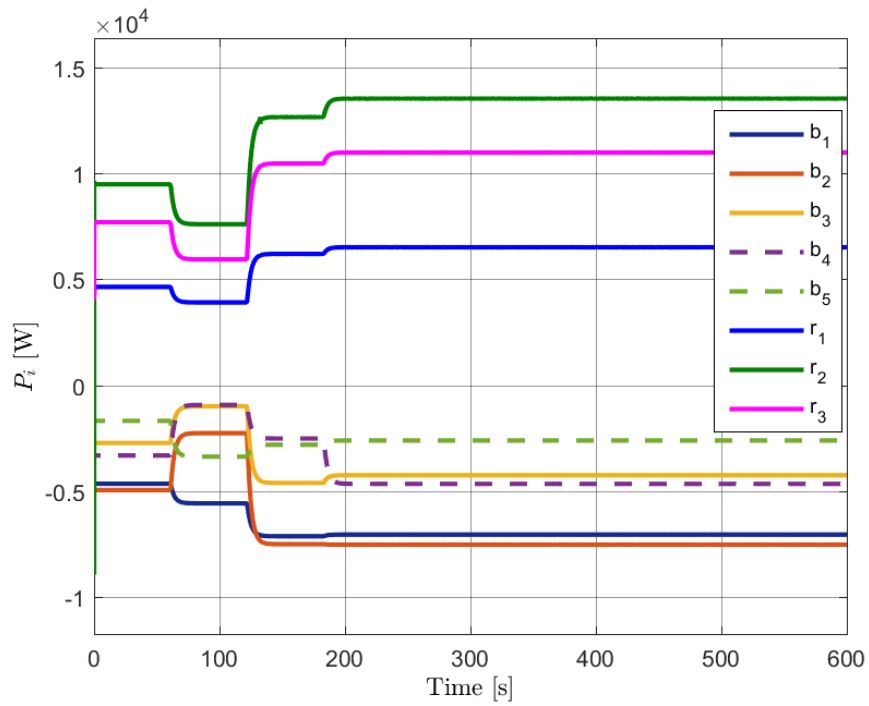


Figure 6.11: Resistive network node powers when subject to the proposed coalitional game.

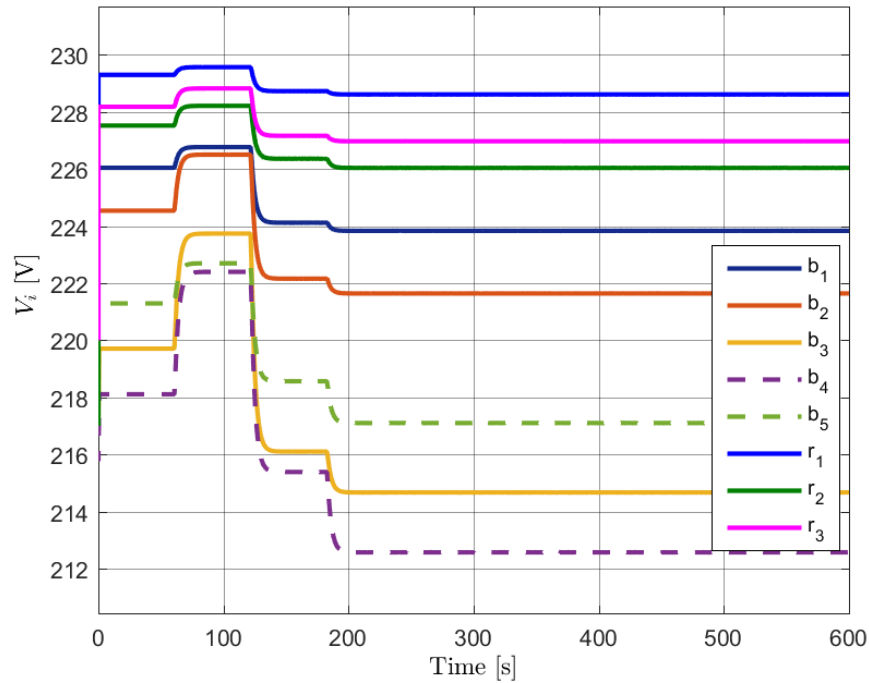


Figure 6.12: Resistive network node voltages when subject to the proposed coalitional game.

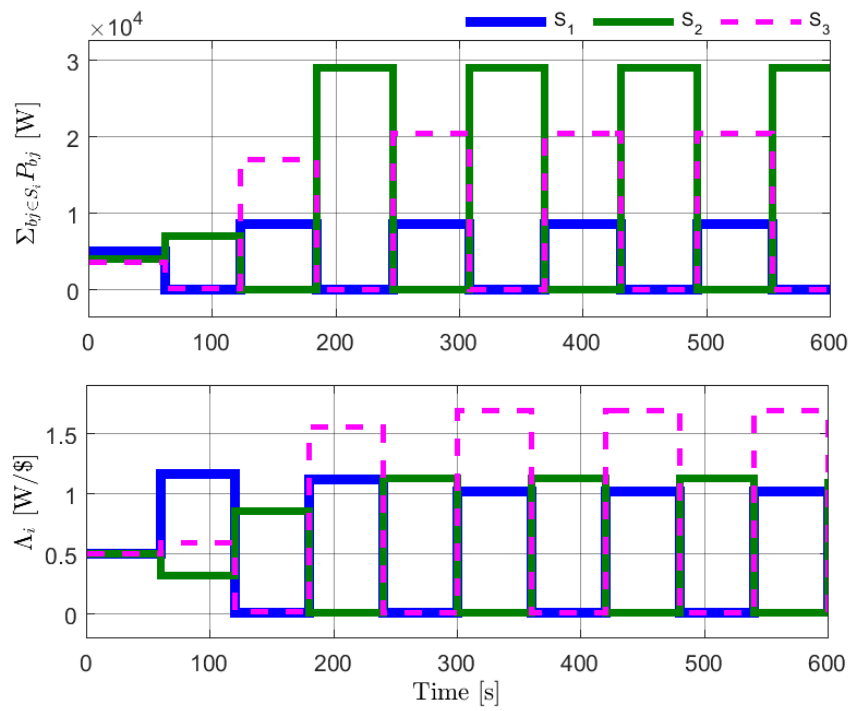


Figure 6.13: Desired cumulative consumptions for each retailer coalition given a respective price.

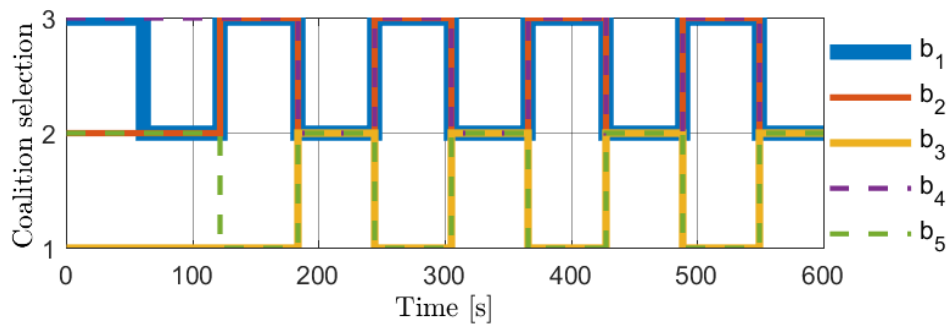


Figure 6.14: Consumers coalition selection when subject to physical dynamics.

described a potential implementation of the present scheme and the integration of it with the physical micro-grid dynamics, together with its corresponding stability analysis. A comparison between single and multiple retailer scenarios has been shown numerically, highlighting the advantages of the latter from an economic point of view.

In this chapter, we have proposed and derived an on-line pricing scheme that encompasses the most important theories and concepts that have been touched on in the present research project. Namely the hierarchical structure of the Stackelberg game, coalitional games where there are competing players, notions of network systems, and the stability of non-linear systems.

Chapter 7

Conclusions

In this thesis, the study of game theory-based pricing schemes and their integration with physical power systems has been carried out. In the sequel, a discussion about the present body of work, its implications, results and general conclusions is presented.

7.1 Discussion and Conclusions

Bringing together the areas of game theory and power systems for this research has been proven to be a great challenge. As mentioned above, because of the interdisciplinary nature of this proposition, there is a knowledge disparity and, to a certain degree, reluctance from both areas to embrace each other. This fact is directly reflected in the literature. The rigorousness of the power systems and control does not compromise for simpler models or the subjectivity of some game-theoretic concepts. Conversely for the game theory community, such realistic approaches have less importance, leading to unrealistic assumptions or outright disregard of the physical systems. From this, one can understand the compromises taken in this research that are reflected in the model switching from Chapter 4 to Chapter 5.

Other discernible compromises arisen from this situation are the choice for simple models in the cost and utility functions of the players, as well as in the choice for linear incentive strategies, since advocating for more complexity would have resulted in a more complicated analysis from the control and systems engineering perspective.

In contrast, from the game theory community, there is an eagerness to see the applicability of the theories and algorithms it proposes. This was illustrated to us directly

during the reviews and the subsequent acceptance of the works proposed in Chapters 4 and 6. Although the ways in which we have connected the two parts of the problem by the means of passing the output of the game through simple dynamics and including the state for the latter in the physical plant appear to be valid, there must be other procedures to couple such parts in a more logical, precise and efficient way.

From the above, we can conclude that the results presented in this thesis help bridge the aforementioned gap, certainly not completely, but they constitute a step closer.

7.2 Impact on the Community

Although our proposed less prescriptive model from Chapter 3 is acceptable only for certain applications, we have made available a tool to represent network systems and be the base for further studies, being on the theoretical or practical aspects, on the market side or otherwise.

The pricing schemes proposed in this study have been formulated with the end-user in mind at all times. The reason behind this is to bring the reader closer to the problem setup in a more engaging and relatable manner. This is very important since an underlying objective of this work is to familiarize people from a power systems or control engineering background to the game-theoretic concepts here touched.

The most palpable contribution from the present research is the insight provided on how the electrical systems would react by subjecting them to the derived pricing schemes; at the same time, conditions for stability are provided, depending on either the parameters of the physical system or the pricing mechanism. This is important since figuring out a definitive on-line pricing scheme for micro-grid systems is still an existing challenge, the work performed here will hopefully help pave the way to their implementation in the near future.

7.3 Future Directions

Given the level of detail of the models proposed in this research, there are several ways the present work can be improved and expanded upon. A non-comprehensive account of approaches is as follows:

Although not taking part in the scope of this study, the ethical dilemmas and repercussions arising from introducing novel market schemes and dynamics have to be thoroughly researched, as with any technological paradigm released to the public, new laws have to be adapted and formulated for proper implementation.

Regarding the physical layer of the problems here presented, several factors can be included such as the impact of stochastic disturbances due to renewable generation, or the existence of failures in a given subset of micro-grid nodes to name some examples. However, these are to be included meticulously since they would likely increase the complexity of the dynamic models and therefore the stability analysis. Another way to extend the present research is investigating the impact and the integration of the proposed pricing schemes on the overall dynamics when there are multiple micro-grids interconnected.

For the game-theoretic part, a logical step forward for the proposed schemes is the introduction of mean-field models for the demand. A more expansive study, specifically for the Stackelberg game, pertains in the inclusion of different functions for the incentive strategy, studying different configurations for both value and cost functions and the analytical conditions that lead to a consensus on price and demand. An investigation on the bounds for the incentive strategy and its tuning that ensure a non-oscillating response is also another path to take.

Further developments for the coalitional game approach dwell in the incorporation of disconnection penalties, quality of the service, among other factors that can be included in the algorithm. Additionally, several approaches/variations for deriving the proposed cost networks can be investigated. Finally, with the same market setup and dynamics as the basis, a plethora of optimization methods can also be implemented for a more efficient and precise performance for the scheme we have proposed.

References

- [1] UK Power Networks, “Regional Development Plan City Road City of London (excluding 33kV),” 2014.
- [2] D. P. Kothari and I. J. Nagrath, *Modern Power System Analysis*. Tata McGraw-Hill Pub. Co, 2003.
- [3] T. Namerikawa, N. Okubo, R. Sato, Y. Okawa, and M. Ono, “Real-Time Pricing Mechanism for Electricity Market with Built-In Incentive for Participation,” *IEEE Transactions on Smart Grid*, vol. 6, no. 6, pp. 2714–2724, 2015.
- [4] D. Bauso, “Nonlinear network dynamics for interconnected micro-grids,” *Systems & Control Letters*, vol. 118, pp. 8–15, 2018. [Online]. Available: <http://linkinghub.elsevier.com/retrieve/pii/S0167691118300896>
- [5] F. Bullo, “Lectures on Network Systems,” 2016.
- [6] M. Roozbehani, M. A. Dahleh, and S. K. Mitter, “Volatility of Power Grids under Real-Time Pricing,” *arXiv preprint:1106.1401*, vol. X, pp. 1–15, 2011.
- [7] A. Loni and F.-A. Parand, “A survey of game theory approach in smart grid with emphasis on cooperative games,” in *2017 IEEE International Conference on Smart Grid and Smart Cities (ICSGSC)*. IEEE, jul 2017, pp. 237–242.
- [8] M. J. Osborne, “A course in game theory,” *Computers & Mathematics with Applications*, vol. 29, no. 3, p. 115, 1995.
- [9] W. Saad, Z. Han, M. Debbah, A. Hjørungnes, and T. Başar, “Coalitional game theory for communication networks,” *IEEE Signal Processing Magazine*, vol. 26, no. 5, pp. 77–97, 2009.

- [10] L. Moreau, “Stability of continuous-time distributed consensus algorithms,” 2004.
- [11] R. O. Saber, J. a. Fax, and R. M. Murray, “Consensus and Cooperation in Multi-Agent Networked Systems,” *Proceedings of IEEE*, vol. 95, no. 1, pp. 215–233, 2007.
- [12] F. Dörfler, M. Chertkov, and F. Bullo, “Synchronization in complex oscillator networks and smart grids,” *Proceedings of the National Academy of Sciences*, vol. 110, no. 6, pp. 2005–2010, 2013.
- [13] F. Dörfler and F. Bullo, “Synchronization and Transient Stability in Power Networks and Non-Uniform Kuramoto Oscillators,” *SIAM Journal on Control and Optimization*, vol. 50, no. 3, pp. 1616–1642, 2012.
- [14] T. Senjyu, M. Tokudome, A. Yona, and T. Funabashi, “A Frequency Control Approach by Decentralized Controllable Loads in Small Power Systems,” *IEEE Transactions on Power and Energy*, vol. 129, no. 9, pp. 1074–1080, 2009.
- [15] L. Dong and Y. Zhang, “On design of a robust load frequency controller for interconnected power systems,” *American Control Conference (ACC), 2010*, pp. 1731–1736, 2010.
- [16] P. Monshizadeh, C. De Persis, N. Monshizadeh, and A. Van Der Schaft, “Non-linear Analysis of an Improved Swing Equation.”
- [17] S. Nabavi and A. Chakraborty, “Structured Identification of Reduced-Order Models of Power Systems in a Differential-Algebraic Form,” *IEEE Transactions on Power Systems*, vol. 32, no. 1, pp. 198–207, jan 2017. [Online]. Available: <http://ieeexplore.ieee.org/document/7452673/>
- [18] Prabha Kundur, “Power System Stability and Control,” p. 1176, 1994.
- [19] H. Bevrani, *Robust power system frequency control*. Springer, 2009.
- [20] J. W. Simpson-Porco, F. Dörfler, and F. Bullo, “Synchronization and power sharing for droop-controlled inverters in islanded microgrids,” *Automatica*, vol. 49, no. 9, pp. 2603–2611, 2013.

- [21] I. A. Hiskens, "Introduction to Power Grid Operation," *Ancillary Services from Flexible Loads CDC'13*, 2013.
- [22] Y. Okawa and T. Namerikawa, "Distributed Optimal Power Management via Negawatt Trading in Real-Time Electricity Market," *IEEE Transactions on Smart Grid*, vol. 8, no. 6, pp. 3009–3019, 2017.
- [23] F. Genis Mendoza, D. Bauso, and T. Namerikawa, "Transient dynamics of heterogeneous micro grids using second order consensus," in *2017 International Conference on Wireless Networks and Mobile Communications (WINCOM)*. IEEE, 2017, pp. 1–6.
- [24] L. Scardovi and R. Sepulchre, "Synchronization in networks of identical linear systems," *Automatica*, vol. 45, pp. 2557–2562, 2009. [Online]. Available: www.elsevier.com/locate/automatica
- [25] Zhongkui Li, Zhisheng Duan, Guanrong Chen, and Lin Huang, "Consensus of Multiagent Systems and Synchronization of Complex Networks: A Unified Viewpoint," *IEEE Transactions on Circuits and Systems I: Regular Papers*, vol. 57, no. 1, pp. 213–224, jun 2009.
- [26] S. Gershgorin, "Über die Abgrenzung der Eigenwerte einer Matrix," *Bulletin de l'Academie des Sciences de l'URSS*, no. 6, pp. 749–754, 1931.
- [27] H. Khalil, *Nonlinear Systems*, third edition ed. Prentice Hall, 2002.
- [28] L. J. S. Allen, *An introduction to mathematical biology*. Pearson/Prentice Hall, 2007.
- [29] M. R. Roussel, "Stability Analysis for ODEs," 2005.
- [30] D. Materassi, M. Roozbehani, and M. A. Dahleh, "Equilibrium price distributions in energy markets with shiftable demand," *Proceedings of the IEEE Conference on Decision and Control*, 2012.
- [31] C. Eksin, H. Delic, and A. Ribeiro, "Demand Response Management in Smart Grids With Heterogeneous Consumer Preferences," *IEEE Transactions on Smart Grid*, vol. 6, no. 6, pp. 3082–3094, 2015.

- [32] A. J. Wood, B. F. Wollenberg, and G. B. Sheble, *Power generation, operation, and control.*, 3rd ed. Wiley, 2013.
- [33] A. H. Mohsenian-Rad, V. W. S. Wong, J. Jatskevich, R. Schober, and A. Leon-Garcia, "Autonomous Demand-Side Management Based on Game-Theoretic Energy Consumption Scheduling for the Future Smart Grid," *IEEE TRANSACTIONS ON SMART GRID*, vol. 1, no. 3, 2010.
- [34] P. Samadi, H. Mohsenian-Rad, R. Schober, and V. W. S. Wong, "Advanced Demand Side Management for the Future Smart Grid Using Mechanism Design," *IEEE Transactions on Smart Grid*, vol. 3, 2012.
- [35] I. Atzeni, L. G. Ordonez, G. Scutari, D. P. Palomar, and J. R. Fonollosa, "Demand-Side Management via Distributed Energy Generation and Storage Optimization," *IEEE Transactions on Smart Grid*, vol. 4, no. 2, pp. 866–876, 2013.
- [36] H. Ehtamo and R. P. Hämmäläinen, "Incentive strategies and equilibria for dynamic games with delayed information," *Journal of Optimization Theory and Applications*, vol. 63, no. 3, pp. 355–369, 1989.
- [37] A. Gupta, S. Schewe, A. Trivedi, M. S. K. Deepak, and B. K. Padarathi, "Incentive stackelberg mean-payoff games," in *Lecture Notes in Computer Science (including subseries Lecture Notes in Artificial Intelligence and Lecture Notes in Bioinformatics)*, 2016, pp. 304–320.
- [38] K. Mizukami and H. Wu, "Two-Level Incentive Stackelberg Strategies in LQ Differential Games with Two Noncooperative Leaders and One Follower," *Trans. of the Society Instrument and Control Engineers*, vol. 2323, no. 66, 1987.
- [39] K. Mizukami and H. S. Wu, "Incentive {S}tackelberg strategies in linear quadratic differential games with two noncooperative followers," in *System modelling and optimization*, 1988, vol. 113, pp. 436–445.
- [40] D. Wang, Xiaolong Qian, and Xiaozheng Jin, "Traffic rate control based on incentive Stackelberg strategy," in *2012 24th Chinese Control and Decision Conference (CCDC)*. IEEE, 2012, pp. 1284–1287.

- [41] D. A. Behrens, J. P. Caulkins, G. Feichtinger, and G. Tragler, “Incentive Stackelberg Strategies for a Dynamic Game on Terrorism,” in *Advances in Dynamic Game Theory*, pp. 459–486.
- [42] X. Vives, “Strategic Supply Function Competition With Private Information,” *Econometrica*, vol. 79, no. 6, pp. 1919–1966, 2011.
- [43] A. Ghosh, V. Aggarwal, and H. Wan, “Exchange of Renewable Energy among Prosumers using Blockchain with Dynamic Pricing,” 2018.
- [44] M. Gouda, S. Danaher, and C. Underwood, “Building thermal model reduction using nonlinear constrained optimization,” *Building and Environment*, vol. 37, no. 12, pp. 1255–1265, 2002.
- [45] B. Asare-Bediako, W. Kling, and P. Ribeiro, “Future residential load profiles: Scenario-based analysis of high penetration of heavy loads and distributed generation,” *Energy and Buildings*, vol. 75, 2014.
- [46] F. Adamek, “Demand Response and Energy Storage for a Cost Optimal Residential Energy Supply with Renewable Generation,” Ph.D. dissertation, Eidgenössische Technische Hochschule ETH Zürich, 2011.
- [47] D. Karlsson and D. J. Hill, “Modeling and identification of nonlinear dynamic loads in power systems,” *IEEE Transactions on Power Systems*, vol. 9, no. 1, pp. 157–166, 1994.
- [48] J. W. Simpson-Porco, F. Dörfler, and F. Bullo, “On Resistive Networks of Constant Power Devices,” vol. 62, no. 8, pp. 811–815, 2015.
- [49] I. Romero Navarro, “Dynamic Load Models for Power Systems, Estimation of Time-Varying Parameters During Normal Operation,” Ph.D. dissertation, 2002.
- [50] W. Saad, Z. Han, H. V. Poor, and T. Başar, “Game-theoretic methods for the smart grid: An overview of microgrid systems, demand-side management, and smart grid communications,” *IEEE Signal Processing Magazine*, vol. 29, no. 5, pp. 86–105, 2012.

- [51] W. Tushar, H. V. Saad, W. and Poor, and D. B. Smith, “Economics of electric vehicle charging: A game theoretic approach,” *IEEE Transactions on Smart Grid*, 2012.
- [52] S.-G. Yoon, Y.-J. Choi, J.-K. Park, and S. Bahk, “Stackelberg-Game-Based Demand Response for At-Home Electric Vehicle Charging,” *IEEE Transactions on Vehicular Technology*, vol. 65, no. 6, pp. 4172–4184, jun 2016.
- [53] M. Yu and S. H. Hong, “A Real-Time Demand-Response Algorithm for Smart Grids: A Stackelberg Game Approach,” *IEEE Transactions on Smart Grid*, vol. 7, no. 2, pp. 879–888, 2016.
- [54] J. Lee, J. Guo, J. K. Choi, and M. Zukerman, “Distributed energy trading in microgrids: A game-theoretic model and its equilibrium analysis,” *IEEE Transactions on Industrial Electronics*, vol. 62, 2015.
- [55] K. Ma, S. Hu, J. Yang, C. Dou, and J. M. Guerrero, “Energy trading and pricing in microgrids with uncertain energy supply: A three-stage hierarchical game approach,” *Energies*, vol. 10, no. 5, 2017.
- [56] A. Belgana, B. P. Rimal, and M. Maier, “Open Energy Market Strategies in Microgrids: A Stackelberg Game Approach Based on a Hybrid Multiobjective Evolutionary Algorithm,” *IEEE Transactions on Smart Grid*, vol. 6, no. 3, pp. 1243–1252, 2015.
- [57] J. Chen and Q. Zhu, “A Stackelberg Game Approach for Two-Level Distributed Energy Management in Smart Grids.”
- [58] N. Liu, X. Yu, C. Wang, and J. Wang, “Energy Sharing Management for Microgrids With PV Prosumers: A Stackelberg Game Approach,” *IEEE Transactions on Industrial Informatics*, vol. 13, no. 3, pp. 1088–1098, 2017.
- [59] L. O. Chua, C. A. Desoer, and E. S. Kuh, *Linear and nonlinear circuits*. McGraw-Hill, 1987.
- [60] F. Dörfler and F. Bullo, “Kron Reduction of Graphs with Applications to Electrical Networks,” *IEEE Transactions on Circuits and Systems I: Fundamental Theory and Applications*, pp. 1–14, 2010.

- [61] C. Luo, Y. F. Huang, and V. Gupta, "Stochastic dynamic pricing for EV charging stations with renewable integration and energy storage," *IEEE Transactions on Smart Grid*, vol. 9, no. 2, pp. 1494–1505, 2018.
- [62] Y. Okawa and T. Namerikawa, "Distributed dynamic pricing based on demand-supply balance and voltage phase difference in power grid," *Control Theory and Technology*, vol. 13, no. 2, pp. 90–100, may 2015. [Online]. Available: <https://link.springer.com/article/10.1007/s11768-015-4131-5>
- [63] T. Malakar, S. K. Goswami, and A. K. Sinha, "Optimum scheduling of micro grid connected wind-pumped storage hydro plant in a frequency based pricing environment," *International Journal of Electrical Power and Energy Systems*, vol. 54, pp. 341–351, jan 2014.
- [64] J. Schiffer, R. Ortega, A. Astolfi, J. Raisch, and T. Sezi, "Conditions for stability of droop-controlled inverter-based microgrids," *Automatica*, vol. 50, no. 10, pp. 2457–2469, 2014.
- [65] A. Bidram, V. Nasirian, A. Davoudi, and F. L. Lewis, *Cooperative Synchronization in Distributed Microgrid Control*, 2017.
- [66] T. L. Vandoorn, J. D. De Kooning, B. Meersman, J. M. Guerrero, and L. Vandevelde, "Automatic power-sharing modification of P/V droop controllers in low-voltage resistive microgrids," *IEEE Transactions on Power Delivery*, vol. 27, no. 4, pp. 2318–2325, 2012.
- [67] M. I. Azim, M. J. Hossain, and H. R. Pota, "Design of a Controller for Active Power Sharing in a Highly-Resistive Microgrid," *IFAC-PapersOnLine*, vol. 48, no. 30, pp. 288–293, 2015.
- [68] C. De Persis, E. Weitenberg, and F. Dörfler, "A power consensus algorithm for DC microgrids," *IFAC-PapersOnLine*, vol. 50, no. 1, pp. 10 009–10 014, jul 2017.
- [69] C. De Persis, E. R. Weitenberg, and F. Dörfler, "A power consensus algorithm for DC microgrids," *Automatica*, vol. 89, pp. 364–375, 2018.

- [70] D. Bauso, L. Giarré, and R. Pesenti, “Non-linear protocols for optimal distributed consensus in networks of dynamic agents,” *Systems and Control Letters*, vol. 55, no. 11, pp. 918–928, 2006.
- [71] J. W. Simpson-Porco, F. Dörfler, and F. Bullo, “Voltage Stabilization in Microgrids via Quadratic Droop Control,” *IEEE Transactions on Automatic Control*, vol. 62, no. 3, pp. 1239–1253, 2017.
- [72] Z. Wang and M. Lemmon, “Voltage and Frequency Stability of Weak Power Distribution Networks with Droop-Controlled Rotational and Electronic Distributed Generators,” pp. 1–32.
- [73] G. C. Konstantopoulos, Q. C. Zhong, B. Ren, and M. Krstic, “Bounded droop controller for parallel operation of inverters,” *Automatica*, vol. 53, pp. 320–328, 2015.
- [74] ———, “Bounded Integral Control of Input-to-State Practically Stable Nonlinear Systems to Guarantee Closed-Loop Stability,” *IEEE Transactions on Automatic Control*, vol. 61, no. 12, pp. 4196–4202, 2016.
- [75] W. Saad, Z. Han, and H. V. Poor, “Coalitional Game Theory for Cooperative Micro-Grid Distribution Networks,” in *2011 IEEE International Conference on Communications Workshops (ICC)*. IEEE, jun 2011.
- [76] C. Wei, Z. M. Fadlullah, N. Kato, and A. Takeuchi, “GT-CFS: A Game Theoretic Coalition Formulation Strategy for Reducing Power Loss in Micro Grids,” *IEEE Transactions on Parallel and Distributed Systems*, vol. 25, no. 9, pp. 2307–2317, sep 2014. [Online]. Available: <http://ieeexplore.ieee.org/document/6565982/>
- [77] R. Pilling, S. Chang, and P. Luh, “Shapley Value-Based Payment Calculation for Energy Exchange between Micro- and Utility Grids,” *Games*, vol. 8, no. 4, p. 45, oct 2017.
- [78] J. Ni and Q. Ai, “Economic power transaction using coalitional game strategy in micro-grids,” *IET Generation, Transmission & Distribution*, vol. 10, no. 1, pp. 10–18, jan 2016. [Online]. Available: <https://digital-library.theiet.org/content/journals/10.1049/iet-gtd.2014.1084>

- [79] L. Han, T. Morstyn, and M. McCulloch, "Incentivizing Prosumer Coalitions With Energy Management Using Cooperative Game Theory," *IEEE Transactions on Power Systems*, vol. 34, no. 1, pp. 303–313, jan 2019.
- [80] M. Yasir, M. Purvis, M. Purvis, and B. T. R. Savarimuthu, "Dynamic Coalition Formation in Energy Micro-Grids," in *Lecture Notes in Computer Science (including subseries Lecture Notes in Artificial Intelligence and Lecture Notes in Bioinformatics)*, 2015, pp. 152–168.
- [81] Y. Xu, E. Hou, and N. Ansari, "Economic coalition strategies for cost reductions in microgrids distribution networks," in *2014 IEEE Global Communications Conference*. IEEE, dec 2014, pp. 2703–2708. [Online]. Available: <http://ieeexplore.ieee.org/document/7037216/>
- [82] A. Chis and V. Koivunen, "Coalitional game-based cost optimization of energy portfolio in smart grid communities," *IEEE Transactions on Smart Grid*, vol. 10, no. 2, pp. 1960–1970, mar 2019.
- [83] J. Mei, C. Chen, J. Wang, and J. L. Kirtley, "Coalitional game theory based local power exchange algorithm for networked microgrids," *Applied Energy*, vol. 239, pp. 133–141, apr 2019.
- [84] A. Mondal and S. Misra, "Dynamic coalition formation in a smart grid: A game theoretic approach," in *2013 IEEE International Conference on Communications Workshops (ICC)*. IEEE, jun 2013, pp. 1067–1071.
- [85] S. Misra and A. Mondal, "DCoE: Game-theoretic dynamic coalition extension with micro-grid failure in smart grid," in *11th IEEE International Conference on Advanced Networks and Telecommunications Systems, ANTS 2017*. IEEE, 2018.
- [86] P. Chakraborty, E. Baeyens, K. Poolla, P. P. Khargonekar, and P. Varaiya, "Sharing Storage in a Smart Grid: A Coalitional Game Approach," *IEEE Transactions on Smart Grid*, vol. 10, no. 4, pp. 4379–4390, jul 2019. [Online]. Available: <https://ieeexplore.ieee.org/document/8416778/>

- [87] D. Bauso, *Game Theory with Engineering Applications*. SIAM's Advances in Design and Control, 2016.
- [88] K. R. Apt and T. Radzik, "Stable partitions in coalitional games," 2006. [Online]. Available: <http://arxiv.org/abs/cs/0605132>
- [89] L. Stoker, "Good Energy formally launches peer-to-peer renewables trading service Selectricity," 2016. [Online]. Available: <https://www.current-news.co.uk/news/good-energy-formally-launches-peer-to-peer-renewables-trading-service-5133>
- [90] Good Energy LTD, "Selectricity - the power of choice — Good Energy," 2018. [Online]. Available: <https://www.goodenergy.co.uk/selectricity/>
- [91] Uswitch Limited, "Uswitch - Energy Comparison - Compare Gas & Electricity." [Online]. Available: <https://www.uswitch.com/gas-electricity/>
- [92] F. Genis Mendoza, D. Bauso, and G. Konstantopoulos, "Online Pricing via Stackelberg and Incentive Games in a Micro-Grid," in *2019 18th European Control Conference (ECC)*. IEEE, jun 2019, pp. 3520–3525.
- [93] F. Milano, F. Dorfler, G. Hug, D. J. Hill, and G. Verbič, "Foundations and challenges of low-inertia systems (Invited Paper)," in *20th Power Systems Computation Conference, PSCC 2018*. Institute of Electrical and Electronics Engineers Inc., aug 2018.
- [94] F. Dorfler, S. Bolognani, J. W. Simpson-Porco, and S. Grammatico, "Distributed control and optimization for autonomous power grids," in *2019 18th European Control Conference, ECC 2019*. Institute of Electrical and Electronics Engineers Inc., jun 2019, pp. 2436–2453.
- [95] B. K. Poolla, S. Bolognani, and F. Dorfler, "Optimal Placement of Virtual Inertia in Power Grids," *IEEE Transactions on Automatic Control*, vol. 62, no. 12, pp. 6209–6220, may 2017.
- [96] Y. Gao, "Existence and uniqueness theorem on uncertain differential equations with local Lipschitz condition," *Journal of Uncertain Systems*, vol. 6, no. 3, pp. 223–232, 2012.

- [97] Q. C. Zhong, “Synchronized and Democratized Smart Grids To Underpin The Third Industrial Revolution,” *IFAC-PapersOnLine*, 2017.
- [98] R. Riaza, “A matrix pencil approach to the local stability analysis of non-linear circuits,” *International Journal of Circuit Theory and Applications*, vol. 32, no. 1, pp. 23–46, jan 2004.
- [99] D. Granot and G. Huberman, “The Relationship Between Convex Games and Minimum Cost Spanning Tree Games: A Case for Permutationally Convex Games,” *SIAM Journal on Algebraic Discrete Methods*, vol. 3, no. 3, pp. 288–292, sep 1982.
- [100] E. Algaba, S. Béal, E. Rémila, and P. Solal, “Harsanyi power solutions for cooperative games on voting structures,” *International Journal of General Systems*, vol. 48, no. 6, pp. 575–602, 2019.
- [101] L. S. Shapley, “Cores of convex games,” *International Journal of Game Theory*, vol. 1, no. 1, pp. 11–26, dec 1971. [Online]. Available: <https://link-springer-com.sheffield.idm.oclc.org/article/10.1007/BF01753431>
- [102] P. H. Le, T. D. Nguyen, and T. Bektaş, “Generalized minimum spanning tree games,” *EURO Journal on Computational Optimization*, vol. 4, no. 2, pp. 167–188, may 2016. [Online]. Available: <https://link.springer.com/article/10.1007/s13675-015-0042-y>
- [103] J. B. Rosen, “Existence and Uniqueness of Equilibrium Points for Concave N-Person Games,” Tech. Rep. 3, 1965. [Online]. Available: <https://www.jstor.org/stable/1911749?seq=1&cid=pdf->
- [104] S. Anily and M. Haviv, “Subadditive and Homogeneous of Degree One Games Are Totally Balanced,” *OPERATIONS RESEARCH*, vol. 62, no. 4, pp. 788–793, 2014. [Online]. Available: <http://dx.doi.org/10.1287/opre.2014.1283>
- [105] E. Baeyens, E. Y. Bitar, P. P. Khargonekar, and K. Poolla, “Coalitional aggregation of wind power,” *IEEE Transactions on Power Systems*, vol. 28, no. 4, pp. 3774–3784, 2013.

-
- [106] D. Lemons and P. Langevin, *An introduction to stochastic processes in physics*. JHU Press, 2002.
- [107] R. Rajagopal, P. Khargonekar, K. Poolla, P. Varaiya, and E. Bitar, “Bringing Wind Energy to Market Aggregation of Renewable Resources View project UV Localization and Routing View project Bringing Wind Energy to Market.” [Online]. Available: <https://www.researchgate.net/publication/228451636>
- [108] T. R. Rockafellar, S. P. Uryasev, and M. Zabarankin, “Deviation Measures in Risk Analysis and Optimization,” *SSRN Electronic Journal*, nov 2005.